Structure-function analysis of C2 domains of multiple C2 domains and transmembrane region proteins, located at plasmodesmata

Auteur : Petit, Jules
Promoteur(s) : Lins, Laurence; Crowet, Jean-Marc
Faculté : Gembloux Agro-Bio Tech (GxABT)
Diplôme : Master en bioingénieur : chimie et bioindustries, à finalité spécialisée
Année académique : 2016-2017
URI/URL : http://hdl.handle.net/2268.2/3039

LIÈGE université
Gembloux
Agro-Bio Tech

STRUCTURE-FUNCTION ANALYSIS OF C2 DOMAINS OF MULTIPLE C2 DOMAINS AND TRANSMEMBRANE REGION PROTEINS, LOCATED AT PLASMODESMATA

JULES PETIT

TRAVAIL DE FIN D'ÉTUDES PRÉSENTÉ EN VUE DE L'OBTENTION DU DIPLÔME DE MASTER BIOINGÉNIEUR ORIENTATION CHIMIE ET BIOINDUSTRIES

ANNÉE ACADÉMIQUE 2016-2017

(CO-)PROMOTEURS: LAURENCE LINS & JEAN-MARC CROWET

LIÈGE université
Gembloux
Agro-Bio Tech

STRUCTURE-FUNCTION ANALYSIS OF C2 DOMAINS OF MULTIPLE C2 DOMAINS AND TRANSMEMBRANE REGION PROTEINS, LOCATED AT PLASMODESMATA

JULES PETIT

TRAVAIL DE FIN D'ÉTUDES PRÉSENTÉ EN VUE DE L'OBTENTION DU DIPLÔME DE MASTER BIOINGÉNIEUR ORIENTATION CHIMIE ET BIOINDUSTRIES

ANNÉE ACADÉMIQUE 2016-2017

(CO-)PROMOTEURS: LAURENCE LINS & JEAN-MARC CROWET

Acknowledgments

First, I would like to thank all the people who supported me during this 6 years journey and helped me to find my way into the bioengineering studies and toward a future that suits me best. My parents and family, who were and are always present for listening, guiding and loving me no matter what. My best friend and roommate Zoé, with whom I spent the best moments of my student life but who also gave me the strength to work hard and never let go. My friends, old and new, who made this Belgian (and Dutch) journey awesome and unforgettable. Jérôme, who made me discover this wonderful country and supported me during the most difficult times. My teachers, who taught me everything and pushed me toward what I've become, and more especially Pr. Luc Willems, to whom I owe the discovery of the LBMI during my third year of bachelor. And more generally all the persons I encountered during this period of my life.

I'd also like to thank those without whom the achievement of this work would have not been possible. Dr Laurence Lins and Dr Jean-Marc Crowet, my promoters, who passed on to me the passion for molecular bioinformatics since my third year of bachelor and guided me during this thesis by teaching, advising, correcting, but also, and more especially, showing me the importance of good professional relationships. I owe them a lot in both my professional and personal developments. I have a special gratitude toward Dr Emmanuelle Bayer, for her infinite kindness and joy, for warmly welcoming me in Bordeaux, giving me extra motivational boosts and for correcting my work. And to my friend, Marie-Aude, for bearing me in her apartment during one month while I was in Bordeaux. From Bordeaux, I also thank Dr Sébastien Montgrand for his welcome and good spirit, Marie Brault for having the patience to teach me confocal microscopy, Dr William Nicolas for his sense of humor – and also for lending me his bike – and Françoise Immel for her gentleness. From the LBMI I thank Dr Magali Deleu for her tenderness and support, Dr Nail Nasir for his dynamic personality and my friend Estelle Deboever for encouraging me this year and particularly this summer.

Through these few lines, I can only express the gratefulness and/or love I have for you all in some quite common words, but be sure that they are sincere and deeper that they might seem: life is not always easy and you, in a way or another, all contributed to the happiness of mine. Frederic Lenoir says that 'Existing is a fact, but living is Art' and I'll add: 'If living is Art, then people are pigments'.

I dedicate this thesis to my grandmother, who prayed daily for my success and loved me until the end.

Abstract

All plant biologists in research history observed the paramount role of cell-to-cell interconnections, so-called plasmodesmata. The plasmodesmata ultra-structure and the elements involved in its regulation are not fully known yet. However, the new viewpoint sees plasmodesmata as specialized membrane contact sites (MCS) – where the endoplasmic reticulum and the plasma membrane get tethered together within the pores – brings us an original hypothesis on the importance of the spoke-like tethering elements. The identity of such elements was not uncovered yet, but recent research has proved plasmodesmata localization of the plant Multiple C2 domains and Transmembrane region Proteins (MCTPs). As members of this family possess all the required features for membrane tethering, they are perfect candidates for being membrane tethers. Indeed, they display a transmembrane domain, that could bind the endoplasmic reticulum membrane, and several C2 domains – known in mammal MCS tethers to bind lipids and/or calcium ions – that could bind the plasma membrane. The objective of our work was to predict the membrane and/or calcium interactions of the C2 domains of two plasmodesmata-located MCTPs: QUIRKY/AtMCTP5, from *Arabidopsis thaliana*, which is involved in morphogenesis regulation and NbMCTP11, from *Nicotiana benthamiana*. For this, we had to establish a series of bioinformatics protocols to delimit the C2 domain sequences, make 3D models and, finally, predict their docking to model plant membrane and possible calcium dependence. The results of the modeling simulations suggested interactions with the membrane, as most of the studied domains were able to interact with the lipids polar heads, but also on more specific features such as phosphatidylinositol phosphate binding sites in NbMCTP11 C2D and calcium binding sites in AtMCTP5 C2D domains. *In vivo* assays on the full length NbMCTP11 proved that the protein localizes at plasmodesmata and truncated mutants showed different phenotypes, revealing different roles of the different parts of the protein. Further analysis has to be carried out on this part but preliminary results showed convergence between mutant localization and domains behavior.

Keywords: *Plant biology; Plasmodesmata; MCTP; C2 domains; Molecular modeling; Molecular dynamics; Calcium-binding; Membrane docking; Lipid interaction.*

Résumé

Les chercheurs en biologie végétale ont toujours observé le rôle primordial des connections intercellulaires chez les cellules de plante, autrement appelées plasmodesmes. La structure détaillée des plasmodesmes ainsi que les éléments impliqués dans leur régulation ne sont pas encore entièrement connus. Cependant, le nouveau point de vue qui perçoit les plasmodesmes comme des sites de contacts membranaires particuliers amène d'intéressantes hypothèses sur l'importance des attaches moléculaires qui lient les deux membranes. La nature de ces éléments n'est pas encore complètement élucidé à ce jour, mais de récentes recherches ont décelé la présence de protéines MCTP (Multiple C2 domains and Transmembrane region Proteins) au niveau des plasmodesmes. Ces dernières semblent posséder toutes les caractéristiques nécessaires au pontage des membranes et sont donc des candidates de choix. En effet, les membres de cette famille de protéines sont constitués d'une région transmembranaire, qui pourrait se lier à la membrane du réticulum endoplasmique, et de plusieurs domaines C2 – connus chez les mammifères comme étant des éléments qui se lient aux membranes et qui peuvent dépendre du calcium – qui pourraient interagir avec la membrane plasmique. L'objectif du présent travail a été de prédire les capacités d'interaction membranaire et de dépendance au calcium des domaines C2 de deux MCTPs associées aux plasmodesmes: QUIRKY/AtMCTP5, du modèle *Arabidopsis thaliana*, qui est également impliqué dans des mécanismes de morphogenèse, et NbMCTP11, du modèle *Nicotiana benthamiana*. Nous avons préalablement établi une série de protocoles bioinformatiques visant à délimiter les domaines C2, modéliser leur structure 3D et enfin prédire leurs comportements. Les résultats de ces simulations nous ont permis de prédire les modes d'interactions des domaines, notamment l'importance des interactions électrostatiques entre les domaines C2 et les têtes polaires des lipides. Nous avons également mis en évidence des caractéristiques plus spécifiques comme la liaison potentielle de C2D de *N. benthamiana* aux phosphatidylinositol phosphates ou bien la coordination d'ions calcium du C2D de *A. thaliana*. Les prédictions d'interaction membranaire ont ensuite été comparés avec les résultats des expériences *in vivo* sur des mutants tronqués de la protéine NbMCTP11, afin de trouver une possible corrélation entre la localisation cellulaire et le comportement moléculaire. Les résultats préliminaires semblent indiquer une certaine cohérence entre la localisation cytosolique et la faible interaction membranaire de certains domaines. L'utilisation d'autres mutants basés sur les prédictions doivent cependant confirmer ces allégations.

Mots clés: *Biologie végétale; Plasmodesmes; MCTP; Domaines C2; Modélisation moléculaire; Dynamique moléculaire; Interaction calcium; Interaction lipides membranaires.*

Table of Contents

List Of Abbreviations

3D: Three Dimensional
APL: Area Per Lipid
CG: Coarse Grained
ElNeDyn: Elastic Network Dynamics
ER: Endoplasmic Reticulum
ESYT: Extended Synaptotagmins
HCA: Hydrophobic Cluster Analysis
MCS: Membrane Contact Site
MCTP: Multiple C2 domains and Transmembrane region Protein
MD: Molecular Dynamics
MP: Movement Protein
PD: Plasmodesmata
PIP(4): Phosphatidylinositol(-4-)phosphate
PKC: Protein Kinase C
PLPC: 1-palmitoyl-2-linoleoyl-3-phosphatidylcholine
PLPS: 1-palmitoyl-2-linoleoyl-3-phosphatidylserine
PM: Plasma Membrane
RMSD: Root Mean Square Deviation
RMSF: Root Mean Square Fluctuation
SA: Salicylic Acid
SEL: Size Exclusion Limit
SYT: Synaptotagmins
TMD: Transmembrane Domain

List Of Figures

Introduction

Before tackling the research core of this thesis, it is important to introduce the context of the study and the different components that are part of it. Indeed, this introduction will allow you to have a better understanding of the biology, tools and stakes behind the project.

First, a very general text aim to position the subject in today's research and society. Next, we will focus on the biology with three main parts, in a decreasing molecular scale way (from cellular to atomic level). The first part explains current knowledge about plasmodesmata (PD): their role, structure and new discoveries. The second describes the newly discovered Multiple C2 domains and Transmembrane regions Protein (MCTP) family and more especially some of its members: AtMCTP5, aka QUIRKY (*Arabidopsis thaliana*), and its *Nicotiana benthamiana* homologue NbMCTP11. The last section refers to C2 domains, which are found in many eukaryotic proteins and share very important features, involving membrane interaction. Finally, the theory and concepts behind the bioinformatics tools necessary to this research will be uncovered.

1/ Context of the study

Everyone knows that one of the most obvious differences between animal and plant cells is the cell wall. And this element becomes quite interesting when it comes to cell communication in plants. Animal cell-to-cell communication and its regulation have been extensively studied (H. Wolburg & A. Rohlmann, 1995; G. Sosinsky & B. Nicholson, 2005; A. Gradilla & I. Guerrero, 2013). The PD are nanometer-scale pores bridging cells across the cell walls, constituting a continuous stream, named symplast, in the plant. However, we don't fully understand how the symplast is regulated yet. How does the plant successfully coordinate signaling responses of neighboring cells that will ultimately impact plant growth, architecture and fitness?

This master thesis is part of a more general project that aims to answer the questions above. The thesis is developed within a partnership between the Laboratoire de Biophysique Moléculaire aux Interfaces (LMBI) of Gembloux Agro-Bio Tech (ULg) and the Laboratory of Membrane Biogenesis (CNRS) of the University of Bordeaux. This original project initiates from the new postulate that sees PD as a specialized Membrane Contact Site (MCS) essential to plant multicellularity. The goal is to gain functional and structural understanding of the PD tether system through interdisciplinary research, since the project combines bioinformatics, biophysics and 3D imaging in a molecular and cellular biology context.

Such an enlightening of the basic mechanisms of plant cell-to-cell communication is

fundamental to the future of plant research in many ways. It could help to better comprehend and solve agricultural issues such as plant growth, diseases propagation and stress responses.

2/ The major position of PD in plant function

At the unicellular level, metabolism and behavior are directly affected, through receptors and signaling cascades, by internal and external triggers. But such a system alone could not work when we level up to multicellular organisms. This multicellularity requires two additional features compared to unicellular species: adhesion and signaling between cells. The extracellular matrix of metazoans allows both adhesion of their cells and close contact for signaling. However, plant cells are surrounded by thick and stiff cell walls made of a microfibrillar complex of homosaccharides (cellulose), heterosaccharides and aromatic polymers (lignin). This wall is a mechanical support for plant growth, a cement between cells that also protects them against biotic and abiotic stresses (R. Sager & J. Lee 2014). This interesting element is nonetheless an obstacle to intercellular transport and communication, and prevents cell movement. Phylogenetic analysis illustrates that almost all multicellular lineages with cell walls develop nanoscopic connections through those walls to interconnect their cells (J. Brunkard & P. Zambryski, 2017). J. Raven (2005) demonstrates that structures analogous to PD evolved in parallel and independently within parenchymatous multicellular lineages. Moreover, there are no existing mutants that lack PD and very few that have strongly altered PD function or formation (I. Kim, F. Hempel, K. Sha et al, 2002; K. Kobayashi, M. Otegui, S. Krishnakumar *et al.*, 2007; Y. Benitez-Alfonso, M. Cilia, A. San-Roman et al, 2009; S. Stonebloom, T. Burch-smith, I. Kim et al, 2009; X. Xu, J. Wang, Z. Xuan et al, 2011; M. Xu, E. Cho, T. Burch-smith *et al.*, 2012; J. Brunkard, A. Runkel & P. Zambryski, 2013). More natural phenomena supports the importance of PD: the presence of functioning PD allows cells to divide synchronously to expend or form complex tissues (K. Ehlers & R. Kollmann, 2000); their shutting down is correlated with senescence or cell death (T. Zhu & T. Rost, 2000). All this ground information puts PD has a vital system for plant life.

2.1/ General presentation of PD

In plants, PD connect virtually all the cells and, because of this almost complete interconnection, the continuous cytoplast that composes the plant is commonly called 'symplast' (as opposed to the apoplast which describes the extracellular space) (R. Erickson, 1986). There are only a few specialized cells, such as the stromata, that are isolated from the symplast, usually through progressive removal of PD pores during cell differentiation (R. Sager & J. Lee, 2014). In a general manner, cytosolic exchange through PD is the 'normal' state for plants, which was transcribed by P. Zambrisky by the “cytosol must flow” (J. Brunkard, A. Runkel & P. Zambryski, 2015; J. Brunkard & P. Zambryski, 2017). Before going in more details with PD various roles, let's review its basic

structure, occurrence and biogenesis.

PD connections were serendipitously discovered by Eduard Tangl but the first structural model was only proposed in 1966 by Lopez-Saez *et al.*, based on electronic microscopy (J. Lopez-Saez, G. Giménez-Martin & M. Risueno, 1966; P. Köhler & Carr, 2006). This model shows PD as a cylindrical, plasma membrane (PM)-lined channels of 20-40nm in diameter and several hundreds nanometers in length. The center of the pores contains a rod-like element called the desmotubule, which is continuous with the endoplasmic reticulum (ER) but only composed of the ER membrane with no lumen (K. Oparka, A. Roberts, P. Boevink *et al.*, 1999). Between the outer PM and the axial desmotubule is a cytoplasmic continuum that links the cells and called cytoplasmic sleeve (originally called cytoplasmic annulus)(fig. 1). The wall matrix around PD has a particular composition and contains callose, a β1-3 glucan whose degradation/synthesis controls PD permeability (J. Knox & Y. Benitez-Alfonso, 2014).

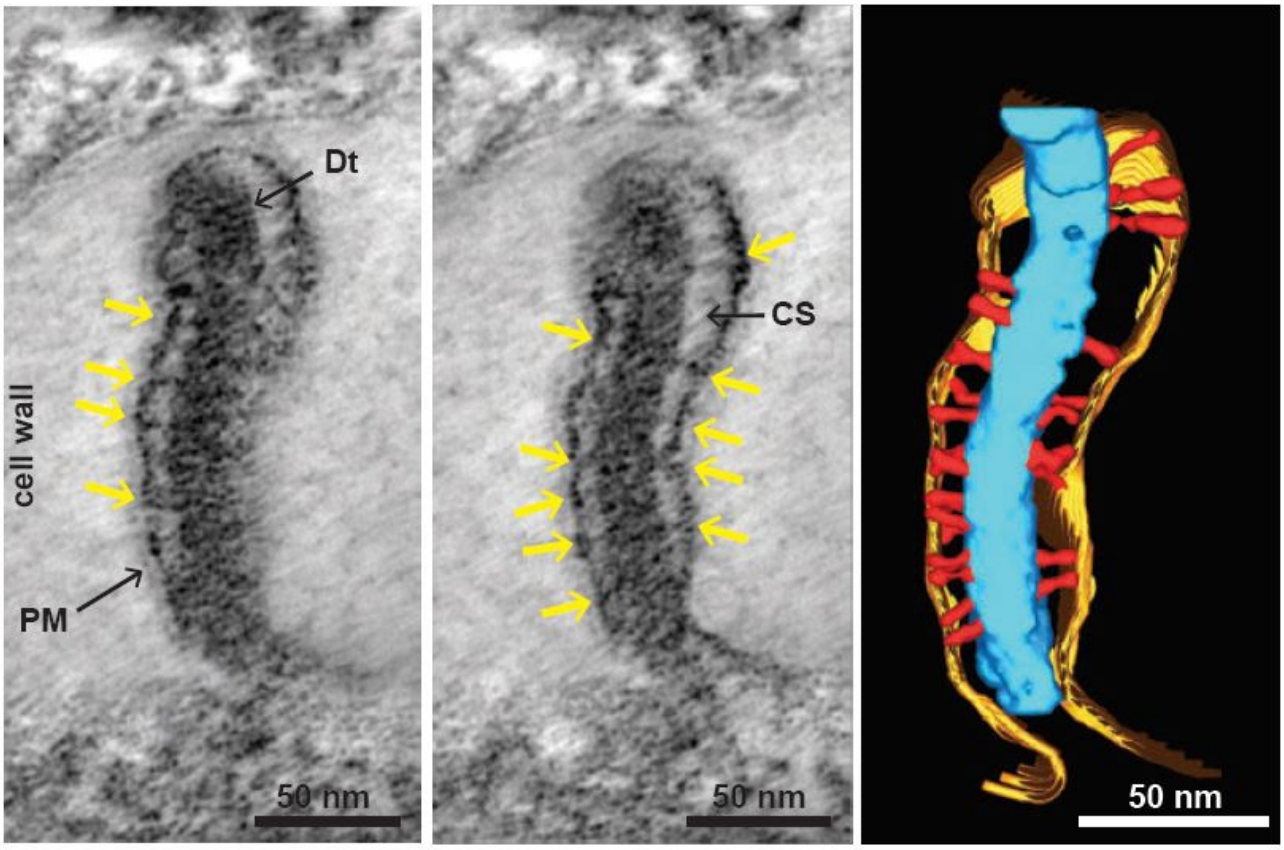

Figure 1: PD ultra-structure from Electron Tomography. The two images on the left show tomographic slices of representative PD from terminal *Arabidopsis thaliana* root tip cells interfaces. Spoke-like tethers are pointed by yellow arrows. The image on the right represent the 3D reconstruction of the same PD. Desmotubule (Dt) in blue, Plasma Membrane (PM) in orange and spoke-like tethers in red (from W. Nicolas, M. Grison, S. Trépout *et al.*, 2017).

The occurrence and structure of PD are subject to variations depending on external and internal factors (reviewed in T. Burch-Smith, S. Stonebloom, M. Xu *et al.*, 2011; R. Sager and J.

Lee, 2014). Usually 1 to 15 PD/µm² of cell wall is assumed but up to 39 PD/µm² can be seen (R. Wayne, 2009). Their distribution can be uniform or aggregated in pitfields.

There are two types of PD between cells. Primary PD, are formed during cytokinesis, when ER strands are trapped by the developing cell plate (W. Nicolas, M. Grison, S. Trépout *et al.*, 2017). Those strands, stretched across the phragmoplast (fig. 2), become lined by PM and finally form the cytoplasmic sleeve. The phenomenon of trapping is likely to be regulated but remains constant over the divisions (C. Faulkner, O. Akman, K. Bell *et al.*, 2008). On the other hand, secondary PD are typically established *de novo* in post-cytokinetic walls between cells of different layers (i.e not sister cells), but can also complement primary PD by insertion of additional branches leading to complex branched PD structures (for review about PD biogenesis, see K. Ehlers and R. Kollmann, 2001; new breakthrough in W. Nicolas, M. Grison, S. Trépout *et al.*, 2017).

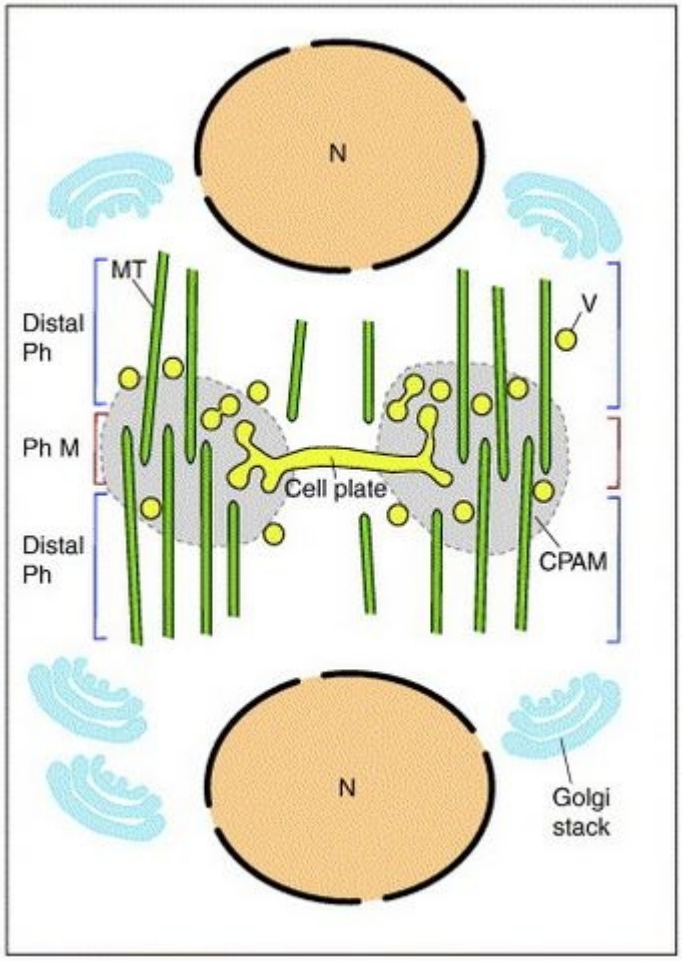

Figure 2: Cytokinesis in plant cells. The new cell plate is formed with the help of the phragmoplast. There are two regions: the phragmoplast midline (Ph) with interdigitating microtubules (MT) and the distal Ph on each side of the midline. A filamentous cell-plate assembly matrix (CPAM) accumulates at the midline to build the new wall. (From M. Otegui, K. Verbrugghe & A. Skop, 2005)

2.2/ Structure-Function Analysis of PD

Despite extensive efforts, we are only beginning to scratch the surface of PD mechanism of action. In the last decade however, we gained substantial understanding of PD molecular structure and thus function-related mechanisms, thanks to the development of new technologies. We can cite as examples tissue-specific omics (M. Salmon & E. Bayer, 2013; M. Grison, L. Brocard, L. Fouillen *et al.*, 2015) and molecular localization studies (C. Thomas, E. Bayer, C. Ritzenthaler *et al.*, 2008; P. Vaddepalli, A. Herrmann, L. Fulton *et al.*, 2014) that helped to reveal novel PD components and their mode of action. The goal of this part is to expose and guide you through the major PD functional axes that have been depicted in the literature, followed by the current reconsideration of the established models.

a) Intercellular Trafficking

Transport between plant cells via PD is mainly passive, thanks to convection generated by cytoplasmic streaming (W. Pickard, 2003). The advantage of such a pathway is the facility and speed of trafficking of hydrophilic elements, in comparison with the effort it would take to the plant if it needed to transport everything across several membrane bilayers. The counterpart of such system is how to prevent cell-to-cell movement of molecules not destined to movement? In other words, if molecules can go freely from one cell to another, how do cells retain certain molecules from leaving or arriving? This needs specific “gate control” and the trapping of molecules not meant to move cell-to-cell. It can be achieved by subcellular targeting to other subcellular compartments (such as nucleus, ER), which is promoted by signal sequences or interactions with other proteins (K. Crawford & P. Zambryski, 2000; H. Cui, M. Levesque, T. Vernoux et al, 2007; J. Schiefelbein, L. Huang & X. Zheng, 2014).

There are a lot of different molecules that can cross the cytoplasmic sleeve of PD: water and ions but also small organic molecules such as hormones, sugars from the photosynthesis, etc (reviewed in A. Roberts & K. Oparka, 2003). Much bigger molecules such as proteins, including transcription factors, and RNAs have also been proved to migrate between cells (reviewed in M. Cilia & D. Jackson, 2004; W. Lucas & J. Lee, 2004; I. Kim & P. Zambryski, 2005), and they have the biggest impact on cell function and response (fig. 3, *top right*).

Although it has been established in some studies that the fluency of trafficking from one cell to another depends on the size of the molecule (K. Crawford & P. Zambryski, 2000; J. Lee, J. Colinas, J. Wang *et al.*, 2006), the cutoff size of PD (defined as SEL -size exclusion limit) has been increasing from under 1kDa (E. Tucker, 1982; P. Goodwin, 1983; H. Weiner, J. Burnell, I. Woodrow *et al.*, 1988) to 70kDa in more recent publications (I. Kim, K. Kobayashi, E. Cho *et al.*, 2005; I. Kim, E. Cho, K. Crawford *et al.*, 2005; J. Brunkard, A. Runkel, P. Zambryski *et al.*, 2015; D.

Paultre, M. Gustin, A. Molnar *et al.*, 2016). Current view suggests that the PD SEL varies according to cell type, developmental stage and various stimuli such as abiotic and biotic stresses. The magnitude of size range supports the necessity of tight regulation for the plant to keep organizational and functional integrity.

Furthermore, increasing complexity of the PD structure, such as the branched channels of nonvascular tissue of old leaves, is correlated with a decrease in molecular transport (K. Oparka, A. Roberts, P. Boevink *et al.*, 1999) (fig. 3, *top left*). This complexity usually arises as cell matures (K. Oparka, A. Roberts, P. Boevink *et al.*, 1999; K. Ehlers & R. Kollman, 2001; K. Ehlers & M. Westerloh, 2013;).

Plant cells can undergo long-term or rapid variations of PD connectivity (R. Sager & J. Lee, 2014). Those changes are crucial for efficient physiological response to spatiotemporal or developmental triggers. And that is the main reason why the regulation of PD permeability is a key toward better understanding of plant biology.

The most extensively studied reversible mechanism of regulation of PD SEL is through callose (β-1,3-glucan) biosynthesis and break down. Callose is mainly found at the neck regions of PD, in the cell wall, where it can form an apoplastic ring that presses the PM against the desmotubule. This “closure” reduces the slot of the cytoplasmic sleeve and is inversely proportional to PD permeability (N. De Storme & D. Geelen, 2014). Callose levels are regulated by two sets of enzymes: synthases (β-1,3-glucan synthases-like proteins (GLS) or callose synthase proteins (CalS)) and hydrolases named β-1,3-glucanases (J. Tilsner, W. Nicolas, A. Rosado *et al.*, 2016). The turnover is triggered by various signals, such as pathogen attack, wounding, cold and other abiotic stresses, but also developmental clues (N. De Storme & D. Geelen 2014; J. Tilsner, W. Nicolas, A. Rosado *et al.*, 2016;). Some signals lead to fast callose response (A. Bilska & P. Sowinski, 2010), indicating that regulation is mainly achieved at the protein level (fig. 3).

Callose levels are very important in the structural remodeling of PD during organogenesis, cell growth and plant development. First, as said before, PD occurs between almost every cell, but some specialized cells undergo permanent isolation. It is the case for mature guard cells forming the stomata (C. Willmer & R. Sexton, 1979; B. Palevitz & P. Hepler, 1985) and the generation of reproduction-related cells like pollen, megagametophytes and zygotes (reviewed in R. Sager & J. Lee, 2014). Furthermore, PD permeability regulation via callose diminishes molecular transport and thus is required for cells to achieve developmental processes. Different stages of embryogenesis of *Arabidopsis* are correlated with temporary PD occlusions (I. Kim, E. Cho, K. Crawford *et al.*, 2005; I. Kim, K. Kobayashi, E Cho *et al.*, 2005; I. Kim & P. Zambryski, 2005; R. Sager & J. Lee, 2014). Lastly, other later developmental processes rely on callose synthesis and degradation. We can cite

sieve plate pore formation in the phloem conducting cells (B. Xie, X. Wang, M. Zhu *et al.*, 2011), flowering by regulation of Shoot Apical Meristem (SAM) size and identity (A. Bergmans, A. Boer, J. Derksen *et al.*, 1997; A. Gisel, S. Barella, F. Hempel *et al.*, 1999; S. Ormenese, A. Havelange, R. Deltour *et al.*, 2000; A. Gisel, F. Hempel, S. Barella *et al.*, 2002; S. Ormenese, A. Havelange, G. Bernier *et al.*, 2002;) and initiation of lateral roots and fiber cell growth by promoting turgor pressure (Y. Benitez-Alfonso, C. Faulkner, A. Pendle *et al.*, 2013; A. Maule, R. Gaudioso-Pedraza & Y. Benitez-Alfonso, 2013).

Figure 3: Cellular processes associated with regulation of molecular trafficking and PD. The top part illustrates opened and closed PD by callose level variation in the neck regions. The *colored dots* represent soluble molecules. It is in association with the inserts 1 and 2, showing close-ups of callose biosynthesis (polymerization of UDP-glucose by callose synthase complexes (CalS) *in dark blue and teal blue*), degradation by β-1,3-glucanase (BG) and regulation by PD callose binding proteins (PDCBs). The bottom part maps the different signaling pathways that lead to callose, and thus PD, regulation. Salicylic acid (SA); Nonexpressor of pathogenesis-related protein 1 (NPR1); PD-localized proteins (PDLPs); Reactive oxygen species (ROS). (from J. Tilsner, W. Nicolas, A. Rosado *et al.*, 2016)

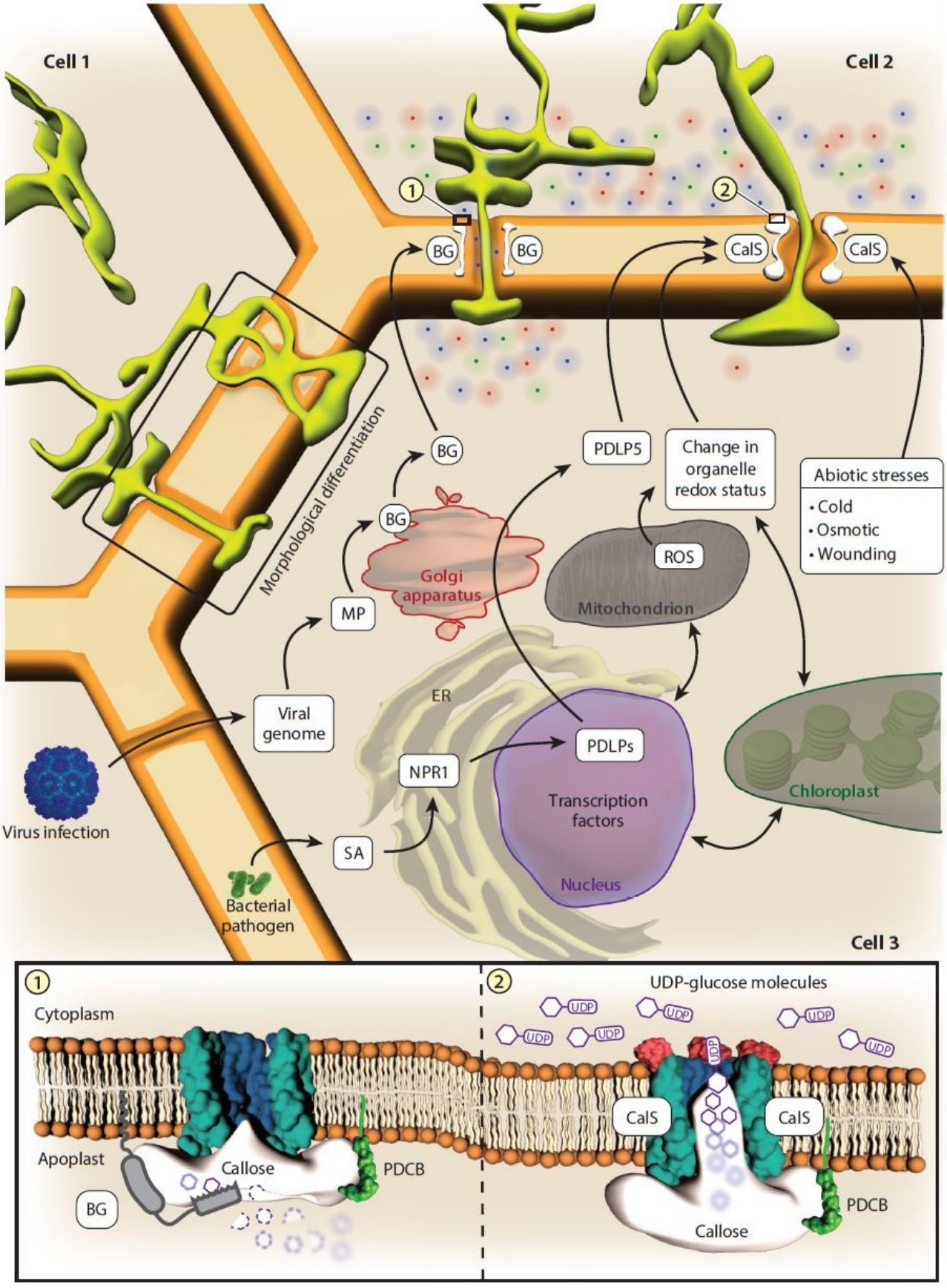
Cell 1
Cell 2
Cell 3
1
2
BG
BG
CalS
CalS
BG
BG
Morphological differentiation
PDLP5
Change in organelle redox status
Abiotic stresses
• Cold
• Osmotic
• Wounding
ROS
Golgi apparatus
Mitochondrion
MP
ER
Viral genome
PDLPs
NPR1
Transcription factors
Chloroplast
Virus infection
SA
Nucleus
Bacterial pathogen
1
Cytoplasm
Apoplast
Callose
PDCB
BG
2
UDP-glucose molecules
UDP
CalS
CalS
PDCB
Callose

PD plays an essential role in plant immunity and defense strategies against pathogen attacks. Callose closure of PD is triggered via the activation of Plasmodesmata-Located Proteins (PDLPs) in response to Salicylic Acid (SA), stimulating SA-response coordinator NPR1 which regulates defense-related genes (J. Lee, X. Wang, W. Cui *et al.*, 2011, X. Wang, R. Sager, W. Cui *et al.*, 2013). SA accumulation is often connected to Reactive Oxygen Species (ROS) synthesis and redox status variation in organelles (chloroplast, mitochondria), which have an impact on Callose Synthase activation (Y. Benitez-Alfonso, M. Cilia, A San Roman *et al.*, 2009; R. Sager & J. Lee, 2014). Viruses exploit PD to spread throughout the plant and have developed strategies to overcome callose closure (reviewed in J. Tilsner, M. Taliansky & L. Torrance, 2014). Indeed, plant viruses genetic material encodes movement proteins (MPs) to facilitate mobility of their genome across PD by increasing SEL. Plants counteract this dissemination by repressing β-1,3-glucanase production or activity (R. Beffa, R. Hofer, M. Thomas *et al.*, 1996; V. Iglesias & F. Meins, 2000; G. Bucher, C. Tarina, M. Heinlein *et al.*, 2001; D. Dobnik, S Baebler, P. Kogovsek *et al.*, 2013). As a response, some viruses produce host factors-interacting MPs that slow down callose-mediated constriction of PD (D. Guenoune-Gelbart, M. Elbaum, G. Sagi *et al.*, 2008; S. Ueki, R. Spektor, D. Natale *et al.*, 2010) and thus promote gating, although gating facilitates antiviral RNA silencing mobility (H. Vogler, M. Kwon, V. Dang *et al.*, 2008).

Callose is surely a major component of PD regulation, but other elements mediate SEL changes. For example, cell walls at PD display microdomains with specific composition and mechanical properties (J. Knox & Y. Benitez-Alfonso, 2014). Cytoskeleton proteins such as myosin and actin are also found in PD (R. White & D. Barton, 2011) (fig. 4). Disruption of myosin, but not actin was shown to alter molecular diffusion between cells (J. Radford & R. White, 2011; W. Nicolas, M. Grison, S. Trépout *et al.*, 2017). However, some viruses evolved actin-degrading MPs that enlarge the SEL (S. Su, Z. Liu, C. Chen et al, 2010). The precise cytoskeleton architecture in the PD remains a mystery and we still need to uncover their exact role in their regulation. Another control of PD permeability has been studied and is quite interesting in the frame of this thesis. E. Tucker (1990) showed that increased levels of calcium ions in the cytoplasm inhibit intercellular movement. Calcium concentration is enhanced by physical alteration of the PM – since the apoplast Ca^{2+} concentration is high –, by cold (T. Holdaway-Clarke, N. Walker, P. Hepler *et al.*, 2000; A. Bilska & P. Sowinski, 2010) or by ROS (J. Foreman, V. Demidchik, J. Bothwell *et al.*, 2003). The precise mechanism by which calcium could regulate PD closure is not known. However, it has been hypothesized that it is linked with callose deposition (J. Tilsner, W. Nicolas, A. Rosado *et al.*, 2016) whereas others support a link with acto-myosin cytoskeleton and calcium-dependent centrin filaments (R. Sager & J. Lee, 2014) (fig. 4). Another possibility is in relation with newly discovered PD-located MCTPs, which are related to calcium-dependent animal synaptotagmins and extended

synaptotagmins.

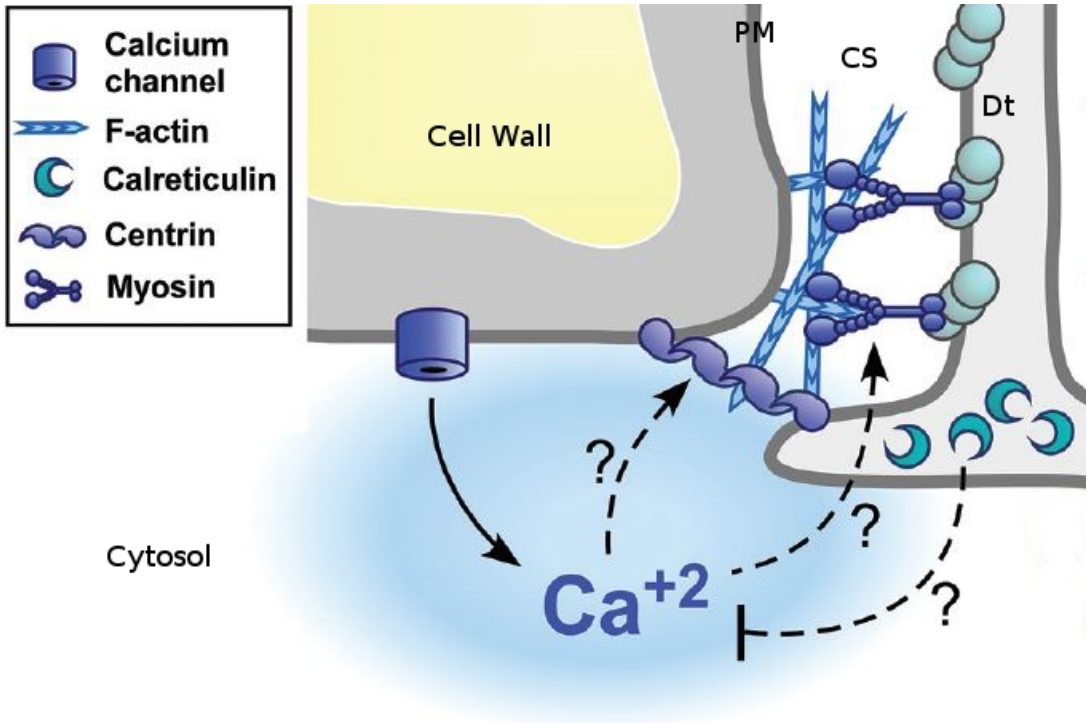

Figure 4: Cytoskeleton elements in PD and Calcium regulation hypothesis. Calcium -dependent proteins such as centrin and myosin have been found in PD, suggesting cytoskeleton-dependent calcium-responsive regulation of PD Size Exclusion Limit (SEL). (from R. Sager & J. Lee, 2014)

b) What we know about PD MCS

Membrane Contact Sites (MCSs) are evolutionary conserved regions where the membranes of two organelles are closely apposed but do not fuse (S. Helle, G. Kanfer, K. Kolar *et al.*, 2013; W. Prinz, 2014; J. Pérez-Sancho, J. Tilsner, A. Samuels *et al.*, 2016). Specific molecular signature and architecture give to MCSs their functional diversity, such as organelle cross talk by information exchange between membranes (M. Eienberg-Bord, N. Shai, M. Schuldiner et *al.*, 2016). In the scope of this thesis, we will focus on the plasma membrane-endoplasmic reticulum (PM-ER) MCS located at PD and more especially on the spoke-like tethers that connect the two membranes (fig. 1). Indeed, the gap between the PM and desmotubule being around 10nm, PD can be classified has a specialized MCS. Many tethers have been identified in mammals and yeasts but not yet in plants PD and we can hypothesize that, like in other eukaryotes, they are critical for membrane junction formation, reshaping and function (A. Manford, C. Stefan, H. Yuan *et al.*, 2012; S. Malmersjö & T. Meyer, 2013; F. Giordano, Y. Saheki, O. Idevall-Hagren *et al.*, 2013; W. Prinz, 2014; W. Henne, J. Liou & S. Emr, 2015; A. Perez-Lara & R. Jahn, 2015; J. Tilsner, W. Nicolas, A. Rosado *et al.*, 2016; J. Pérez-Sancho, J. Tilsner, A. Samuels *et al.*, 2016). The tethering machinery is central to MCS function and inter-organelle crosstalk, i.e. exchange of information, transfer of molecules and

collaborative action (M. Eienberg-Bord, N. Shai, M. Schuldiner et *al.*, 2016), presumably with consequences on developmental organization like those discussed above for plants.

All described tethers gather three main features: ER-anchoring motifs, high-affinity lipid-binding motifs that can interact with PM and a molecular length sufficient to bridge the two membranes (J. Tilsner, W. Nicolas, A. Rosado *et al.*, 2016). As a matter of fact, a study on extended synaptotagmins (E-SYT) in mammals has shown that the spacing between membranes is defined by the molecular identity of the tethers and that dynamic molecular rearrangements directly affects MCS plasticity (R. Fernandez-Busnadiego, Y.. Saheki & P. De Camilli, 2015) (fig. 5b). The recent development of PD isolation techniques and PD-focused proteomic analyses (L. Fernandez-Calvino, C. Faulkner, J. Waalshaw *et al.*, 2011; M. Salmon & E. Bayer, 2013; C. Faulkner & E. Bayer, 2017) allowed the investigation of tether candidates (Bayer unpublished data). The review of J. Tilsner, W. Nicolas, A. Rosado *et al.* (2016) exposes the ongoing thinking concerning putative tethers in PD context.

The first family defined as ER-PM tether is plant synaptotagmins (SYTs), homologous to MCS tethers mammalian extended synaptotagmins (E-SYT) and yeast tricalbins (Tcb) (F. Giordano, Y. Saheki, O. Idevall-Hagren *et al.*, 2013; J. Pérez-Sancho, S. Vanneste, E. Lee *et al.*, 2015). SYT1 (also called SYTA), which has been found in PD proteome (L. Fernandez-Calvino, C. Faulkner, J. Walshaw *et al.*, 2011), is recruited at PD upon virus attack – and promotes viral propagation, suggesting molecular trafficking alteration – (A. Levy, J. Zheng & S. Lazarowitz, 2015). The protein possesses transmembrane domain that could insert into ER and C2 lipid-binding domains that possibly interact with PM anionic lipids. SYT1's roles seem to be mechanical support of PM as a result of scaffold formation (J. Pérez-Sancho, S. Vanneste, E. Lee *et al.*, 2015) but it also enhances PM resistance to stress exposure and membrane repair by sensing calcium levels (A. Schapire, B. Voigt, J. Jasik *et al.*, 2008; T. Yamazaki, Y. Kawamura, A. Minami *et al.*, 2008; A. Schapire, V. Valpuesta & M. Botella, 2009). This indicates that ER-PM MCS components could play a role in calcium signaling. Even more interesting, SYTs carry a cytosol-exposed synaptotagmin-like mitochondrial lipid-binding protein (SMP) domain present in other MCS tethers (A. Toulmay & W. Prinz, 2011) which could favor lipid exchange in crosstalk context, like in animal E-SYT (C. Schauder, X. Wu, Y. Saheki et *al.*, 2014).

Another tether candidate is the vesicle-associated membrane protein (VAMP)-associated protein (VAP) family, whom member VAP27 co-localizes with SYT1 (J. Pérez-Sancho, S. Vanneste, E. Lee *et al.*, 2015) and connects both membrane through NET3C, actin and microtubule networks (P. Wang, T. Hawkins, C. Richardson *et al.*, 2014). P. Wang, C. Richardson, T. Hawkins *et al.* (2016) go even further by bringing evidence that VAP27 localizes in PD MCS, that its mobility is influenced by cell wall and that it is vital for ER-cytoskeleton interaction and plant development.

3/ MCTP family: a new PD-specific tether candidate

The hunt for ER-PM tethers in PD systems is on going, and a newly identified PD-associated protein family is in the line of sight of Emmanuelle M. Bayer and her research group at the Laboratory of Membrane Biogenesis of Bordeaux. The Multiple C2 domains and Transmembrane regions Proteins (MCTPs) have a very good potential to be tethers. First, their structural feature is similar to those of mammalian E-SYT and plant SYT discussed above. Their denomination is quite explicit concerning their architectural constitution: the N-terminal side is composed of a succession of C2 domains while the C-terminal side contains several (two to four) transmembrane regions. Moreover, among the 17 identified MCTPs in *Arabidopsis*, two have already been more thoroughly studied and proved to be located at PD, but never proposed to act as membrane tethers. Those two proteins, namely AtMCTP4/Flowering locus T-Interacting Protein 1 (FTIP1) and AtMCTP5/QUIRKY (QKY), play significant roles in PD-mediated cell-to-cell signaling during developmental processes, as loss-of-function mctp5/qky mutants for instance present abnormal organ structures (L. Fulton, M. Batoux, P. Vaddepalli *et al.*, 2009; L. Liu, C. Liu, X. Hou *et al.*, 2012; C. Trehin, S. Schrempp, A. Chauvet *et al.*, 2013; P. Vaddepalli, A. Herrmann, L. Fulton *et al.*, 2014). This information supports the idea that PD is not only an inert channel but acts as a signaling hub, which can generate and/or relay non-cell-autonomous developmental signals and more.

3.1/ General presentation

The multiple TransMembrane Domains (TMDs) at the C-terminus are hydrophobic segments by definition but some of them can be divided into smaller TMDs, approaching the wedge-shape Reticulon topology. Comparable to Reticulons (I. Sparkes, N. Tolley, I. Aller *et al.*, 2010), the insertion of MCTPs in the ER/desmotubule could favor or stabilize high membrane curvature (K. Knox, P. Wang, V. Kriechbaumer *et al.*, 2015) (fig. 5a). Some C2 domains, that would partly insert in one of the membrane leaflets (L. Chon, J. Osterberg, J. Henderson *et al.*, 2015), could also be associated with specific membrane curvature at PD (K. Ward, J. Ropa, E. Adu-Gyamfi *et al.*, 2012; M. Zanetti, O. Bello, J. Wang *et al.*, 2016). Dynamic response and reshaping of the MCS may be triggered by the putative ability of MCTP C2 domains to dock to the membrane for instance in a calcium-dependent manner. Indeed, many animal SYT and E-SYT display calcium binding pockets (E. Chapman, 2008; N. Gustavsson & W. Han, 2009; J. Xu, T. Bacaj, A. Zhou *et al.*, 2014) and conformational changes of the cytosolic domains upon calcium gradient variations, leading to shortening of the inter-membrane distance at ER-PM MCS in animal cells (R. Fernandez-Busnadiego, Y. Saheki & P. De Camilli, 2015; C. Chang, T. Hsieh, T. Yang *et al.*, 2013) (fig. 5b).

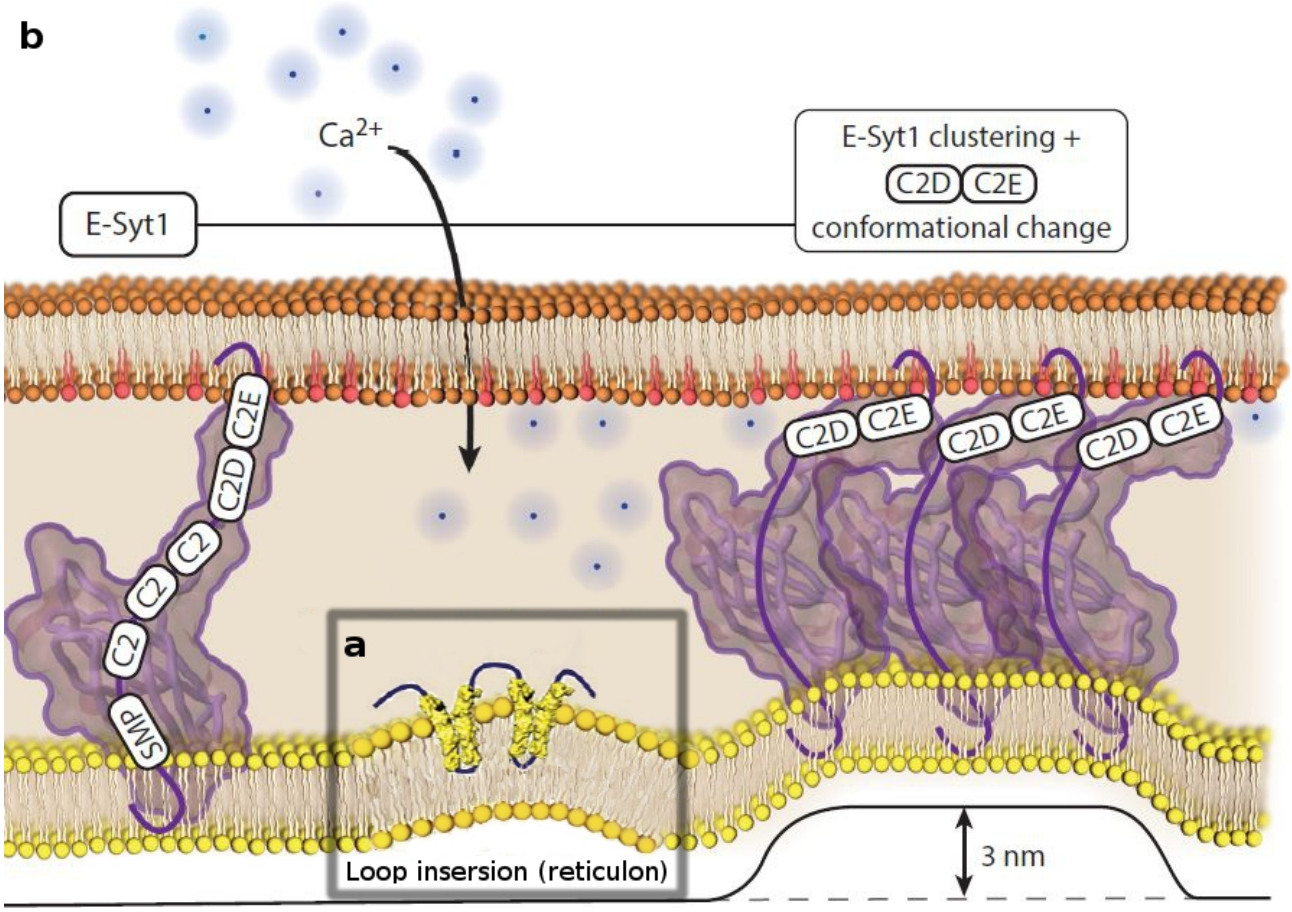

Figure 5: Putative characteristics of MCTPs upon structural analysis. (a) The Transmembrane regions of MCTPs could insert in the ER membrane (*yellow*) in a reticulon-like manner, resulting in specific membrane curvature. (b) Extended-Synaptotagmins (E-Syt) possess multiple C2 domains that can interact with lipids of the plasma membrane (*orange and red*). E-Syt1 forms cluster and undergo conformational changes in response to calcium ion entry in the cytosol, leading to reduction of the gap between the membranes. (from J. Tilsner, W. Nicolas, A. Rosado *et al.*, 2016).

Even if none of the MCTPs features a SMP domain related to lipid transfer (K. Kopec, V. Alva & A. Lupas, 2010; C. Schauder, X. Wu, Y. Sahek *et al.*, 2014), protein association and complex formation, for instance with a receptor-kinase at the PM as shown with QKY (C. Trehin, S. Schrempp, A. Chauvet *et al.*, 2013; P. Vaddepalli, A. Herrmann, L. Fulton *et al.*, 2014), could still coordinate ER-PM crosstalk.

3.2/ The quirks of AtMCTP5 and its kind

AtMCTP5, also named QUIRKY (QKY), is, at this time, the most well known member of the MCTP family. The function of QKY in plant development was uncovered in 2009 (L. Fulton, M. Batoux, P. Vaddepalli *et al.*, 2009) and studied afterward in a tissue morphogenesis context solely (C. Trehin, S. Schrempp, A. Chauvet *et al.*, 2013; P. Vaddepalli, A. Herrmann, L. Fulton *et al.*, 2014). The protein is associated with STRUBBELIG (SUB), an atypical (leucine-rich repeat) receptor-like kinase that regulates intercellular communication during many organogenesis events

such as floral organ shape, stem height and shape, leaf shape and root patterning (D. Chevalier, M. Batoux, L. Fulton *et al.*, 2005; S. Kwak, R. Shen & J. Schiefelbein, 2005; L. Fulton, M. Batoux, P. Vaddepalli *et al.*, 2009; P. Vaddepalli, L. Fulton, M. Batoux *et al.*, 2011).

The discovery of P. Vaddepalli, A. Herrmann, L. Fulton *et al.* (2014) – together with the PD proteome research by L. Fernandez-Calvino, C. Faulkner, J. Walshaw *et al.* (2011) – places the MCTP family onto a new scene. Expression of QKY and SUB tagged with fluorescent proteins in plant showed they co-localizes in PD (P. Vaddepalli, A. Herrmann, L. Fulton *et al.*, 2014). More interestingly, AtMCTP5 is not required for SUB localization and conversely, SUB is not required for QKY localization, but the two proteins are physically interacting at PD. These results imply that even if the two proteins interact, their PD localization rely on individual features. From here, it is engaging to lean on the identification of the PD-targeting domains of QKY. The conclusions of the paper concerning the structure-function of QKY are still uncertain but several ideas arise. First, the C-terminal of QKY is essential for its localization and its PD localization is essential for its function. Secondly, the PRT_C domain containing the TMD might be necessary to anchor the protein to the PM, as the C2-only construct show ER-like patterning. Lastly, solely the C2 domains C and/or D seem important for PD targeting since construct lacking A and B behave similarly to the full length protein in terms of localization. (fig. 6). What P. Vaddepalli, A. Herrmann, L. Fulton *et al.* (2014) did in this research is of great matter, but they did not see QKY as an PD ER-PM MCS tether, and thus did not conducted experiments to investigate the tethering properties of the different mutants.

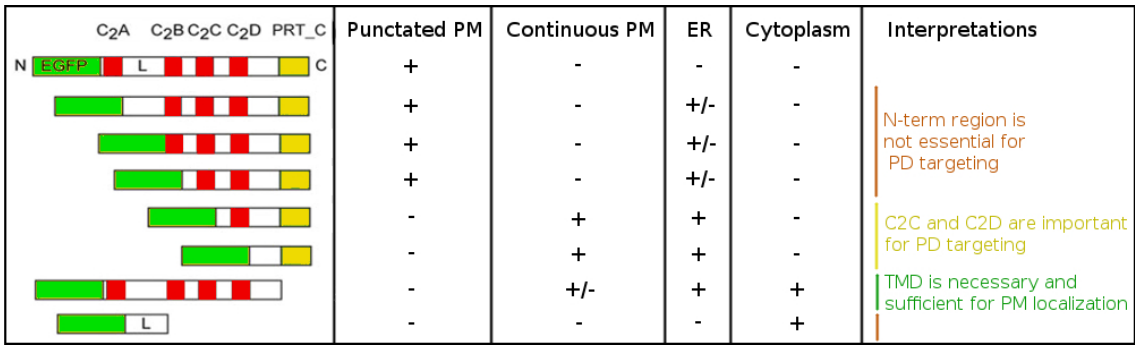

Figure 6: Results of QKY truncated mutant localization in *Arabidopsis* root cells (P. Vaddepalli, A. Herrmann, L. Fulton *et al.*, 2014).

4/ C2 domains touchdown

First we will see how C2 domains are spread across the phylogenetic tree and compose many different proteins. Then we will dress a list of the various functions associated with the C2 domains, in association with amino acid nature and structural composition.

4.1/ General presentation

Pfam database (http://pfam.xfam.org/) gathers more than 50,000 C2 domain sequences in more than 800 eukaryote species (family PF00168). Indeed, C2 domains are among the most abundant eukaryotic lipid-binding domains and act in various cellular mechanisms. The members of the C2 super-family were classified in seven major families: PKC-C2 (**P**rotein **K**inase **C**), PI3K-C2 (**P**hospho**I**nositide **3**-**K**inase), PTEN-C2 (**P**hosphatase and **TEN**sin), AIDA-C2 (**A**xin **I**nteractor, **D**orsalization **A**ssociated), B9-C2 involved in centrosome migration and ciliogenesis, DOCK-C2 which are Rac/CDC42 GDP exchange factors, NT-C2 acting in endocytotic recycling and organelle positioning (D. Zhang & L. Aravind, 2010). C2 domains are ubiquitous units but their low sequence conservation and their presence in so many different structural and functional types of proteins make them difficult to identify from genomic analysis (W. Cho & R. Stahelin, 2006). Their extremely high divergence suggests various ways of interactions.

In mammalians, the PKC-C2, PTEN-C2 and PI3K-C2 families were the most extensively studied so far. They show a wide variety of structural architectures – linked to the nature and sequence of the amino acids that compose the loops and form the binding sites – but quite narrow physiological roles: membrane dynamics and repair (dysferlin) (L. Glover & R. Brown Jr, 2007), vesicular transport and dynamics (synaptotagmins), GTPase regulation (Rabphilin)(T. Südhof, 2004; J. Guillen, C. Ferrer-Orta, M. Buxaderas *et al.*, 2013), tethering for enzymatic domains (PKC, PLC)(A. Newton, 1995; T. Bunney & M. Katan, 2011). The PKC-C2 family being the only family showing calcium-binding capabilities, it is possible that this specific feature appeared with the emergence of vesicular trafficking and membrane repair systems (D. Zhang & L. Aravind, 2010). In yeast, tricalbins – structurally related to E-SYT – have been examined because they are involved in membrane-trafficking processes (C. Creutz, S. Snyder & T. Schulz, 2004; T. Schulz & C. Creutz, 2004).

4.2/ Review of C2 specificities

The conventional C2 domain structure is two face-to-face antiparallel β-sheets with a hydrophobic core. The loops bridging β-strands vary in structure, length and amino-acid composition but the general connectivity follows one of the two existing topologies: the PLC-like variant known as the P-family and the synaptotagmin-like variant called S-family. The main difference is position of the N- and C-termini, close to the calcium-binding region in S-family but at the opposite side in the P-family. However, no significant functional differences have been associated with this classification (E. Nalefski & J. Falke, 1996; W. Cho & R. Stahelin, 2006; S. Corbalan-Garcia & J. Gomez-Fernandez, 2014). The β-sandwich allows the domains to independently fold and be autonomously stable (J. Clark, L. Lin, R. Kriz *et al.*, 1991; B. Davletov

& T. Sudhof, 1993; E. Chapman & R. Jahn, 1994; E. Nalefski, L. Sultzman, D. Martin *et al.*, 1994; T. Yamaguchi, H. Shirataki, S. Kishida *et al.*, 1993)(fig. 7). The C2 domains are one-of-their-kind in the membrane-interacting cluster in the way that they have neither specific nor conserved features that bind lipids. However, two global interacting phenomena have been observed, using two distinct sites: the top loops (associated with calcium coordination, interacting in a calcium-dependent or independent manner) and the shallow depressed cationic β-groove (W. Cho & R. Stahelin, 2006). D. Zhang & L. Aravind (2010) propose that at least one of the two regions is functional in any C2 domain. Identification of charged electrostatic surfaces or exposed hydrophobic residues can help to emphasize on those putative interacting regions (D. Murray & B. Honig, 2002) but there is no simple way to analyze the specificity and/or selectivity of C2 domains interaction. For example, synaptotagmins usually bind anionic phospholipids through non-specific electrostatic interactions (B. Davletov & T. Sudhof, 1993)) while PKCα and PLCδ1 stereo-specifically recognize a lipid headgroup (N. Verdaguer, S. Corbalan-Garcia, W. Ochoa *et al.*, 1999; B. Ananthanarayanan, S. Das, S. Rhee *et al.*, 2002; R. Stahelin, J. Rafter, S. Das *et al.*, 2003).

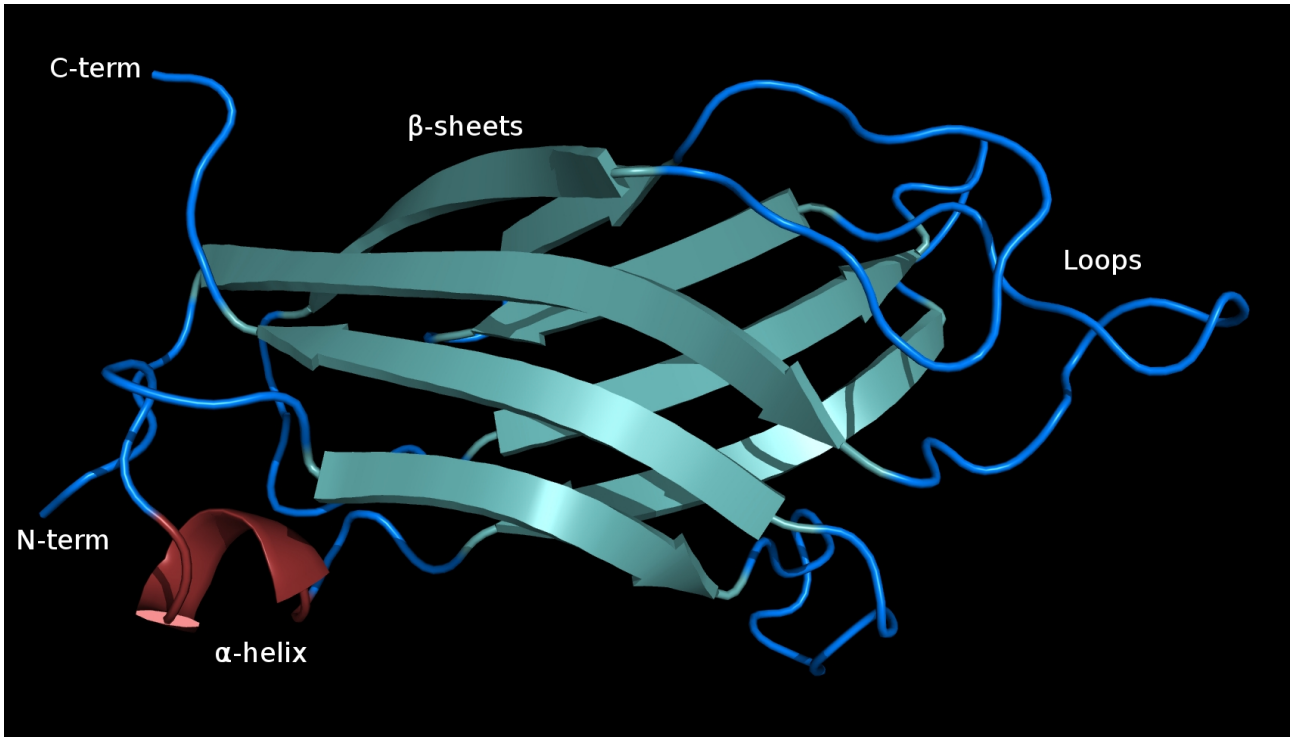

Figure 7: General architecture of a C2 domain. This P-family C2 domain 3D structure illustrates the eight antiparallel β-sandwich in *light blue*, with the loops connecting the β-strands in *marine blue*. Additional secondary structures such as α-helices (*red*) can be found in the loops.

As explained before, there are two sites available for membrane lipid binding, but there are many different modes of interaction. For example, phosphatidylcholine (PC) selectivity is favored by the affinity of tryptophan for the choline head group (W. Yau, W. Wimley, K. Gawrisch *et al.*, 1998; S. Baker, R. Othman & D. Wilton, 1998; M. Gelb, W. Cho & D. Wilton, 1999; S. Han, K.

Kim, R. Koduri *et al.*, 1999); aromatic and aliphatic residues in loops preferentially insert in PC environment because of the low desolvation energy barrier (D. Murray & B. Honig, 2002). W. Cho & R. Stahelin (2006) reviewed all the known C2-lipid interaction: they listed all types of lipids that can be bound to C2 domains with various interaction mechanisms. Angle of membrane approach and ionic gradient can also lead to contrasting selectivity (D. Han, S. Ok-Ho, M. Machius *et al.*, 2004).

The PKC-C2 domains can be calcium-dependent and their function modulated by calcium concentration. The acidic residues (aspartates) and backbone oxygens in the Calcium-Binding Loops (CBL1-3) are usually responsible for the coordination of up to four ions, as directed mutagenesis survey illustrates (M. Medkova & W. Cho, 1998; J. Ubach, X. Zhang, X. Shao *et al.*, 1998; L. Bittova, M. Sumandea & W. Cho, 1999), but the binding properties are not widely conserved because of the expansive primary and tertiary arrangements. For that reason, structural calcium-dependent electrostatic switch analysis (X. Shao, C. Li, I. Fernandez *et al.*, 1997) and/or machine learning tools are needed to go toward calcium-binding sites prediction (D. Murray & B. Honig, 2002; W. Zhou, G. Tang & R. Altman, 2015) if experimental data are not available. Calcium coordination is in some cases enhanced by loops conformational changes (J. Grobler, L. Essen, R. Williams *et al.*, 1996) and/or anionic lipid interaction (X. Zhang, J. Rizo & T. Sudhof, 1998). It is interesting to notice that some calcium binding domains do not interact with membranes but may be involved in protein-protein interactions or trigger protein conformational changes (W. Cho & R. Stahelin, 2006; Y. Saheki & P. De Camilli, 2017). In a general manner, C2 domains that are calcium-dependent, and thus have cationic residues, are more attracted by anionic lipids.

Hydrophobic interaction with the membrane as a result of loop penetration has been observed in some cases. This interaction is favored by the presence of aromatic or aliphatic residues at the extremity of the loops (fig. 8). The penetration depth varies from 6 to 12 angstrom below the phosphate plane and the orientation of the domain during docking is also subject to variation (A. Ball, R. Nielsen, M. Gelb *et al.*, 1999; A.Frazier, M. Wisner, N. Malmberg *et al.*, 2002; N. Malmber, D. Van Burskirk & J. Falke, 2003; S. Kohout, S. Corbalan-Garcia, J. Gomez-Fernandez *et al.*, 2003; S. Malkova, F. Long, R. Stahelin *et al.*, 2005; A. Ausili, M. Berglin, H. Elwing *et al.*, 2013; N. Chon, J. Osterberg, J. Henderson *et al.*, 2015).

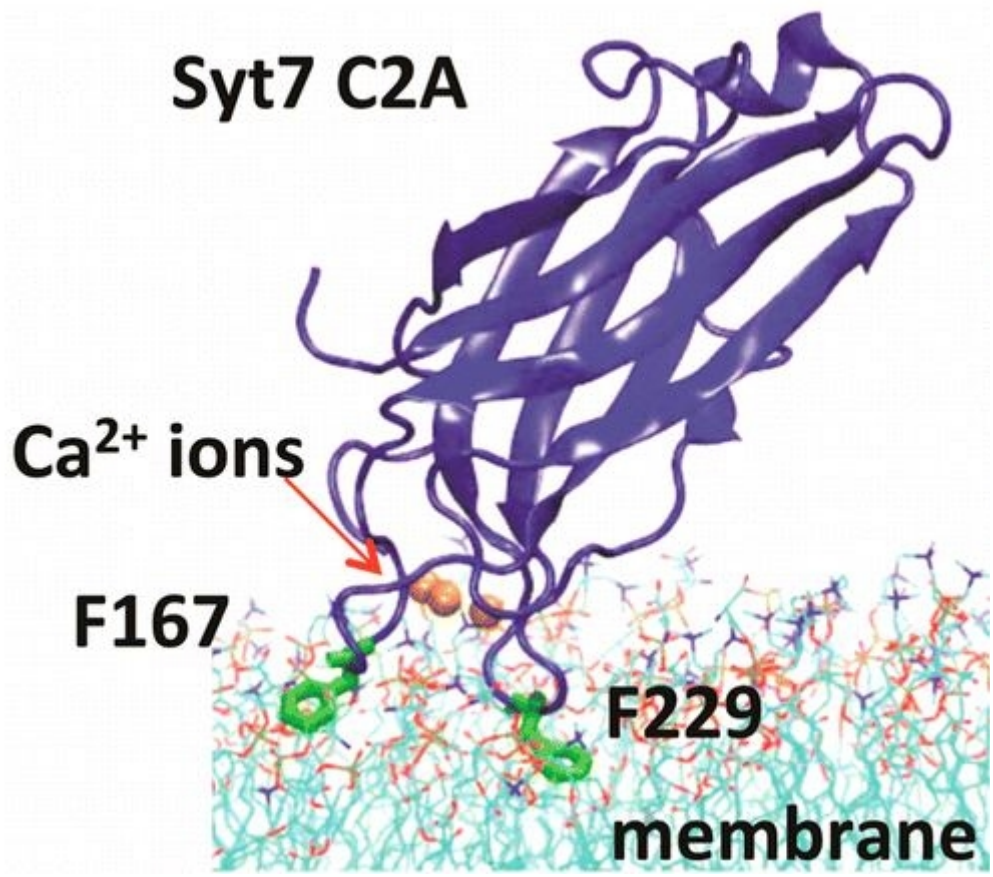

Figure 8: Calcium-dependent-loop-penetrating membrane docking of mammalian SYT7. The membrane penetration is favored by the phenylalanine residues having hydrophobic interactions with the lipid acyl chains. (From N. Chon, J. Osterberg, J. Henderson *et al.*, 2015)

The β-sheet interaction is made by a series of basic and aromatic residues. Indeed, the concavity, also called β-groove, contains a cationic patch of lysine, tryptophan and tyrosine, among others. Two residues in particular are more important: a residue at the beginning of strand 2 and another at the end of strand 5 can interact on the surface of the domain through hydrophobic or aromatic stacking interactions (D. Zhang & L. Aravind, 2010). This region is essential for structural and functional roles, as it can specifically bind phosphatidylinositol bis-tris phosphate (fig. 9), a lipid family involved in key membrane mechanisms (S. McLaughlin & D. Murray, 2005; M. Guerrero-Valero, C. Ferrerota, J. Querol-Audi *et al.*, 2009). The specificity is probably due to a well-defined architecture.

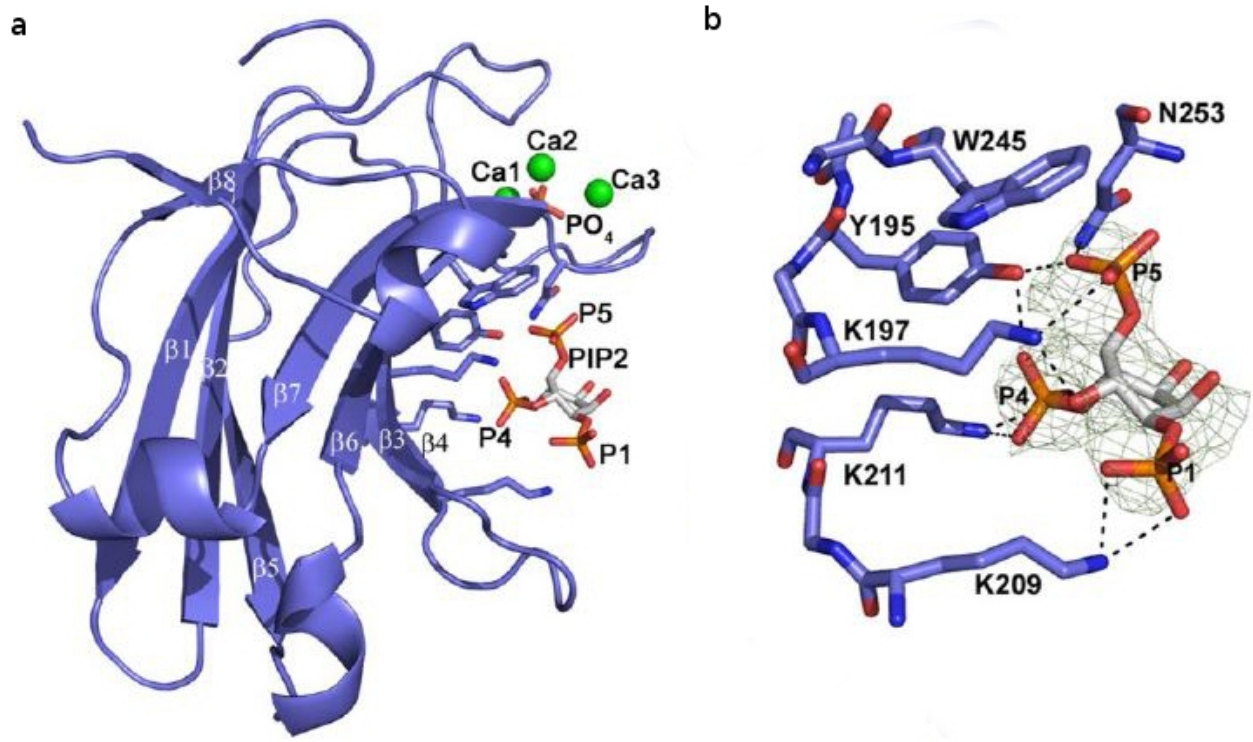

Figure 9: PKCα-C2 interaction with phosphoinositol-4,5-bisphosphate (PIP_2). (a)The β-groove has a lysine rich cluster and specific aromatic residues to interact with the phosphate oxygen atoms. (b) Zoom of the binding pocket.(From M. Guerrero-Valero, C. Ferrerota, J. Querol-Audi *et al.*, 2009)

5/ The power of molecular bioinformatics

Bioinformatics is a rising science as the computational power and improvement of technology are explosively growing since a couple of decades. This science is also very broad as it now touches almost all biological and human-related surveys. Here, we will focus on what we can call “molecular bioinformatics”, which focuses on the understanding of molecular structures and mechanisms.

Besides the experimental exploration, some techniques give atomic-scale resolution of molecule architecture and interactions, which are very interesting informations for unwrapping their roles and functionings.

This chapter aims to explain main tools and concepts that are used in this master thesis for the analysis of C2 domain sequences. Starting with the beginning, one can learn quite some information from raw protein sequence, based on the nature and chaining of the amino acids. Then, based on the fact that sequence and subsequent 3D structure having biological function is better conserved than non-functional sequence, 3D structures of proteins can be built from the primary sequence. Finally, molecular dynamics open the way to the study of molecule's behavior in a more biological environment.

5.1/ What can be learned from a protein sequence ?

Proteins are made of a chain of amino acid linked by peptidic bonds. These units have different properties based on the nature of their side chain: aliphatic, aromatic, polar, charged; and their sequence can be correlated to the secondary, tertiary and quaternary scaffolds. The propensity of each amino acid for a peculiar secondary structure allows us to predict the regions that will be β-strands, α-helices, bends, turns, coils, etc… (D. Buchan, F. Minneci, T. Nugent *et al.*, 2013). One special way to visualize the protein sequence is to use Hydrophobic Cluster Analysis (HCA) representation that allows the highlighting of hydrophobic and polar patches in the sequence (C. Gaboriaud, V. Bissery, T. Benchetrit *et al.*, 1987). The hydrophobic clusters are mainly associated to secondary structures and are often very conserved in homologous proteins (G. Faure & I. Callebaut, 2013), which is interesting for C2 domains analysis/comparison since their have well conserved structure pattern but low sequence similarity.

5.2/ Homology modeling : crossroad between sequence, evolution and structure

With the rise of structural protein data (for example Protein Data Bank (PDB); www.rcsb.org/pdb), genomic data and sequence comparison tools (such as BLAST; http://blast.ncbi.nlm.nih.gov) together with the increase of computer calculation power, homology modeling became an easy and common way to build 3D models from primary sequence and homologous templates when the experimental 3D structure is not available. Indeed, it is possible to determine the structure of a protein if the structures of homologous proteins (from ~30% sequence identity) are experimentally determined (by X-ray or NMR) with enough resolution. Several servers and softwares are available to perform this task, with more or less accuracy (K. Arnold, L. Bordoli, J. Kopp *et al.*, 2006; B. Webb & A. Sali, 2014). If templates with enough sequence similarity cannot be found, other servers offer 3D building using a mix of techniques, such as threading, *de novo* folding and molecular dynamics (MD) (D. Kim, D. Chivian & D. Baker, 2004; http://robetta.bakerlab.org).

Resulting models have to be looked with a critical point of view and tested for their validity. Usually, researchers examine if the overall structure of the model (N. Guex & M. Peitsch, 1997; The Pymol Molecular Graphic System, Version 1.8 Schrödinger, LLC; W. Humphrey, A. Dalke & K. Schulten, 1996), the energy (M. Wiederstein & M. Sippl, 2007) and Ramachandran plot (G. Ramachandran, V. Ramakrishnan & V. Sasisekharan, 1963) seem accurate. The final verification is to test stability over time by few steps of MD (see below).

MD are a very powerful tool to study molecular behaviors and interactions. The molecule is represented by spheres or beads (atoms or groups of atoms depending on the method) of specific mass, size and properties that follow Newton equations in a 3D system. The atoms are connected by bonds which follow the classical physics of springs. Position and speed of the beads at each time step of the simulation give a trajectory of the molecule in the system during a chosen period of time.

The different types of interactions and their parameters are sorted out of experimental data and quantum mechanics calculations. The force field is defined by all the equations applied on the system that mimic the natural interactions and environment of the atoms and allow potential energy calculation. There are then two types of interactions in MD: bonded interactions, defined by bond length, angles and dihedral angles and non-bonded ones, like electrostatic and Van Der Waals interactions. It is interesting to note that the Born-Oppenheimer approximation, which states that electronic and nuclear motions can be separated, gives us the possibility to only consider the nuclei movements during the simulations. Dealing with nuclei as defined particles, and thus working with partial charge, allows a great gain of time. However, it also results in the impossibility to simulate covalent bond reorganization nor changes in partial atomic charges. The potential energy of all those interactions is used to calculate the force applied on each atom and thus the trajectory by the mean of classic physics of particle equations. The initial speed is randomly attributed from the Maxwell-Boltzmann distribution based on system temperature.

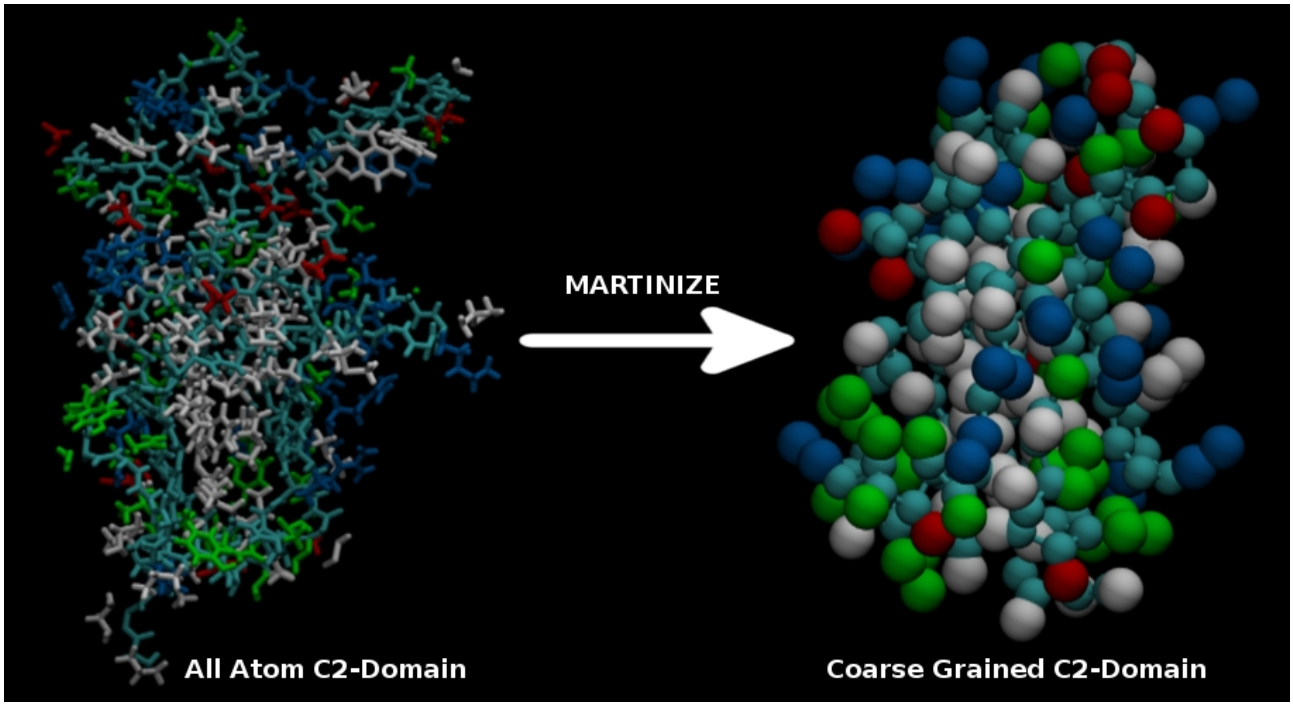

Figure 10: Coarse grained transformation of a C2 domain using MARTINI. Cyan color represent the backbone of the domain. The side chain colors correspond to the residue properties: blue for basic residues, red for acidic, green for polar and white for apolar.

As the atomistic simulations of protein membrane docking represents a considerable amount of computational time, the use of coarse grained (CG) force field are usually considered (M. Chavent, A. Duncan & M. Sansom, 2016). MARTINI is a CG force field that consists of gathering four atoms (hydrogens are not taken into account) into one particle we call bead (S. Marrink, H. Risselada, S. Yefimov *et al.*, 2007; X. Periole & S. Marrink, 2013) Each bead is characterized by a mass, charge, type and position. This approximation allows to simplify each amino acid residue into one to five beads and thus longer time-scale simulations can be performed (fig. 10). To give an illustration, the same system on the same computer would take two weeks for a 250ns in all atom simulation whereas 2,5µs run of CG would take only 28 hours. Of course the CG doesn't give the resolution to identify specific atomic interactions, but the method is still very interesting to distinguish behaviors and docking sites. A very interesting fact is the possibility to reverse the coarse grained system back into all atom after the docking, allowing a further dynamic study of the molecular system (T. Wassenaar, K. Pluhackova, R. Böckmann *et al.*, 2014).

5.4/ Molecular Dynamics of C2 domains

A few MD simulations have been performed on C2 domains already but, to our knowledge, only in mammalian. (L. Banci, G. Cavallaro, V. Kheifets *et al.*, 2002; D. Manna, N. Bhardwaj, M.Vora *et al.*, 2008; C. Lai, K. Landgraf, G. Voth *et al.*, 2010; N. Chon, J. Osterberg, J. Henderson *et al.*, 2015). They mainly focus on the specific calcium-dependent interactions of Protein Kinase C α and β with anionic lipids such as phosphatidylserine and phosphatidylinositol bis or trisphosphate (L. Banci, G. Cavallaro, V. Kheifets *et al.*, 2002; D. Manna, N. Bhardwaj, M.Vora *et al.*, 2008; C. Lai, K. Landgraf, G. Voth *et al.*, 2010). SYT7 C2 domain docking in calcium-dependent manner was also studied (N. Chon, J. Osterberg, J. Henderson *et al.*, 2015). In all cases, the proteins were known *a priori* to interact with membranes lipids in the presence of calcium. For this reason, the simulations were performed with membrane-docked structures as initial states and carried out on few hundreds of ns at most.

Objectives

The objective of our work was to investigate the potential docking of the individual C2 domains of MCTPs on the PM, at a molecular level using molecular bioinformatics approaches, to decipher the role of MCTP proteins in the ER-PM membrane tethering, in the context of PD function.

The primary goal was to accurately define the C2 domains from the MCTP sequences (sequence analysis), then, 3D models needed to be built for each individual C2 domain (structure homology) for further structure-function analysis. The prediction of the ability of the C2 domains to interact with the plant PM was one of the main objectives of this work. This question was investigated using MD. The second main objective was the evaluation of C2 domain's specific binding sites (calcium, PIP). Finally, *in vivo* and *in planta* co-localization of MCTP truncated mutants using fluorescence microscopy was performed to complement MD and reveal the role of the C2 domains for the PD localization.

Methodology

1/ Primary sequence analysis and C2 domain delimitation

Since C2 domains are highly variable, prediction of C2 domain localization in proteins, including MCTPs, from databases such as Pfam (http://pfam.xfam.org/) are quite approximate. Refining the C2 domains delimitation is hence mandatory.

The analysis was carried out with AtMCTP5 (QKY) of *Arabidopsis thaliana* and NbMCTP11 of *Nicotiana benthamiana*, since QKY is already identified in literature, both are localized in PD and NbMCTP11 is used experimentally in the Bordeaux's lab. The process is an integrative combination of several bioinformatics tools available on internet. Pfam domain recognition output from BLASTp (https://blast.ncbi.nlm.nih.gov/Blast.cgi) on the full protein shows approximate localization of the C2 domains. Combination of secondary structure prediction (PSIPRED; http://bioinf.cs.ucl.ac.uk/psipred/; D. Buchan, F. Minneci, T. Nugent *et al.*, 2013) and hydrophobic cluster analysis (HCA; http://mobyle.rpbs.univ-paris-diderot.fr/cgi-bin/portal.py?form=HCA#forms::HCA; C. Gaboriaud, V. Bissery, T. Benchetrit *et al.*, 1987) allowing to better define structured domains (L. Lins, A. Couvineau, C. Rouyer-Fessard *et al.*, 2001) provides stronger and more accurate predictions of the delimitation of each C2 domain.

PSIPRED can predict the strands with high accuracy by using PSI-BLAST based feed-forward neural network. The information of PSIPRED output is then merged to the HCA output to better define functional domains. Hydrophobic Cluster Analysis (HCA) is a specific visualization of a protein sequence. Figure 11 explains how HCA is made: the sequence is wrapped around a cylinder (fig. 11a), which is then opened (fig. 11b) and duplicated (fig. 11c) to restore all the neighbors of each amino residue. A code is used to have an immediate view of the clusters and their properties (fig. 11d) (red for negatively charged, blue for positively charged, green and contoured for hydrophobic, red star for Proline, black diamond for Glycine, black frame for Threonine and dotted black frame for Serine) (see fig. 15 for colors).

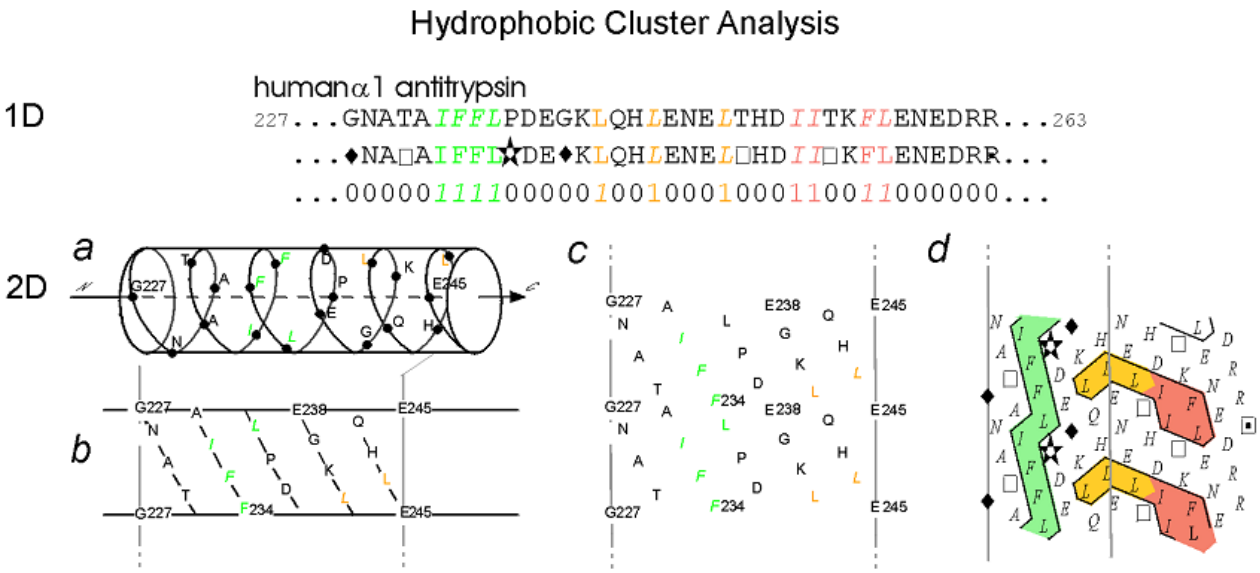

Figure 11: Hydrophobic Cluster Analysis. http://mobyle.rpbs.univ-paris-diderot.fr/cgi-bin/portal.py?form=HCA#forms::HCA

The 17 members of *Arabidopsis thaliana* MCTP family, gathering 59 C2 domains, were dissected by this protocol. In a first step, classical alignment using Clustal Omega (http://www.ebi.ac.uk/Tools/msa/clustalo/) of the members allowed the segregation of the C2 into so-called "sub-families": short (three C2) and long (four C2) MCTPs. The short ones seem lacking the first C2 domain, whereas the C2B-C-D (three next C2 domains) are conserved in all members (except AtMCTP3). Then, this multiple sequence alignment, which gives a more global view and a point of comparison with QKY is used as additional support for the C2 domain delimitation refining. The resulting refined alignment is also referential to predict/verify putative key amino-residues involved in docking and/or calcium coordination (Annexe 2).

2/ Homology modeling

For homology modeling, each domain first served as input in the SWISSMODEL web server (https://swissmodel.expasy.org/) (K. Arnold, L. Bordoli, J. Kopp *et al.*, 2006) for template search against the PDB databank containing known 3D structures. SWISSMODEL uses a combination of BLASTp (Basic Local Alignment Sequence Tool) and HHblits (HMM-HMM-based lightning-fast iterative sequence search) for alignment with PDB templates. In order to enhance the quality of the model, several templates were picked, based on different criteria: full sequence coverage, highest identity percentage (minimum 25%), no ligand interactions and the best resolution for templates. Next, T-COFFEE multiple structural alignment (http://tcoffee.crg.cat/) was carried out between the MCTP C2 sequences and the chosen templates. This alignment was then manually adapted to be used as input for MODELLER (B. Webb & A. Sali, 2014).

MODELLER is a modeling software allowing to generate 3D models based on alignment of the protein under investigation with known templates. It is based on the satisfaction of spacial restraints by which a set of geometrical criteria are used to create a probability density function for the location of each atom in the protein.

It uses different python scripts: the model_mult.py script was used with the alignment file (.ali) of the sequence of interest along with the sequences and the 3D structures of the templates (.pdb) as input. The program calculates several models (.pdb) and also gives a general "process" file (.log). The molpdf score associated with each model, at the end of the .log file, sums the restraints of the molecule and thus informs us about the model quality. The best-score models were quality checked with the PROSA-WEB server (https://prosa.services.came.sbg.ac.at/prosa.php; M. Wiederstein & M. Sippl, 2007), which provides energy-related information along the primary sequence for the 3D construct. This server gives three kind of information: the z-score indicates overall model quality, the plot residue score gives local knowledge-based energy levels and interactive molecule view of the 3D structure, with colors associated to residue energy. The presumably most accurate model (from the scores and the 3D viewing) was screened for local energetic problems using the plot of residue scores. This plot has two Y zones: the negative values is low energy and thus assumed stable whereas the positive values usually correspond to problematic parts of the model. There are also two lines, corresponding to two different ranges of smoothing. The bold line averages energy on 40 residues and the fine line averages on 10 residues. The goal fixed here was to keep the bold line under 0 and have the less peaks possible above 0 for the fine line. The script loop_refine.py recalculates a specified region of the chosen model. The outputs are the same: .pdb files for the models, and a .log with the molpdf scores. The process was performed as many times as necessary, until few acceptable models are found. Those models were then visualized and Ramachandran plots were made using the Swisspdbviewer software (N. Guex & M. Peitsch, 1997) to choose the model fitting the spatial restraints at best (Annexe 1).

Finding no model satisfying structural quality led us to use the automated ROBETTA server (http://robetta.bakerlab.org/; D. Kim, D. Chivian & D. Baker, 2004), which calculates models by cutting the protein into fragments then using complementary approaches such as homology, threading, *de novo* folding and MD to generate the full model. This tool performs well but is however time-consuming.

3/ Molecular dynamics

All the MD calculations were performed using GROMACS (M. Abraham, T. Murtola, R. Schulz *et al.*, 2015) in a Linux environment. Practically, there are several steps before the actual simulation. The first input file commonly used is the .pdb file, here the selected model. The

topology of the models (.top and .itp files), meaning the ensemble of parameters and equations that will be used to describe these molecules for a given force field, have to be settled. Then, a box is defined around these molecules and solvent and ions are added to the system. Once the system is complete, energy minimization serves to lead the system in a more stable state by removing the steric clashes and inappropriate geometry. Non-restrictive box sides are used during the simulations: an atom trespassing one side will continue its trajectory from the opposite side. A first simulation is then done with atomic position restraints on the studied molecule, to allow the water and ions to rearrange around it, and to set up the system to the wanted pressure and temperature. This step is called equilibration. Lastly, the main simulation run (called production) can be launched for the wanted period of time, typically in the order of nanoseconds, as one time step of simulation is in the order of few femtoseconds. All those commands are usually encoded in a home-made linux bash script and the Gromacs parameters are written in specific files (.mdp). Before each run (minimization, equilibration, production), the grompp command compiles the structure, topology and parameters into one file (.tpr). Without going into much details, the main outputs of a simulation are the system at the last step (.gro) and the compressed trajectory file (.xtc).

Every energy minimization step is following the steepest descent algorithm (intergrator=steep). In atomic simulations, the electrostatics are set on fast smooth Particle-Mesh-Ewald (PME) (T. Darden, D. York & L. Pedersen, 1993) (coulombtype=pme), with a Coulomb cut-off of 1.0 (rcoulomb=1.0). For GPU acceleration of the calculations, Verlet cutoff scheme was used. The protein equilibration was done using an isotropic Berendsen exponential relaxation pressure coupling, to efficiently scale the box. The reference temperature for coupling was set to 300K. The constraint algorithm used was LINCS (LINear Constraint Solver) (B. Hess, H. Bekker, H. Berendsen *et al.*, 1997). The general time-step was 2 femtoseconds. The equilibration lasted 1000ps. To verify the stability of the previously made models, the production runs were simulated for 50ns in basic solvent system (water, sodium and chlorine ions). This is what will be called “stand-alone” simulations hereafter.

In a general manner, the .gro and .xtc outputs are loaded into the VMD (Visual Molecular Dynamics) software (W. Humphrey, A. Dalke & K. Schulten, 1996) to have a first look at the simulation and spot potential issues.

The evaluation of the stability of the protein structure is drawn from the Root Mean Square Deviation (RMSD) and the Root Mean Square Fluctuation (RMSF) graphs. The first one is a calculation of the deviation of the global protein structure (typically, only the alpha carbons of the backbone are used), based on a fit with an initial structure, over time (formula below). The second is doing the same calculation but each amino acid residue deviations are summed up for the whole simulation, giving the protein sequence as x axis instead of time.

$$RMSD = \sqrt{\frac{1}{N}\sum_{i=1}^{N}(x_{ci} - x_{di})^2 + (y_{ci} - y_{di})^2 + (z_{ci} - z_{di})^2}$$

Secondary structures of the domains can also be analyzed using the DSSP algorithm (W. Kabsch & C. Sander, 1983). Plots can be made to study the stability of the protein secondary structure over the entire simulation.

4/ Calcium-binding sites prediction

When the model is stable as assessed by MD, calcium binding sites can be predicted. For known C2 domains, the binding site is made by a cluster of aspartate residues located on connective loops (J. Xu, T. Bacaj, A. Zhou *et al.*, 2014; S. Corbalan-Garcia & J. Gomez-Fernandez, 2014). Such a cluster was first visually checked: this gives a clue on the promising candidates before going more thoroughly in the prediction.

The prediction is based on three distinctive steps: machine learning algorithm, statistic R script and MD.

First, the machine learning FEATURE, together with the 2015 CALCIUM MODEL (W. Zhou, G. Tang & R. Altman, 2015), was used for high resolution calcium-binding site prediction. The algorithm scores each cell of a 3D 0.48Å grid based on calcium-binding features and micro-environments of known (PDB) structures. The grid was set up across the system with a home-made python script.

Next, the R script identifies the list of potential calcium sites with the scores of the grid points.

The last step is a verification of the coordination strength in a MD stand-alone system with 50mM of Ca^{2+}. Identified calcium-binding sites are furnished with calcium ions and two equilibration steps of 1ns were performed: the first one with restraints on protein and calcium positions and the second one on protein alpha carbons and the calcium ions. The second one allow the side chains to rearrange and possibly coordinate the Ca^{2+}. Finally, a 50ns run was done without any restraints, to see whether the calcium ions stay in place or not. The mobility of the ions was assessed by calculating the distance between the coordinates of the ion at each frame and the coordinate points of its initial localization using MDAnalysis.

5/ Atomistic membrane building using Charmm-Gui

The atomistic membrane bilayer was built on Charmm Gui web server (http://www.charmm-gui.org/). Chosen options were Heterogeneous Lipid building in rectangular box to add 256 lipids. Two lipids were used, based on the SYT7 C2A docking work (Chon et al, 2015) and adapted to

plants membrane composition: 1-palmitoyl-2-linoleoyl-3-phosphatidylcholine (PLPC) and 1-palmitoyl-2-linoleoyl-3-phosphatidylserine (PLPS) in a PLPC-3:1-PLPS ratio (96/96 PC for 32/32 PS). System was neutralized with 0.1M NaCl using the Monte-Carlo ion placing method.

The Charmm Gui membrane system was made to be used in Gromacs. Parameter files (.mdp) from Charmm Gui output were used to perform the sequential equilibration steps needed for the membrane stability before the insertion of the protein. For this, the Charmm36-nov2016 (J. Huang & A. Mackerell Jr, 2013) force field and the TIP3P (W. Jorgensen, J. Chandrasekhar, J. Madura *et al.*, 1983) water model were selected in Gromacs v5.0.. Once equilibrated, the membrane was simulated in stand alone for 50ns using the production .mdp file provided by Charmm-Gui.

6/ Atomistic membrane docking simulations

The building of the pre-docking system, i.e. the manual placement of the C2 domain above the stable membrane, was performed manually using PyMol (The PyMOL Molecular Graphics System, Version 1.8 Schrödinger, LLC). First, water and ions were removed. The C2 domains were placed with the loops of the non-termini side downwards, facing the lipids. Z axis of resulting .pdb file was increased so the box was large enough to contain the two objects and the protein wouldn't be able to interact with both layers at the same time (because of the periodic boundaries). The scp (H. Berendsen, J. Postma, W. van Gunsteren *et al.*, 1981) water model was used for solvation. Note that the Van Der Waals radius of the carbon atoms was artificially increased to 0.5 to prevent the water molecules to be inserted inside the bilayer. The radius was then set back to initial value right after solvation. Na^+/Cl^- ions were added to neutralize the system. Three sequential equilibration steps were needed after the minimization: NPT with lipid restraints so solvent can equilibrate first with no membrane deformation, NVT and NPT (see below). The production run was launched for 250ns. To see if the systems were having the same behavior, two repetitions were done.

The equilibration step is performed in two distinct phases. The first one is the NVT, for constant Number of particles, Volume and Temperature, to stabilize the temperature of the system. The second one is conducted to stabilize the pressure and density of the system. Its name is NPT, for constant Number of particles, Pressure and Temperature.

7/ Martini CG transformation, ElNeDyn and stand-alone dynamics

The martinize.py scprit was used to transform the protein from atomic representation to coarse grained (CG) representation of the MARTINI force field (S. Marrink, H. Risselada, S. Yefimov *et al.*, 2007; X. Periole & S. Marrink, 2013), rendering the system less complex and enabling longer simulations to study the docking mechanisms. The script clusters 4 heavy atoms into one bead with assigned properties (fig. 12), making for example a two beads CG valine (one

for the backbone, one for the side chain) from a 7 atoms atomistic valine.

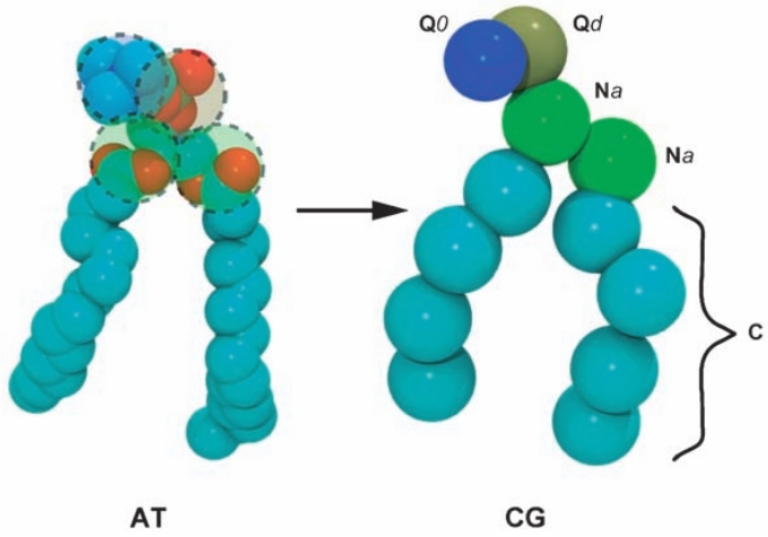

Figure 12: Atomistic to CG representation of phosphatidylcholine. (S. Rouse, T. Carpenter & M. Sansom, 2010)

The clustering of atoms into beads leads to the loss of secondary structures, notably because hydrogen bonds are not represented. To avoid deconstruction of the protein, ElNeDyn – for Elastic Network Dynamic – is used to constraint the secondary structure of the atomic protein onto the CG scaffold (X. Periole, M. Cavalli, S. Marrink *et al.*, 2009). Manual modifications of this network can be done to improve the mimetic of the natural molecule, for example to restrain β-strands and α-helices and set free loops (C. Globisch, V. Krishnamani, M. Deserno *et al.*, 2013). In order to optimize the network, amino acid residues involved in stable β-strands or α-helices secondary structures were listed based on the atomic simulation DSSP plot. Then, the protein .itp file was modified by hand, removing every elastic that binds a non-listed residue.

Classic stand-alone simulations (50ns run) on the "free loops" CG domains were necessary to verify two things: first the stability by calculating RMSD, secondly the recovery of the natural behavior of the protein (RMSF comparison with the atomic simulations) (Annexes 3 & 4).

8/ INSANE and CG membrane docking simulations

The membrane bilayer is also made in CG style, using INSANE script (T. Wassenaar, H. Ingolfsson, R. Böckmann *et al.*, 2015). The python script insane.py was used on the martinized protein. The -dm option sets the distance between the protein mass center and membrane. Placement of the protein in the chosen conformation (non-termini side loops downward) was done using the editconf gromacs command before the bilayer addition. Insane added 288 lipid molecules (108/108 PLPC for 36/36 PLPS) to fill the box in the XY plane (fig. 13).

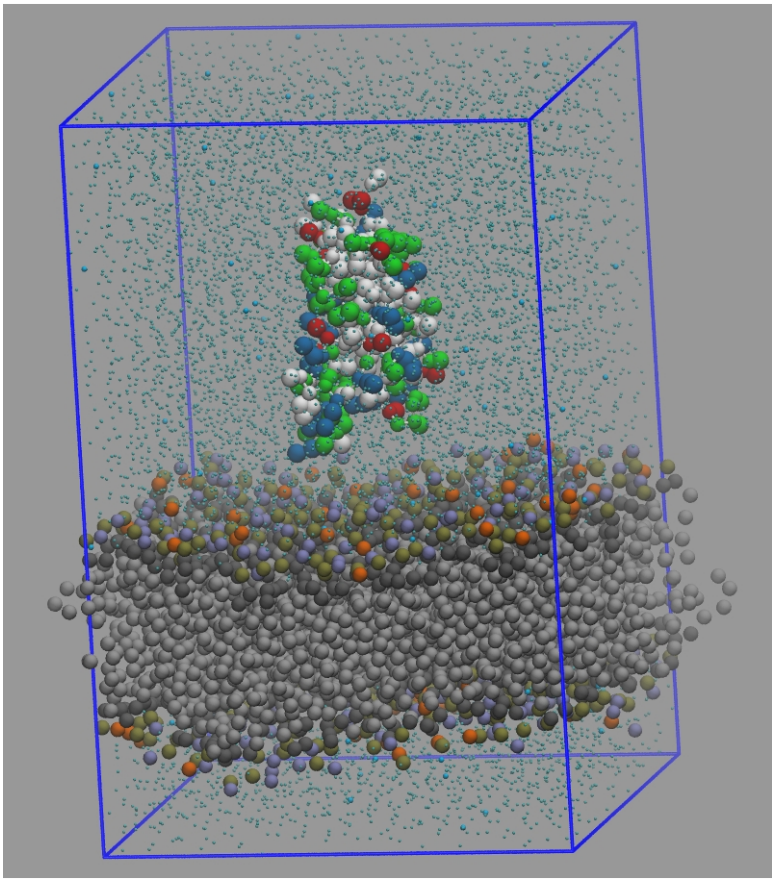

Figure 13: System set up for CG simulation. The box around the system is highlighted in *blue*. The water is represented with small *cyan* beads and the sodium ions in larger *cyan* beads. The protein is positioned above the membrane bilayer, non-termini loops facing down. The residue color is consistent to their nature: *blue* for basic, *red* for acidic, *green* for polar and *white* for apolar. The acyl chains of the lipids are in *light gray* and the glycerol beads in *dark gray.* The phosphate beads are in *khaki*, choline beads in *iceblue* and serine beads in *orange*.

Na^+/Cl^- neutralization and docking simulations were launched on the established system. Coulomb_type was set to “reaction-field” (I. Tironi, R. Sperb, P. Smith *et al.*, 1995). Because of the presence of the membrane, the coupling is set to semiisotropic Berendsen (H. Berendsen, J. Postma, W. van Gunsteren *et al.*, 1984) during equilibration and semiiisotropic Parrinello-Rahman (M. Parrinello & A. Rahman, 1981) for production. The time-step is 10 femtosecond in CG force field. Equilibration was done in 500ps. Production run was 2.5 microseconds. Each simulation was repeated four times

Resulting trajectories were visualized on VMD to analyze whether or not the domain was interacting with the membrane lipids.

9/ Adding PIP4 in the system for specific interaction analysis

Additional simulations were done in the case of NbMCTP11 C2D domain using the docked system as input and by adding one or five PIP4 (phosphatidylinositol-4-phosphate) per leaflet, replacing one or five PLPC molecules. PIP4 topology file was made by manually modifying the 1-palmitoyl-2-oleoyl-3-(phosphatidylinositol-3,4-biphosphate) (POP2) available in martini topology. The PLPC molecules to be replaced were chosen in a clear area of the leaflet, quite far from the protein, using VMD. The replacement itself occurred in the input .gro file.

No equilibration step was needed here after the minimization since the system was taken from a previous simulation and no major modifications were done. Four repetitions were also performed with the same parameters as the docking.

10/ Reverse CG to atomistic

The reverse or backward process (T. Wassenaar, K. Pluhackova, R. Böckmann *et al.*, 2014) consists of mapping back atoms from a CG system. The initram.sh script follows a series of steps. The first step uses the backward.py script, which takes the mapping information (.map files) of each molecule to distribute the atoms along the molecule topology (fig. 14*middle*). The .map file allocates the atoms coordinates in the given order and following the center of mass indicated by the named beads (fig. 14*left*). Performing backward on a protein is different in the way that the backbone and side chains conformations of the amino residues are known (angles, distances) and used to recover the atomic structure. The other steps of the initram.sh script are minimization and equilibration processes, which allow the system to evolve in correct atomic positions (fig. 14*right*).

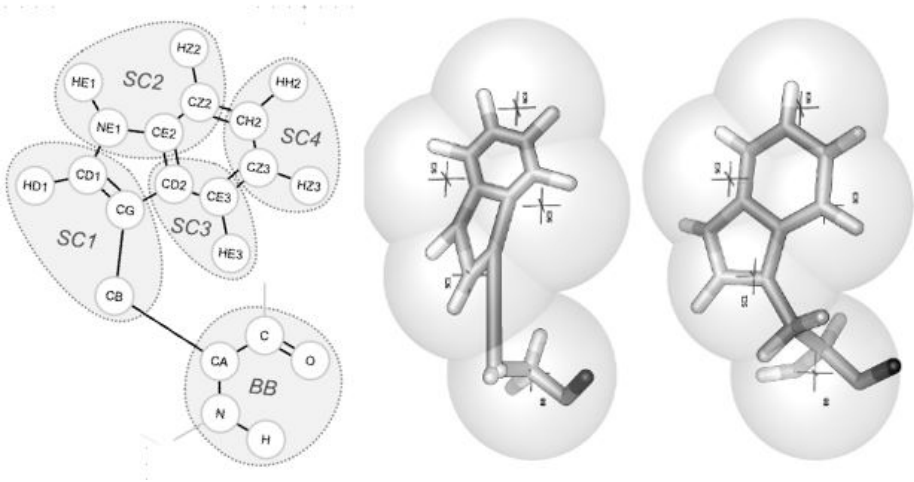

Figure 14: CG to atomistic representation of tryptophan. *Left*, atomistic structure and associated CG beads. *Middle*, atomistic structure after "backward". *Right*, atomistic structure after initram minimization steps. (S. Rouse, T. Carpenter & M. Sansom, 2010)

The command calling for initram also join a .gro file of the CG system to be reversed and the topology file gathering the atomic molecules of the system. In this work, the reverse was done in Gromos force field with the option -to gromos. It is important to note that the reverse must be done in Gromacs v4.6.. .

After the system was reversed back in atoms, minimization, NVT and NPT equilibration and production runs were done, in order to allow the rearrangement of the interaction and verify its stability. The NVT run was 100ps, the NPT 1ns and the production run was 25ns.

11/ CG membrane properties

The area per lipid (APL) is a characteristic of every membrane. It is dependent on the membrane composition and temperature, among other external elements. The Gromacs command "gmx energy" allows to get the XY dimensions of the simulation box for each time frame during every simulation. The total area of the box was then divided by half the total number of lipids (i.e. the number of lipids of one leaflet) to obtain the APL.

The membrane thickness was calculated with MDAnalysis (see below).

12/ MDAnalysis

MDAnalysis is an object-oriented Python library used to analyze MD trajectories (http://www.mdanalysis.org/; N. Michaud-Agrawal, E. Denning, T. Woolf *et al.*, 2011; R. Gowers, M. Linke, J. Barnoud *et al.*, 2016). It was used here to extract several informations from the CG simulations.

The membrane thickness was extracted from each frame of the simulation trajectories by subtracting the Z position of the center of geometry of the phosphate from the upper leaflet by the Z position of the center of geometry of the phosphate from the lower leaflet.

In order to translate the trajectory into a simpler graph to analyze the docking dynamics, the minimal Z position of the C2 domain relative to a phosphate plane was calculated for each frame. This position and the Z position of the phosphate plane were normalized to the center of geometry of the complete membrane, so the output graph would be easier to read: the center of the membrane hence corresponds to y = 0.

The unwrapping of the information concerning the quantity and nature of the interactions was also carried out using MDAnalysis. First, we recorded the global number of interactions of every charged or polar amino acid (lysine, histidine, arginine, aspartate, glutamate, serine, threonine, asparagine, glutamine), for each simulation. The count increases each time the terminal bead of these residue types were located in a radius of 5 angstroms around the lipid polar head

beads (choline, serine or phosphate). The same method was used to quantify the PIP4 interactions, with the 5 angstrom radius around either of the two phosphates. To reveal which particular residue was involved in the interactions, we dissected the recording of the salt bridges by counting their number involving individual amino acids, chosen on the basis of trajectory visualization.

After merging the four trajectories, centering and fitting the rotation and translation of the β-skeleton of the protein, PIP4 positions were analyzed using a python script and MDAnalysis tools. The PIP4 isosurfaces were calculated with a 3D density grid correlated with the occurrence of PIP4 molecules at each point (as in C. Arnarez, S. Marrink & X. Periole, 2013). VMD software was used to translate the density into isosurfaces. The PIP4 bulk density was calculated from the protein-free leaflet.

13/ Transient expression of MCTP constructs and Confocal Microscopy

For transient expression in *N. Benthamiana*, leaves of 3 weeks-old plants were pressure-infiltrated with GV3101 *Agrobacterium* strains, previously electroporated with the relevant binary plasmids. Prior to infiltration, agrobacteria cultures were grown in Luria and Bertani medium with appropriate antibiotics at 28°C for two days then diluted to 1/10 and grown until the culture reached an OD_{600} of about 0.8. Bacteria were then pelleted and resuspended in water at a final OD_{600} of 0.3 for individual constructs, 0.2 each for the combination of two. The ectopic silencing suppressor 19k was co-infiltrated at an OD_{600} of 0.15. The infiltration itself was performed by making a puncture on the abaxial face of the leaf. Then, a 1mL syringe is used to infiltrate the agrobacteria solution on the same side while maintaining a pressure with a finger on the other side of the leaf. Agroinfiltrated *N. benthamiana* leaves were imaged 3-4 days post infiltration at room temperature using a confocal laser scanning microscope Zeiss LSM 880 equipped with fast AiryScan using X63 oil lens. For that ~ 2 cm leaf pieces were removed from plants and mounted with the lower epidermis facing up onto glass microscope slides. For GFP and YFP imaging, excitation was performed with 2-8% of 488 nm laser power and fluorescence emission collected at 505-550 nm and 520-580 nm, respectively. For RFP and mCherry imaging, excitation was achieved with 2-5% of 561 nm laser power and fluorescence emission collected at 600-650 nm. For co-localisation sequential scanning was systematically used to avoid cross-talk contamination.

Results

PART 1 : QUIRKY/AtMCTP5 analysis

This first part aims at establishing protocols for sequence analysis, homology modeling and MD for predicting C2 domains and their potential lipid binding properties, using the well known AtMCTP5/QKY from *Arabidopsis thaliana*. Indeed, bioinformatics analysis of the MCTP family in plants was never performed before. An accurate protocol needs to be set up in order to facilitate further analysis on other MCTPs and support future research.

1/ C2 domain delimitation

The C2 domain identification and delimitation was done by using a combination of several bioinformatics tools. Since it is known that C2 domains have a conserved β-sheet structure, secondary structure prediction was appropriate to locate the 8 β-strands along the protein sequence. HCA (C. Gaboriaud, V. Bissery, T. Benchetrit *et al.*, 1987) allows to spot very rapidly the patterns in the sequence but not the secondary structure in a precise way. The combined use of both PSIPRED, which allows accurate secondary structure prediction (D. Buchan, F. Minneci, T. Nugent *et al.*, 2013), and HCA is perfect to have a quite complete information from the protein sequence alone, granting a precise delimitation of every of the four C2 domains out of the full length protein (fig. 15).

The average length of the C2 domains is around 130-140 amino acids, as for mammalian C2 domains (W. Cho & R. Stahelin, 2006). Note that the C2C domain of QKY is peculiar since the last loop is very long and composed of almost only glycine residues (fig. 15).

2/ Homology modeling

Homology modeling is a very common technique to predict the 3D structure of a sequence from related established structures (review in J. Kopp & T. Schwede, 2004). The sequence of each delimited C2 domain was aligned to known C2 domains from the PDB (Protein DataBank), containing experimental structures. Those PDB structures are defined as templates for the homology modeling.

Hereafter is a summary table of the chosen PDB templates for each domain, after running the SWISSMODEL template search (K. Arnold, L. Bordoli, J. Kopp *et al.*, 2006).

Domain	Template name	PDB – ID	% identity
C2A	Munc 13-1	3kwt	35,71
	E3 ubiquitin-protein ligase NEDD4-like	2nsq	30,16
	E3 ubiquitin-protein ligase NEDD4	3b7y	28,80
C2B	Extented Synaptotagmin 2	4npj	25,93
	E3 ubiquitin-protein ligase NEDD4-like	2nsq	25,64
C2C	Intersectin 2	3jzy	25,21
	Extented Synaptotagmin 2	4npj	24,35
	Human MCTP2	2ep6	23,73
C2D	Human MCTP2	2ep6	26,23
	Intersectin 2	3jzy	25,62
	Extented Synaptotagmin 2	4npj	24,37

The name of each template is associated with the PDB identification code and the percentage of identity between the template and the corresponding C2 domain of QKY.

Once the PROSA-WEB results seem acceptable (see the Methods' section for the criteria; Annexe 1 for example) (M. Wiederstein & M. Sippl, 2007), the structures were visualized on SwissPDBviewer (N. Guex & M. Peitsch, 1997) to have a look at the Ramachandran plots (Annexe 1). The residues outside of the areas with acceptable phi/psi angle values are confronted to high energy conformations. The more residues are found in these “steric clash regions”, the less stable the protein is. For the predicted models, there were very few amino residues with sterics clashes, which were exclusively found in the loops, and thus we considered them as stable.

3/ ROBETTA modeling

This tool was used for the C2B domain of QKY. Indeed, the multiple alignment quality between the templates and the C2B sequence was low: the β-strands were not well aligned. Hence MODELLER (B. Webb & A. Sali, 2014) was not able to correctly compute a stable model, as assessed by the PROSA-WEB results. This problem led us to use the ROBETTA server (D. Kim, D. Chivian & D. Baker, 2004) and the calculated models were much more satisfying in terms of quality.

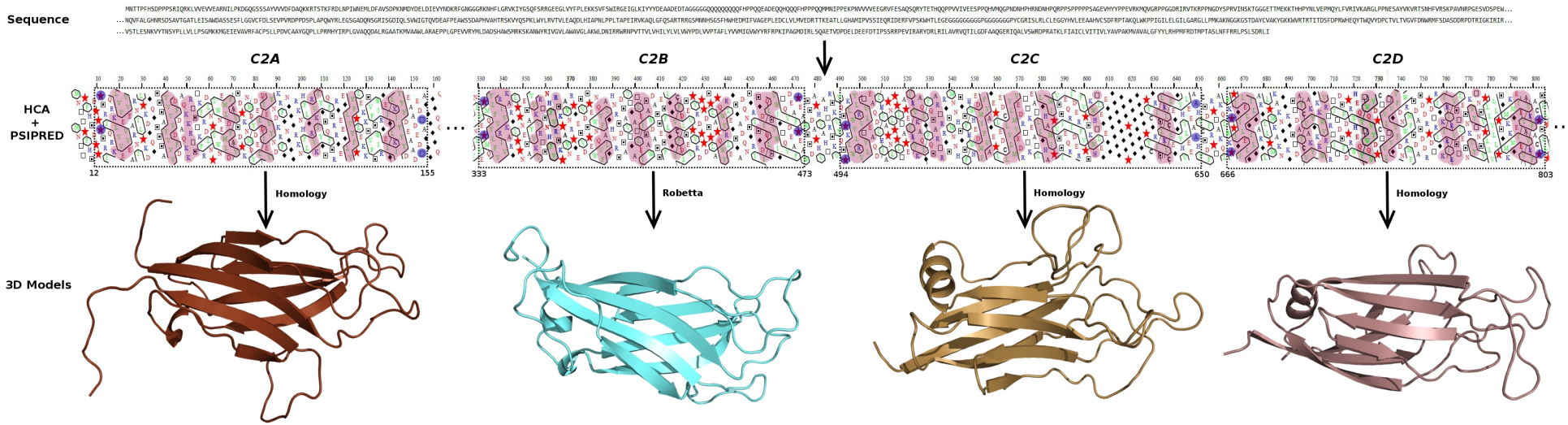

Figure 15: Delimitation and Modeling of QKY C2 domains. The raw MCTP sequence (top) is processed with HCA (middle; *blue* points are the beginning and end residues of each domain, with their sequence number below the dot frame) and psipred (predicted β-strands highlighted in *pink*). The delimited sequences of each C2 domain were modeled in 3D (bottom) using structure homology (C2A, C, D) or Robetta server (C2B).

4/ Molecular Dynamics for stability

Since a model with accurate quality was built for each C2 domain, MD were run to assess the stability of individual QKY C2 domain structures. The first MD run on all-atom stand-alone revealed quite high RMSD compared to average stable protein structures, suggesting non stable structure. Indeed, the RMSD value was fluctuating between 0.4 to 0.7nm when one would expect a maximum 0.4nm for a stable protein (fig. 16). However, a very interesting feature was observed from the RMSF plot: it shows important differences in values, as some regions of the protein have a very low value (~0,1nm) and others have a higher value (~0,6nm). In fact, this peak-gap skyline matches perfectly to the loop-β strand alternation in the secondary structure (fig. 17). The trajectory visualization corroborates this information, since no secondary structure deconstruction was observed in the β-sheet skeleton but loops showed high flexibility and thus mobility.

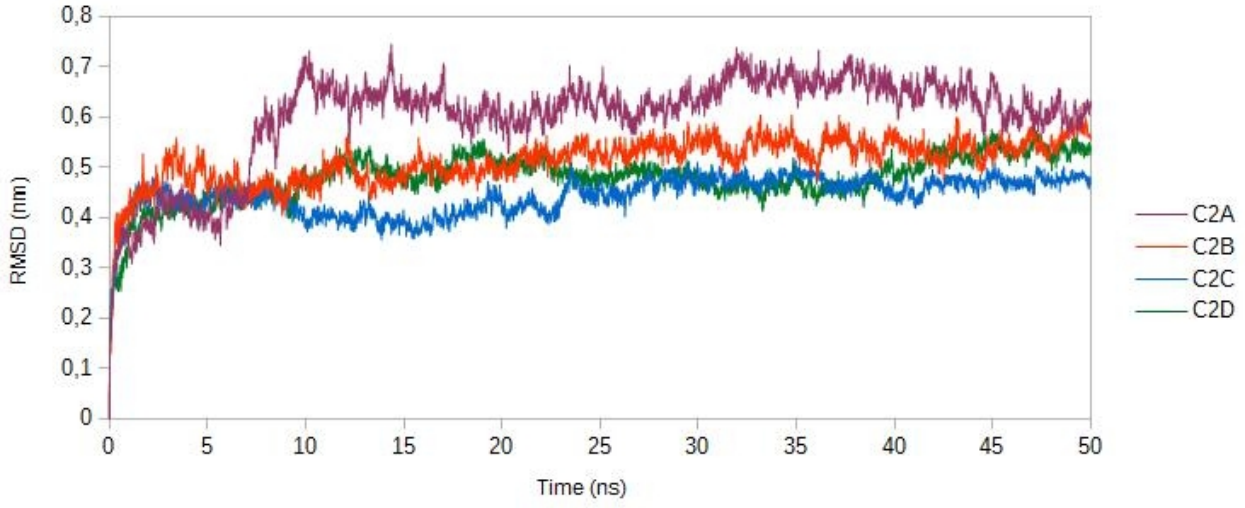

Figure 16: RMSD plot of QKY C2 domains.

All four QKY C2 domains display the same behavior. We can draw out of this that the β-sheets make the C2 domains stable despite the moving loops. From this calculation, we can assume that C2 domains can be analyzed independently from the rest of the protein and gives us preliminary clues about the potential role of loop rearrangement for calcium and/or lipid binding.

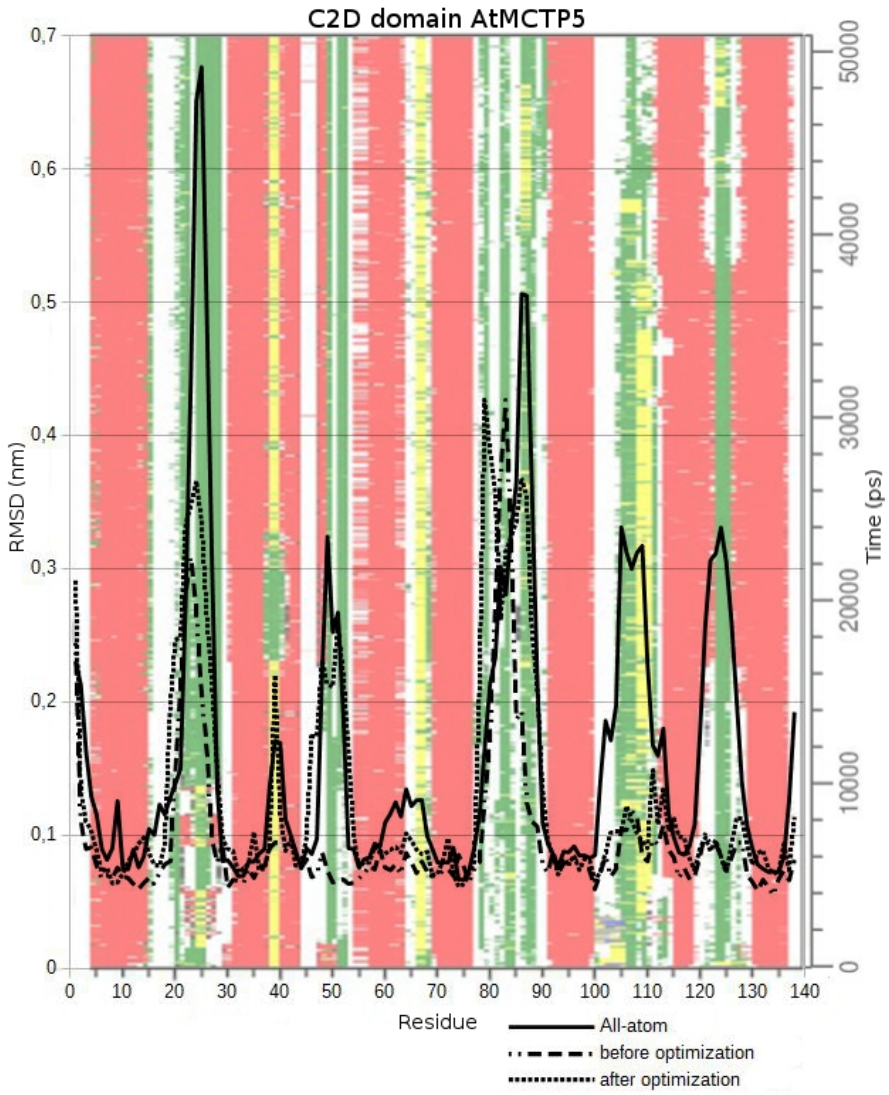

Figure 17: Coarse grained structure optimization of C2D. This figure compile information from both atomistic and coarse grain stand-alone simulations. The background color represent the DSSP (secondary structure over time) of the 50ns atomistic simulation. Red color indicates β-strands whereas the other colors are loops and turns. The continuous black line is the RMSF associated with the DSSP. The dotted lines are RMSF of the coarse grained structures, before optimization (dash-dot) and after (dots).

5/ Calcium-binding sites prediction

Calcium binding is one of the known interaction C2 domains can have, and this information can be very important to justify ionic gradient dependency of the protein and conditional membrane docking. This property is however not conserved in all C2 domains and it is very difficult to estimate whether or not binding occurs and, if so, how many and where the calcium ions are bound. This part of the work aims at finding a protocol for such a calcium-binding prediction, using various tools.

The primary idea was to compare the calcium-binding site of a calcium-bound structure

from the PDB (for example E-Syt2, 4npk) with the QKY C2 structures and look if the residues involved in the coordination were conserved. Most known calcium-binding C2 domains in the literature, including E-Syt2, have a cluster of aspartate residues located in the loops (Xu et al, 2014). On that basis in the case of QKY, only the C2D domain had enough aspartate residues to be qualified for further analysis (fig. 18A).

The first prediction assay was based on MD performed on E-Syt2 calcium-free structure (4npj). The idea was to make a stand-alone simulation of the domain in a box containing calcium ions (0,1M) and see if interactions with Ca^{2+} occurred and generated the calcium-bound structure (4npk).

The prediction was unsuccessful (no binding of Ca^{2+}) so we used a machine-learning (FEATURE) and statistic (R)-based technique (W. Zhou, G. Tang & R. Altman, 2015). A control test was first done on 4npj in order to check the method. The prediction gave sites corresponding to the 4npk calcium-bound (fig. 18B). FEATURE was then performed on all four QKY domains to verify the sequence analysis. Indeed, only C2D domain had high score sites predicted in the region of interest and linked to the presence of aspartates. The scores of C2D were however lower than those of E-Syt2 (fig. 18C). To summarize, we predicted that C2D would be able to interact with two calcium ions.

To add an extra verification step, MD simulations of the structures bound to their calcium ions were carried out. The concept leans on the distance calculation between the initial position of each calcium ion (from PDB in Esyt2 and predicted for C2D) and their new position at each frame, during the 50ns simulation. If the ion is not well stabilized by coordination, it will be released and the distance will increase. The system also contained free ions in solution at a concentration of 50nM to avoid osmotic problems and permit potential replacements in the binding pockets. Again, the method was first tested with E-Syt2 crystallized with calcium (4npk). The C2D domain was not optimized for coordination as it is in 4npk, and a supplemental equilibration step with position restraints on protein backbone and calcium ions was first run. This allows the side chains to rearrange around the ions and maximize coordination before the system was set free for the production run. E-Syt2 4npk showed complete stabilization of calcium 1 during the whole simulation, calcium 2 unhooked at 15ns and calcium 3 did not seem well stabilized from the beginning (fig. 18D). The two highest scores of C2D were stabilized for approximately 5 and 10ns before being released in the solvent (fig. 18E). It is interesting to note that these results are in accordance with the score values given by FEATURE: higher the score is, stronger the coordination is. Furthermore, calcium-binding is sometimes related to lipid-binding (W. Cho & R. Stahelin, 2006), where the polar heads of anionic lipids complete the coordination. A possible hypothesis is that C2D can sequester the ions better when it is bound to a membrane.

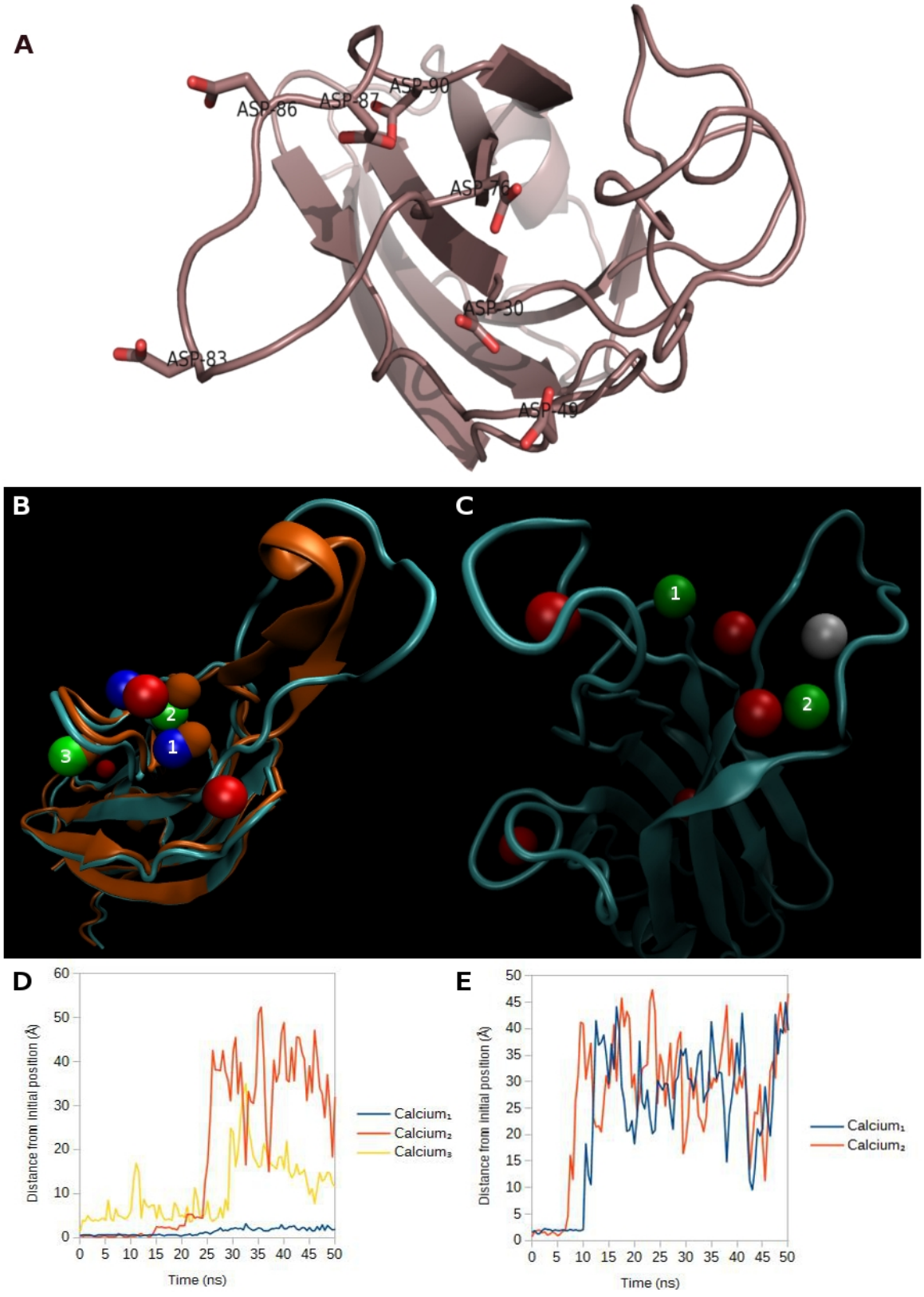

Figure 18: Calcium-binding sites prediction. (A) C2D visualization with the aspartate cluster in the loop region. **(B)** Human Extended Synaptotagmin 2 used as control for calcium-binding sites prediction (FEATURE and R). *Orange* cartoon and beads correspond to the calcium-bound structure (4npj). *Green* cartoon is the calcium-free structure (4npk). The *blue*, *green* and *red* beads are the predicted sites. **(C)** QKY C2D domain with the predicted sites as beads. **(B,C)** Colors of the beads match the FEATURE scores: *blue* for x>200, *green* for 200>x>100, *white* for 100>x>10 and *red* for x<10. **(D,E)** MD simulations of 4npk and C2D with the high score beads. The calcium numbers refer to the numbers showed in **B** and **C**.

6/ All atom simulation of QKY C2D domain in interaction with a membrane

The following membrane docking simulations and analysis were only carried out with the C2D domain of QKY. The reason behind this choice was time-related: setting a protocol and understand the tools can be time-consuming and we preferred to start with one domain only. C2D was chosen because it is one of the two domains (C2C and C2D) shown to be necessary for the PD localization (P. Vaddepalli, A. Herrmann, L. Fulton *et al.*, 2014) and was more "classic" than the C2C domain (which has a peculiar long glycine loop). Furthermore, C2D was the only domain to stand out during the calcium binding prediction.

The initial trial for C2 domain docking was inspired by the work on SYT7 membrane docking (N. Chon, J. Osterberg, J. Henderson *et al.*, 2015). Two lipids were chosen to build the membrane on Charmm-Gui: 1-palmitoyl-2-linoleoyl-3-phosphatidylcholine (PLPC) and 1-palmitoyl-2-linoleoyl-3-phosphatidylserine (PLPS) in a PLPC-3:1-PLPS ratio. Those lipids are major components of the plant biological membrane. The PLPS have anionic polar head whereas PLPC is neutral, giving two different types of possible interactions with the protein. Since docking of MCTP C2 domains to a membrane has never been done before, we chose to remain simple concerning the membrane composition and stick to those two lipids in a first place.

The system was launched in two parallel 250ns production simulations. Several issues were faced for those all-atom simulations. The first inconvenient was the duration of the calculations themselves and the computational monopolization: each calculation took its own computer for 15 days. This problem led us to another one: the impossibility to do more than two repetitions of the same system, which is hardly an acceptable minimum. Furthermore, the two simulations resulted in an interaction of the protein with the membrane, but in different conformations, and 250ns seemed too little for proper membrane docking and stabilization.

We drew out of this that the simulations had to be longer (microsecond scale) to better predict the membrane docking mechanism if happening. All-atom simulations were no longer suitable for this kind of calculations, so we turned on to CG simulations.

7/ CG docking

The transformation of the domain into CG representation was carried out within a MARTINI force field (S. Marrink, H. Risselada, S. Yefimov *et al.*, 2007; X. Periole & S. Marrink, 2013).

CG transformation causes a loss of secondary structure. In order to maintain it, ElNeDyn (Elastic Network Dynamic) (X. Periole, M. Cavalli, S. Marrink *et al.*, 2009) creates an artificial

mesh of elastic bonds that keeps the secondary structure in the CG simulation. However, the previous MD assays showed that only the β-skeleton is fixed in the native protein while the network is originally calculated for the whole protein, including loops. Manual ElNeDyn optimization needed to be done to set free the loops and mimic the native domain's behavior (C. Globisch, V. Krishnamani, M. Deserno *et al.*, 2013). This step was based on the knowledge of the atomic secondary structure (with the help of DSSP algorithm and molecular visualization).

Figure 17 displays the optimization process: the raw ElNeDyn networked domain (dash-dot line) is not behaving the same way as the native atomistic domain (continuous line) in the loop regions (no peaks). After optimization, loops number two and three developed a more “natural” behavior with appearance of peaks. We also see that the last two loops would need additional optimization. However, depending on the case, some regions cannot be well optimized without altering the stability of the whole protein.

Two CG repetitions of 2,5µs were then carried out. Slight differences in the membrane interaction led us to extend the simulation duration to 5µs (fig. 19B, rep1 and rep2). The results were not different after the extra 2.5µs but they still brought information that the docking is stable over time (up to 5µs) and that 2.5µs simulations are long enough to study the docking mechanism. To deal with the conformation variations, two additional repetitions (fig. 19B, rep3 and rep4) were performed, of 2.5µs each.

The resulting simulations revealed that the C2D interacts quite rapidly with the membrane but stays on the surface instead of inserting deeply in the leaflet (fig. 19).

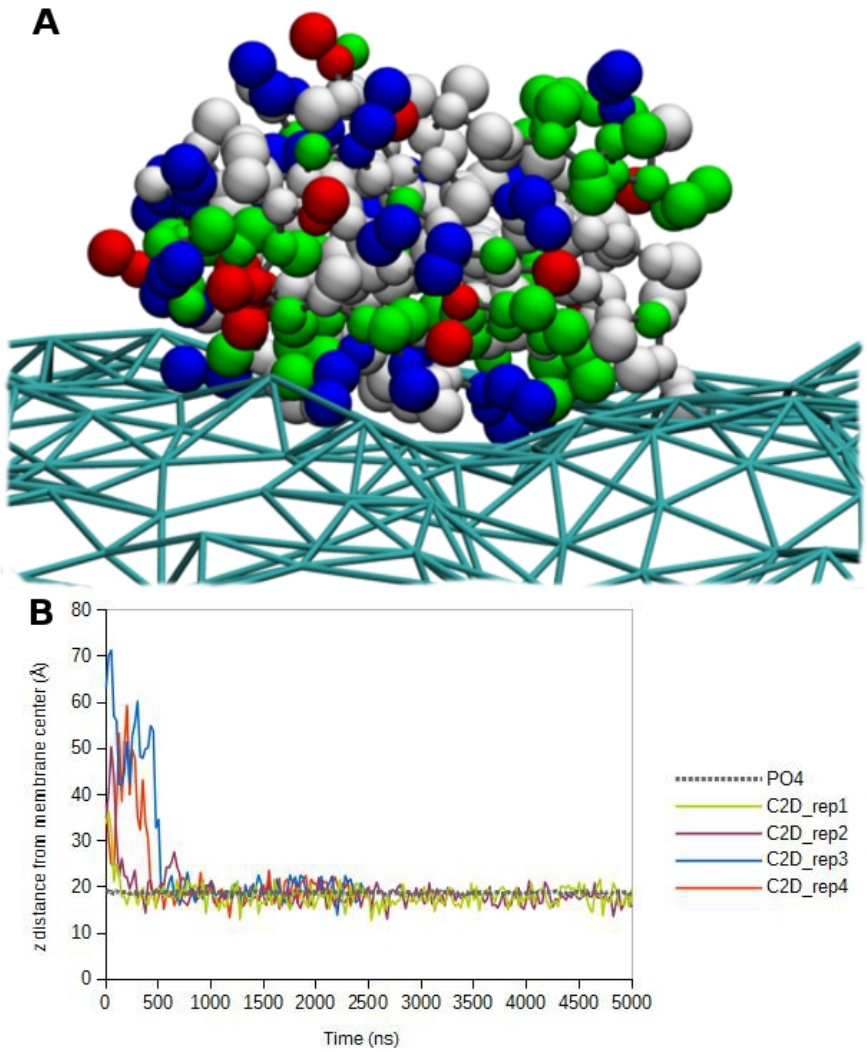

Figure 19: C2D membrane docking analysis. (A) 3D visualization of the membrane docked CG domain onto the phosphate plane (*cyan* network). Colors correspond to amino acid properties (*blue* for basic, *red* for acidic, *green* for polar and *white* for apolar). **(B)** Graph of the docking simulations. The y=0 line represent the center of geometry of the whole membrane. The *gray* dot line is the phosphate plane and the colored lines represent the minimal distance between the protein and the membrane center, for each repetition.

PART 2: NbMCTP11 Analysis

The analysis of QUIRKY served then for the analysis of *Nicotiana benthamiana* NbMCTP11 protein, the one currently studied *in vivo* at the Laboratory of Membrane Biogenesis of Bordeaux.

The protocol established with AtMCTP5 was hence applied on NbMCTP11 to give molecular-scale complementary support and information to the *in vivo* biological assays. All domains of NbMCTP11 were analyzed in parallel. Multiple alignments of the MCTP members from *Arabidopsis* show enough conservation in terms of domain positions and structures to safely utilize the same protocol (Annexe 2).

1/ Delimitation, Modeling and Stability of the NbMCTP11 C2 domains

The sequence analysis of NbMCTP11 resulted in the delimitation of four C2 domains: C2A [M1 to P135], C2B [D262 to A395], C2C [A426 to T573] and C2D [P589 to T725]. C2A 3D structure was established with MODELLER using human MCTP2 (2ep6), human E3 ubiquitin-like ligase NEDD4-like protein (2nsq) and Munc13-1 (3kwt) as templates. The three other domains were modeled with the ROBETTA server. All the predicted domains display the conserved β-sheets (fig. 20).

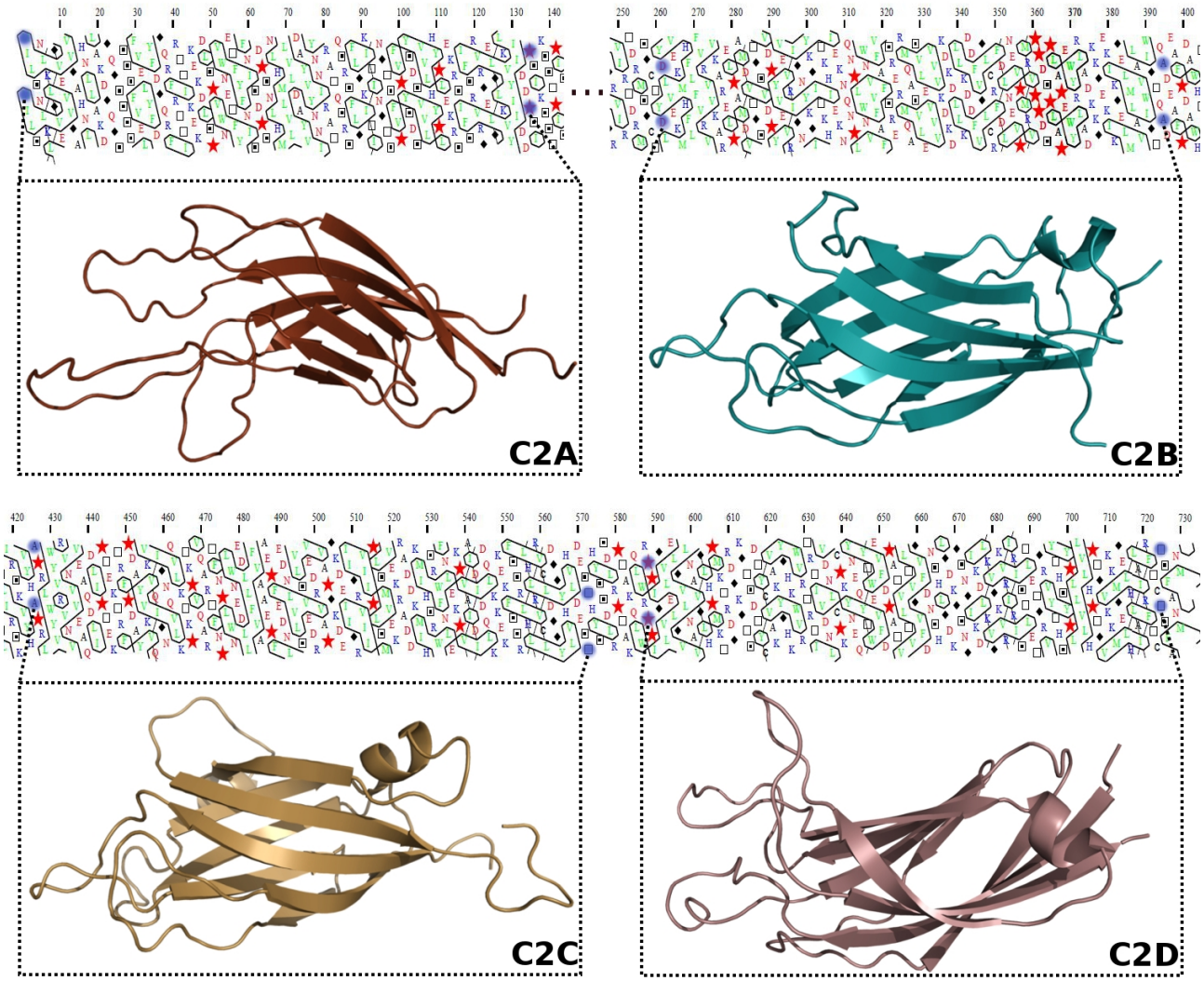

Figure 20: Modeling results of NbMCTP11. The HCA sequence (top) of each domains (delimited by the *blue* points) used for their 3D modeling. PSIPRED results are not shown on this figure but were also used, as in QKY.

Each model was then simulated through GROMACS MD in a stand-alone system. RMSD and RMSF/DSSP calculations (Annexe 3) showed stability and similar behavior as the QUIRKY C2 domains. We can observe from the DSSP plot that only C2B maintains its α-helix throughout the entire simulation (Annexe 4).

The CG structures were made and optimized like for QKY C2D domain. ElNeDyn was used and the six main loops were set free (the second loop being a short β-turn) in C2A, B and C domains. The α-helix inner network of C2B was kept but the helix was still made loose from the β-skeleton. Stand-alone simulations were satisfying for all those domains (see RMSF plots, annexe 4). For C2D, we were only able to optimize three of the loops but the resulting domain was considered close enough to the native protein from the RMSF comparison (Annexe 4). The three freed loops being the most mobile and the more important ones for putative docking.

All the CG domains were then placed in a simulation box for membrane docking analysis with a lipid bilayer composed of PLPC-3:1-PLPS ratio. Four repetitions of 2.5µs were performed on each domain.

2/ CG membrane analysis

Area per lipid (APL) and membrane thickness were analyzed for each system. The APL is not significantly different between the systems, nor the thickness (fig 21), indicating no significant membrane perturbation.

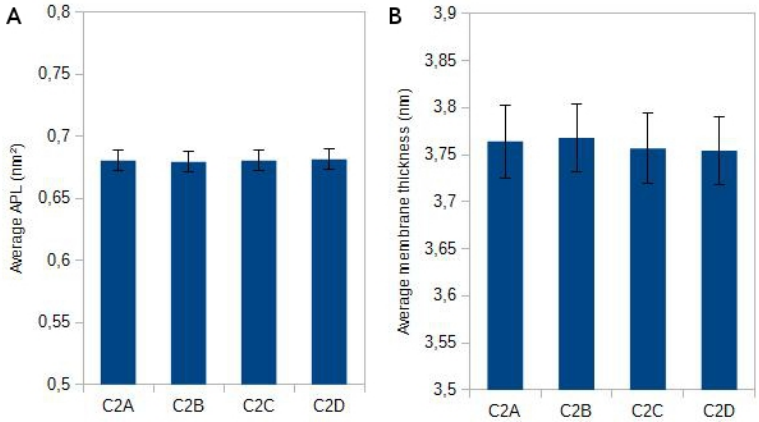

Figure 21: Membrane analysis. (A) Average Area Per Lipid of each domain on all repetitions. **(B)** Average membrane thickness of each domain on all repetitions.

3/ C2A domain Analysis

3.1/ Docking to CG membrane

The four repetitions resulted in three loop docking on the membrane, two with the same way of interacting (rep1 and rep3) and one showing interaction with the termini side (rep2); rep4 didn't interact. Two additional repetitions were then simulated to try to pin out one main behavior of C2A: one gave the same loop docking as rep1 and 3 but the other one had an interesting path (rep5): C2A interacted in the same way as rep2 but in the last nanoseconds of the simulation, the domain detached from the membrane (fig. 22B). This undocking points out a possible instability of the termini-side membrane interaction in comparison with the loop docking of rep1, 3 and 6, that we only consider in the following analysis.

Figure 22 A and B shows that C2A can interact with the membrane but is not deeply inserted into the leaflet and stays at the level of the phosphate plane. The interaction is mainly stabilized by interaction between lipid phosphate groups and positively charged Arginines and, to a lesser extend, Lysines (fig. 22C). Two apolar residues a few angstroms below the phosphate plane (fig. 22A) are also involved: ILE117 and PHE118.

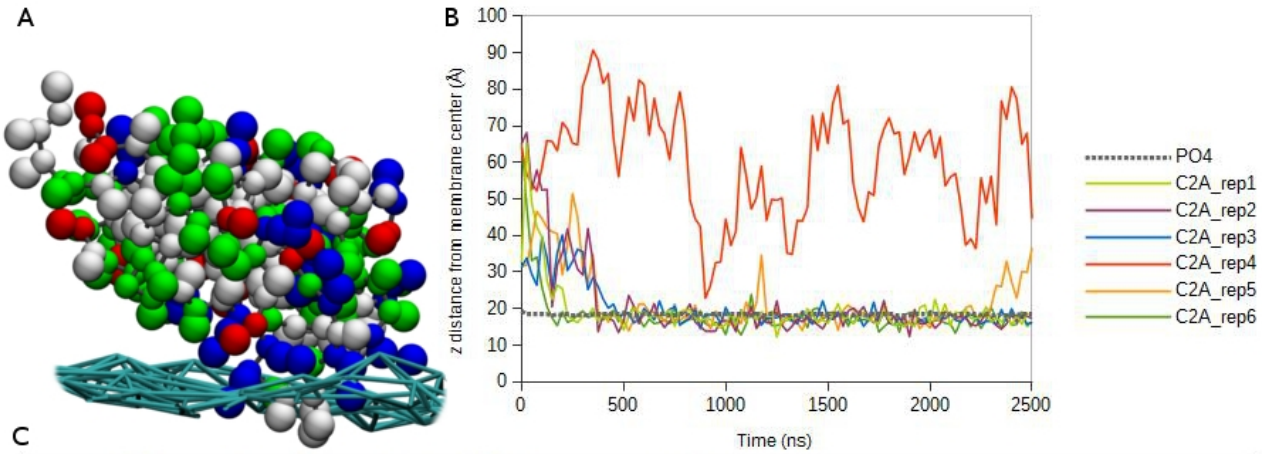

C

C2A	Total - 467 -	PLPS - 50,43 % -	PLPC - 49,57 % -	Residue name
Lysine	16,90%	19,09%	14,68%	K114, K91
Arginine	43,79%	45,97%	41,58%	R120, R115, R86, R81, R122
Serine	20,61%	20,51%	20,72%	S116, S87, S119, S85
Sum interactions	81,30%	85,57%	76,98%	

Figure 22: Membrane docking analysis of C2A. (A) 3D visualization of the docked domain onto the phosphate plane (*cyan* network). Colors correspond to amino acid properties (*blue* for basic, *red* for acidic, *green* for polar and *white* for apolar). **(B)** Graph of the distance between the membrane center and the protein. The y=0 line represent the center of geometry of the whole membrane. The *gray* dot line is the phosphate plane and the colored lines represent the minimal distance between the protein and the membrane center, for each repetition. **(C)** Summary table of the interactions. The top line displays the total number of interactions and the distribution of those interactions between PLPS and PLPC (in percent). The last line sums the percentages of the table, to show the importance of each residue (K, R, S) during the interaction.

We can observe that the number of interactions of C2A with PLPS and PLPC is of the same magnitude (50/50). However, since the negatively charged PLPS are minor in the membrane composition compared to PLPC, they might be essential to the membrane docking. This should be further tested to assess the role of PLPS in the docking.

3.2/ Reverse simulation

We then performed reverse simulation from CG to all atom, to visualize the polar connections between the protein and the lipids with atomistic details (fig. 23A) but also to check any possible conformational changes in the protein secondary structure with the DSSP plot (fig. 23B). All the 3D images of reverse are taken from the last frame (at 25ns).

The C2A domain interacts with five PLPS and three PLPC in the image. The interaction involves both side chains and backbone atoms (fig. 23A). The secondary structure of the docked domain is similar to the stand-alone structure meaning there is no significant conformational change (fig. 23B; Annexe 4).

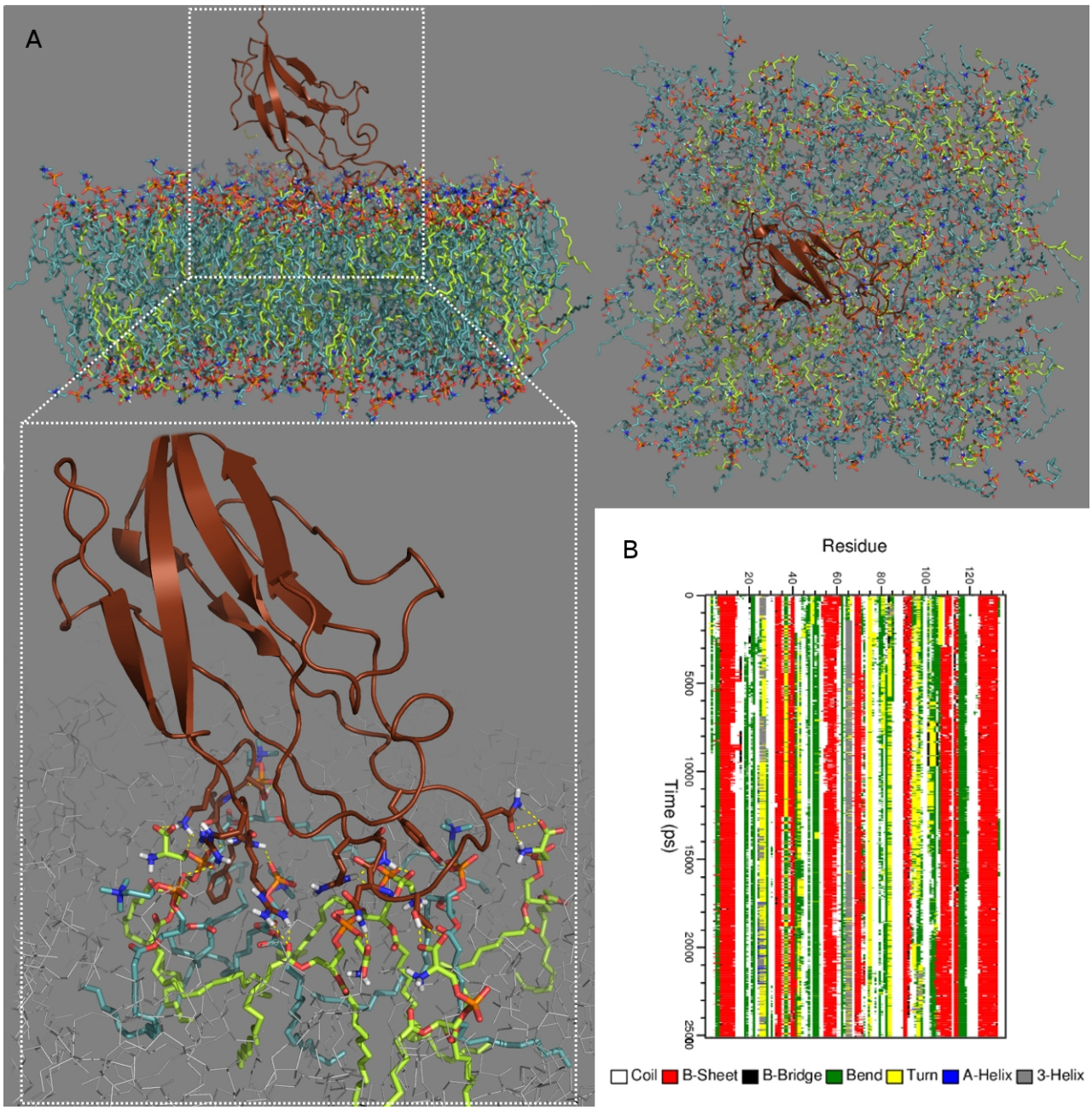

Figure 23: C2A reverse simulation analysis. (A) *Top right* image is the C2A domain (*brown*) docked onto the membrane, global view from above. *Top lef*t is the same, global side view. *Bottom left* is a close up of the interaction, only the interacting lipids are colored, the others are represented as *gray* sticks. PLPC are shown in *light blue* and PLPS in *light green*. Only the side chains and/or main chains of the residues that are involved in polar contacts are represented as bold sticks. Phosphate atoms are *orange*, oxygen are *red*, nitrogen *blue* and polar hydrogen *white*. The polar contacts are displayed through the *yellow* dotted lines. **(B)** DSSP plot of the reverse simulation.

4/ C2B domain Analysis

4.1/ Docking to CG membrane

The C2B domain did not show interaction with the lipids of the membrane but instead stayed in the solution (fig. 24A). This is assessed by the plot of the distance of the protein to the membrane center (fig. 24B**)**, as the domain moves closer and farther from the leaflet without real

interaction. This behavior was observed in all four repetitions.

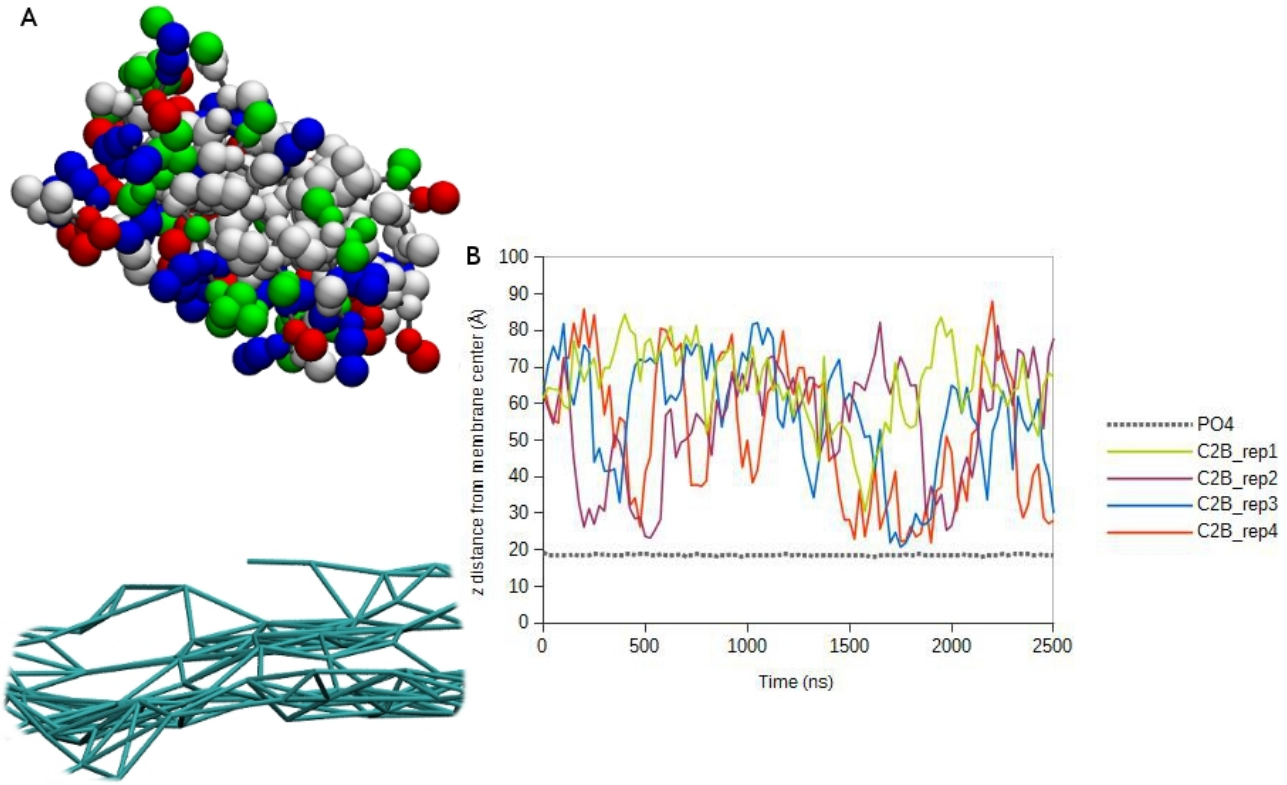

Figure 24: Membrane docking analysis of C2B. (A) 3D visualization of the domain above the phosphate plane (*cyan* network). Colors correspond to amino acid properties (*blue* for basic, *red* for acidic, *green* for polar and *white* for apolar). **(B)** Graph of the distance between the membrane center and the protein. The y=0 line represent the center of geometry of the whole membrane. The *gray* dot line is the phosphate plane and the colored lines represent the minimal distance between the protein and the membrane center, for each repetition.

4.2/ Putative calcium-binding

3D structure screening for putative calcium-binding sites was successful for the C2B domain, as it is the only of the four C2 domains to display a clear cluster of seven aspartate residues in the loop region (fig. 25). Rearrangement of the loops and side chains could easily coordinate one or more calcium ions.

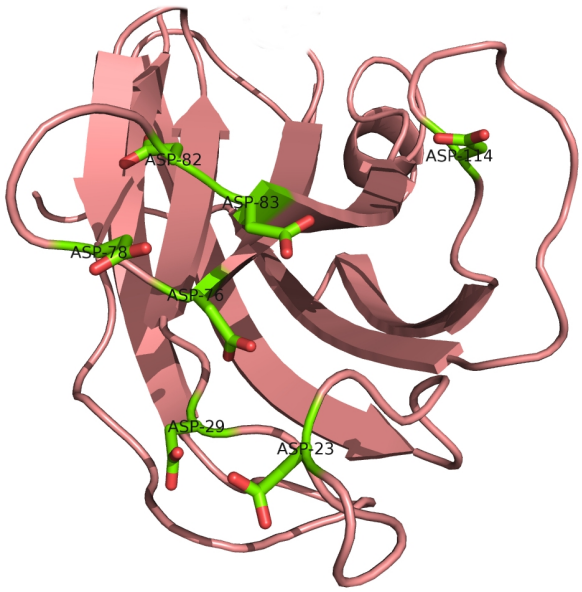

Figure 25: Aspartate cluster in C2B loops.
Asparatate residues are displayed as *green* sticks, with the corresponding numbering.

Due to lack of time, this was not predicted but the protocol to follow would be the same (established for QKY, see above).

5/ C2C domain Analysis

5.1/ General comments

The third domain required some additional work because the sequence analysis and simulations were primarily done on a long version of the domain (161 amino acids). This longer domain, compared to the three others (around 130-140 amino acids), displayed a larger final loop. This feature was in correlation with the previously delimited QKY C2C domain, which has a long glycine-rich final loop. However, after performing the modeling and docking simulations (which resulted in two non-docking behavior and two membrane docking with different sites of interaction), sequencing results of Dr Jens Tilsner for the cDNA constructs (see experimental part) showed that the NbMCTP11 sequence used for the *in vivo* assays was lacking 13 residues (LKKEKFSSRLHLR) located inside the longer final loop of C2C. It is difficult to say if this repetition is an annotation problem or a natural variant. Anyhow, the shorter version being the correct one, and to be in accordance with the *in vivo* experiments, we decided to resume the C2C analysis from the modeling. The extra amino acids were deleted and the two extremities "glued" back together using MODELLER. All the verification and docking simulations were done afterward.

The four repetitions showed that C2C docked onto the membrane after up to 1.5µs, i.e. relatively late in the simulation. Trajectory analysis enables us to observe that the docking is always occurring with the same side of the protein (fig. 26A), but the angle between the protein and the leaflet could vary. The interaction never occured deeper than the phosphate plane (fig. 26A, B). This interaction at the lipid surface would suggest a weak attachment to the membrane, as reflected by the total number of interactions (fig. 26C). It is also possible that the membrane composition used in the simulation is not suitable for C2C docking.

A

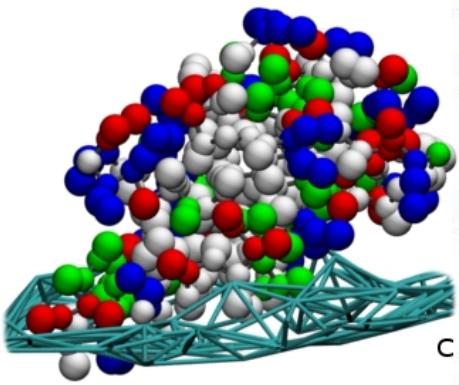

B

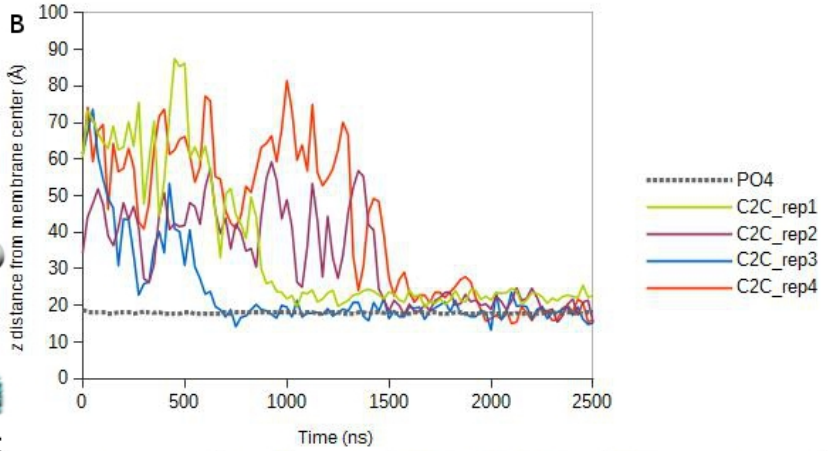

C

C2C	Total - 304 -	PLPS - 41,17 % -	PLPC - 58,83 % -
Lysine	32,37%	42,91%	25,00%
Arginine	22,02%	23,95%	20,67%
Aspartic acid	16,84%	9,18%	22,21%
Glutamic acid	12,90%	6,79%	17,18%
Sum interactions	84,13%	82,83%	85,06%

Figure 26: Membrane docking analysis of C2C. (A) 3D visualization of the docked domain onto the phosphate plane (*cyan* network). Colors correspond to amino acid properties (*blue* for basic, *red* for acidic, *green* for polar and *white* for apolar). **(B)** Graph of the distance between the membrane center and the protein. The y=0 line represent the center of geometry of the whole membrane. The *gray* dot line is the phosphate plane and the colored lines represent the minimal distance between the protein and the membrane center, for each repetition. **(C)** Summary table of the interactions. The top line displays the total number of interactions and the distribution of those interactions between PLPS and PLPC (in percent). The last line sums the percentages of the table, to show the importance of each residue (K, R, D, E) during the interaction.

The analysis of the residues involved in the interaction showed that not only negatively charged residues (E, D) are implied (fig. 26C) but also apolar residues (fig. 26A). This could suggest an affinity for neutral lipids, but also potential interaction with calcium ions that could mediate lipid docking. This hypothesis could however not be tested by MD currently, since no calcium mediated lipid binding has been tested for C2 domains using this predictive method, to our best knowledge.

5.3/ Reverse simulation

The domain interacts with five PLPS and three PLPC at this time frame (fig. 27A). The number of interactions is quite low compared to the surface area available for contact (in comparison to C2A, fig. 22, which surface is smaller) (fig. 27A). The secondary structure is similar to the stand-alone simulation but we can note the appearance of a small β-strand in the last loop (fig. 27B).

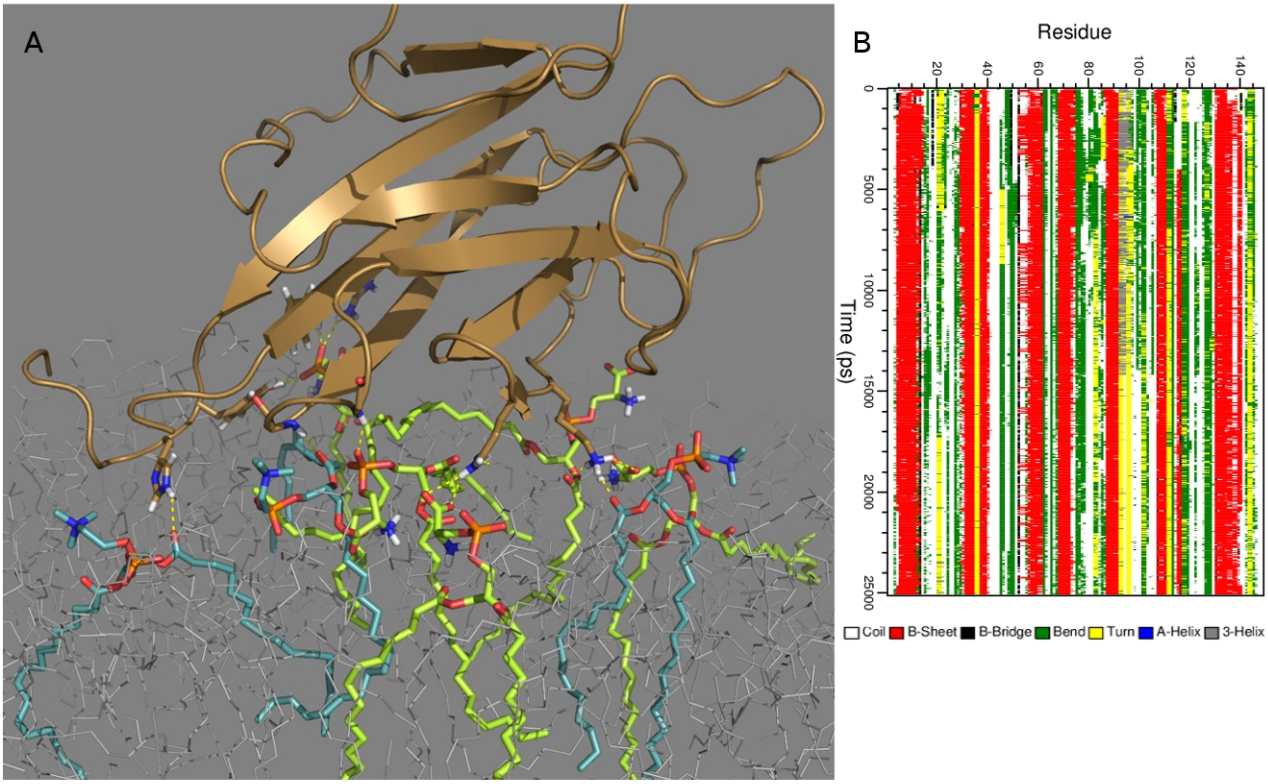

Figure 27: C2C reverse simulation analysis. (A) The C2C domain (*sand yellow*) docked onto the membrane. This is a close up of the interaction and only the interacting lipids are colored, the others are represented as *gray* lines. PLPC are shown in *light blue* and PLPS in *light green*. Only the side chains and/or main chains of the residues that are involved in polar contacts are represented as sticks. Phosphate atoms are *orange*, oxygen are *red*, nitrogen *blue* and polar hydrogen *white*. The polar contacts are displayed through the *yellow* dotted lines. **(B)** DSSP plot of the reverse simulation.

6/ C2D domain Analysis

6.1/ Docking to CG membrane

The C2D domain showed the fastest docking and the strongest interactions. Indeed, all repetitions were the same, with C2D deeply attached to the lipid leaflet after 500ns (fig. 28A, B). The interaction is made by both loops and β-strands residues, along the domain (essentially Cterm loop and strands 6 and 7) (fig. 28A). Several apolar residues of the Cterm loop find their way deeper in the leaflet, below the phosphate plane (fig. 28A, B), and many polar residues strengthen the bonding (fig. 28A, C). Basic residues, mainly lysines (as 8 lysines are involved in almost 30%

of the total number of interactions) (fig. 28C), are spread all around the domain and contribute to ~65% of the electrostatic bridges. The total number of electrostatic interactions is the highest of the four domains. The interaction is also very specific, as trajectory analysis shows exactly the same conformation in all four simulations.

A

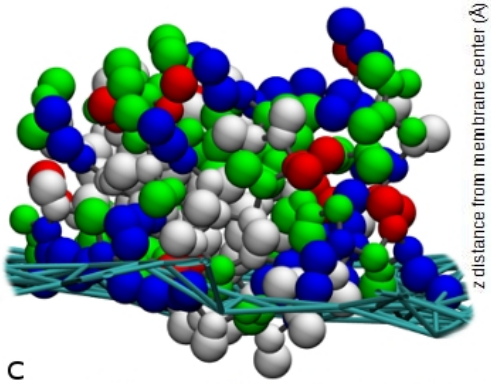

B

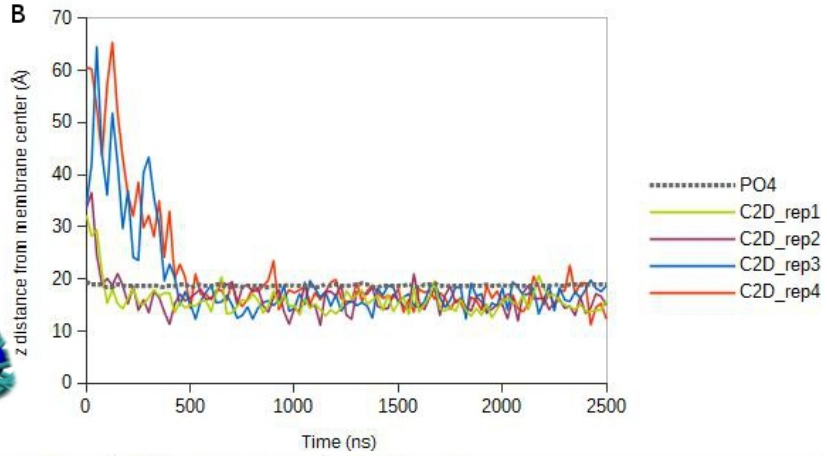

C

C2D	Total - 894 -	PLPS - 56,50 % -	PLPC - 43,50 % -	Residue name
Lysine	28,73%	29,06%	28,30%	K123, K94, K124, K91, K20, K35, K25, K88
Histidine	12,67%	14,50%	10,29%	H110, H129, H17, H118, H38
Arginine	22,35%	23,96%	20,26%	R98, R106, R96, R22
Serine	7,50%	6,24%	9,13%	S100, S111
Threonine	22,43%	23,32%	21,29%	T104, T101, T70, T120, T67, T21, T109
Sum interactions	93,68%	97,08%	89,27%	

Figure 28: Membrane docking analysis of C2D. (A) 3D visualization of the docked domain onto the phosphate plane (*cyan* network). Colors correspond to amino acid properties (*blue* for basic, *red* for acidic, *green* for polar and *white* for apolar). **(B)** Graph of the distance between the membrane center and the protein. The y=0 line represent the center of geometry of the whole membrane. The *gray* dot line is the phosphate plane and the colored lines represent the minimal distance between the protein and the membrane center, for each repetition. **(C)** Summary table of the interactions. The top line displays the total number of interactions and the distribution of those interactions between PLPS and PLPC (in percent). The last line sums the percentages of the table, to show the importance of each residue (K, H, R, S, T) during the interaction.

The membrane interaction seems to involve more PLPS than PLPC, suggesting affinity for anionic lipids. This hypothesis is supported by the high number (17) of interacting basic amino residues.

6.2/ Reverse simulation

The number of interacting lipids is considerable. The non-termini loops seem stretched on the leaflet, increasing the surface area and thus the number of possible interactions (fig. 29A). A very interesting feature is the immediate appearance of the α-helix at the termini side, which wasn't present in the stand-alone simulation (Annexe 4). Moreover, this helical structure looks very strong as it stays intact during the whole 25ns. The β-strands are also modified: some got smaller or fragmented, others, small ones, emerge in loops (fig. 29B). It is obvious that the interaction impacts

quite considerably the domain secondary structure, even if the β-skeleton remains present.

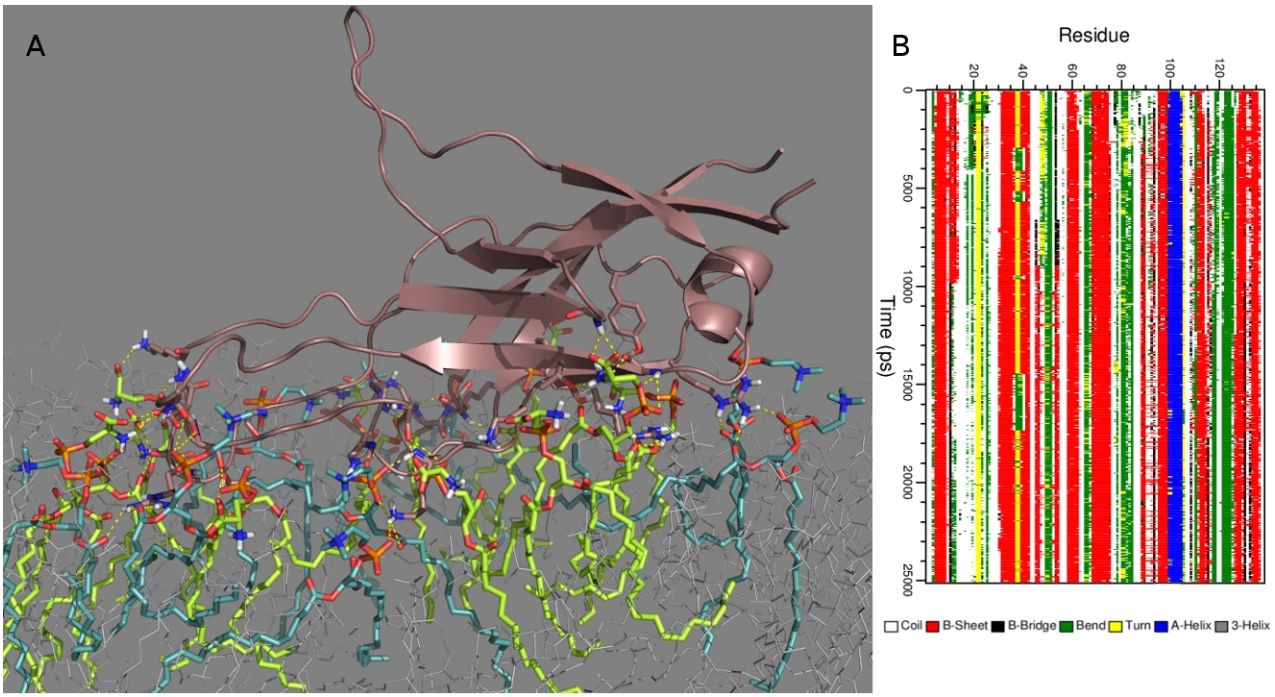

Figure 29: C2D reverse simulation analysis. (A) The C2D domain (*pink*) docked onto the membrane. This is a close up of the interaction and only the interacting lipids are colored, the others are represented as *gray* lines. PLPC are shown in *light blue* and PLPS in *light green*. Only the side chains and/or main chains of the residues that are involved in polar contacts are represented as sticks. Phosphate atoms are *orange*, oxygen are *red*, nitrogen *blue* and polar hydrogen *white*. The polar contacts are displayed through the *yellow* dotted lines. **(B)** DSSP plot of the reverse simulation.

6.3/ CG simulations in the presence of PIP4

It has been established that the presence of phosphatidylinositol-4-phosphate (PIP4) lipid molecules is an essential determinant for the plant PM identity, as it confers the inner electrostatic potential signature. Such a unique electrostatic field at the membrane surface controls the function of PM-associated proteins, thus having major roles in plant signaling and development (G. Hammond, M. Fischer, K. Anderson *et al.*, 2012; M. Simon, M. Platre, M. Marquès-bueno *et al.*, 2016). The propensity of NbMCTP11 C2D domain to interact with anionic lipids during the CG simulations (see above) led us to seek for more specific interactions with PIP4 molecules. The article from M. Guerrero-Valero, C. Ferrerorta, J. Querol-Audi *et al.* (2009) provide a detailed view of phosphatidylinositol-4,5-bisphosphate (PI(4,5)P2) interaction in mammals, which could be used as a template for searching a similar binding site in the C2D structure. Visualization using PyMol revealed that the β-groove of C2D presents similar residues to those located in the PI(4,5)P2 binding site.

Figure 30 compares the PKCα C2 domain bound to PI(4,5)P2 to the putative PIP-binding

site found on NbMCTP11 C2D domain. Even if the arrangement is a little different, all the residues needed for the PIP(4,5)P2 interaction are conserved: three lysines, one tryptophane, one tyrosine and one asparagine. This similarity pushed us to test the hypothesis by performing simulations of the docked C2D domain in the presence of PIP4.

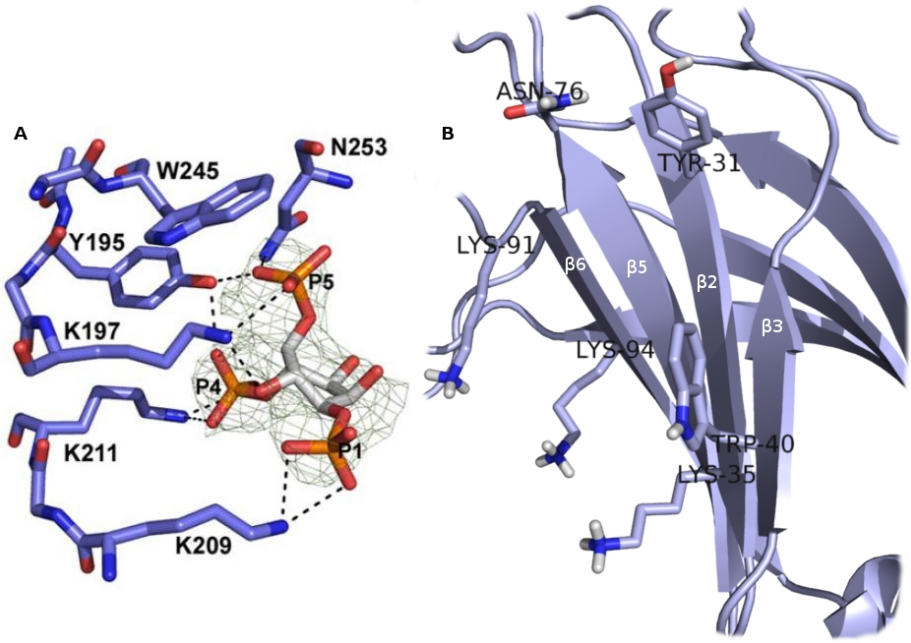

Figure 30: PIP-binding site comparison. (A) Phosphatidylinositol-4,5-bisphosphate binding site from M. Guerrero-Valero *et al.* (2009). **(B)** C2D β-groove with similar residues.

The choline head of one PLPC molecule was first replaced by an inositol-4-phosphate head, on each side of the membrane in the CG calculations. The four repetitions of 2.5µs resulted in PIP4 binding by the domain. However, only one repetition showed interaction at the β-groove site, the others were interacting elsewhere. We drew out of this that the C2D domain might interact with PIP4 at multiple places, and therefore possibly interact with several PIP4 at the same time. To enlighten these questions, we placed four additional PIP4 molecules on each bilayer side, for a total of five PIP4 per side, and simulated again four repetitions of 2.5µs.

We observed that C2D can indeed interact with PIP4 and up to five PIP4 can interact with the protein at the same time. Since only fives molecules were present, it is possible that more than five PIP4 could interact.

During simulations, PIP4 are moving inside the membrane and spend increasing amount of time at specific positions around the protein according to their interacting preferences. By taking into account all the simulation frames and using the protein as an immobile target around which lipids are moving, probabilities to find PIP4 beads at certain positions of space can be computed. In fact, if these computations are made for all points of a 3D grid, envelopes, named isosurfaces, can

be drawn around spacial regions having a higher probability to find PIP4 beads at a defined cut-off.

Figure 31A displays the C2D domain in CG representation and three isosurfaces calculated from the PIP4 4-phosphate only. The yellow isosurface correspond to the superior limit of the bulk apparition that is the maximal probability observed for the PIP4 4-phosphate in the leaflet without protein, the orange represent five times the yellow density and violet twenty times. We can see that PIP4 interacts in one main region that goes from the β-groove to the loop region. The violet region matches perfectly the β-groove site that was predicted. Orange regions show additional but secondary binding sites.

Isosurfaces were also calculated on the PIP4 phosphatidyl phosphate group. Figure 31B demonstrates that the interactions with this phosphate (pink isosurfaces; PO4) are segregated from the PIP4 4-phosphate (orange isosurface; P2). From the image, we can observe that the two phosphate types are located in two parallel buoys, the inositol ring being located in between.

The total number of interactions with PIP4 molecules was on average 335 on the four simulations, with a 50-50 distribution between PIP4 4-phosphate and PIP4 phosphatidyl phosphate (fig. 27C). PLPC and PLPS interactions were relatively similar to the PIP4-free docking (average 800 interactions), with a slight decrease in the PLPS interactions number.

Lysines 91 and 94 identified in the binding pocket in figure 30B are hence the most involved in the PIP4 interaction and lysines contribute to 61% of the total interaction (70% of the P2 interactions)(fig. 30C).

Interaction of one C2 domain with specific anionic lipids of the PM, and especially PIP4, is a very important information that supports the tethering hypothesis of MCTPs. Furthermore, on the basis of the sequence analysis and C2 domain delimitation, multiple alignment of the seventeen members (Annexe 2) show that the main PIP4-binding residues are well conserved in the C2D domains. PIP4 could therefore be an important feature of MCTP's C2D domains.

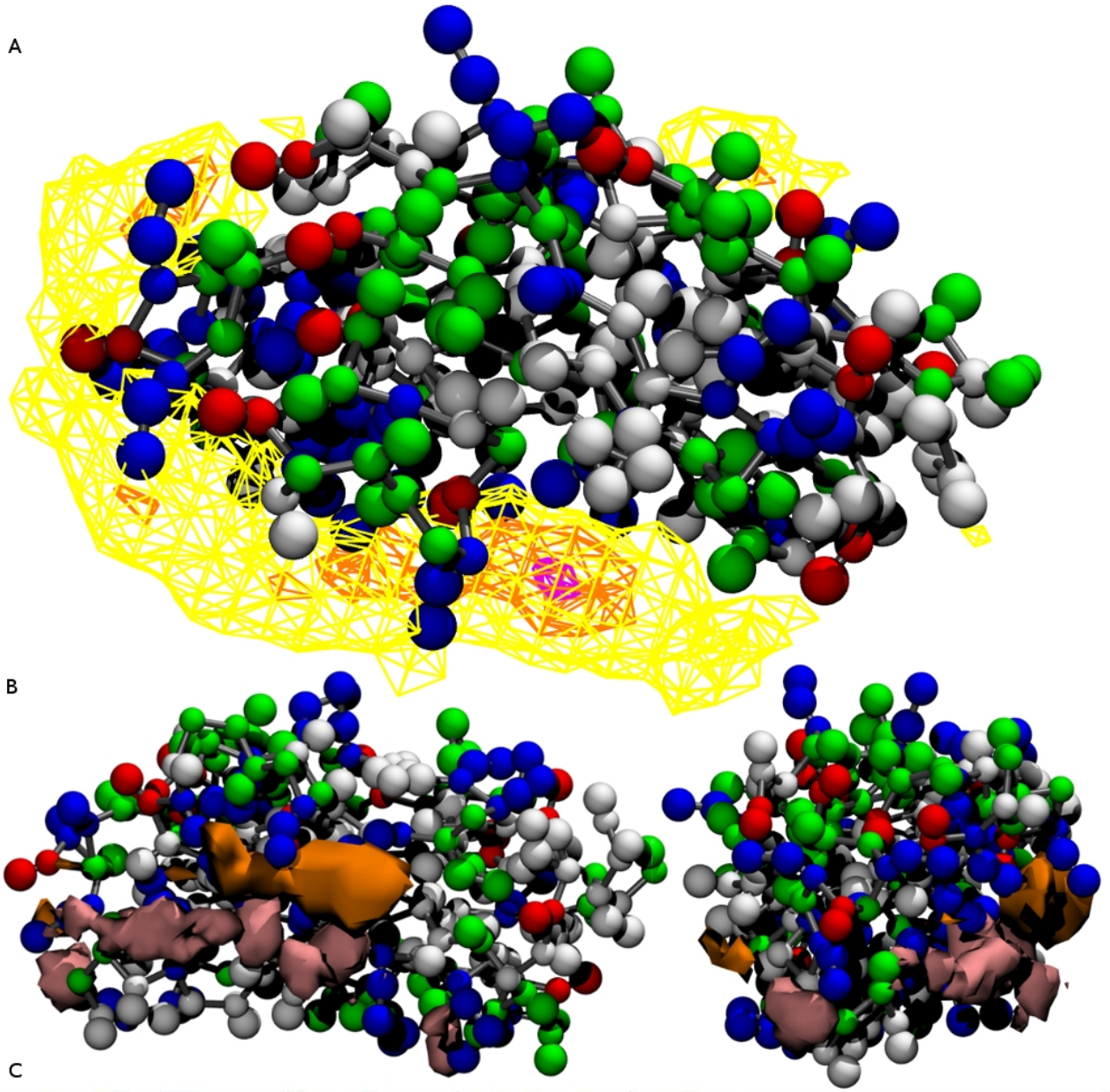

C2D – PIP4	Total - 335 -	P2 - 53,69 % -	PO4 - 46,31 % -	Residue name
Lysine	61,35%	70,32%	50,97%	K94, K91, K123, K20, K35, K25, K88, K82, K124
Histidine	9,86%	5,75%	14,62%	H118, H78, H110, H17, H38, H129
Arginine	15,74%	11,87%	20,22%	R22, R96, R98, R106
Threonine	10,76%	9,46%	12,26%	T70, T120, T21, T104, T101, T109
Sum interactions	97,71%	97,40%	98,07%	

Figure 31: C2D - PIP4 interaction analysis. (A) PIP4 density surfaces around the C2D domain calculated on PIP4 4-phosphate localization. *Yellow* surface correspond to the bulk (isosurf = 0,0002), *orange* to five times the bulk (isosurf = 0,001) and *violet* to twenty times the bulk (isosurf = 0,004). **(B)** Side views of the five times bulk isosurfaces. *Orange* represent the P2 phosphate and *pink* the PO4 phosphate. **(C)** Summary table of the PIP4 interactions. The top line display the total number of interactions and the distribution of those interactions between P2 and PO4 (in percent). The last line sums the percentages of the table, to show the importance of the presented residues during the interaction. The first column show the main residue types involved, with the associated colors.

To further analyze the molecular details of the interaction, we reversed the CG simulation to all atom representation. We see on figure 32A that the PIP4 molecules mainly interact on the loop and β-groove region, corresponding to the CG results. The CG structure used for the reverse transformation had the protein in interaction with five PIP4 molecules. After 25ns of the atomistic simulation, two of the PIP4 molecules have moved away from the protein. This information, together with the CG trajectory analysis, suggests more transient interactions for the secondary sites than for the main binding pocket.

Furthermore, DSSP analysis shows a secondary structure arrangement more similar to the stand-alone protein (fig. 32B; Annexe 4). PIP4 interaction also triggers the formation of an additional α-helix in the first loop, in the non-termini side.

Comparison between the stand-alone, reverse for PLPC/PLPS simulation and reverse for PIP4 simulation brings interesting views on conformational changes of the C2D domain, in correlation with the lipid composition of the membrane.

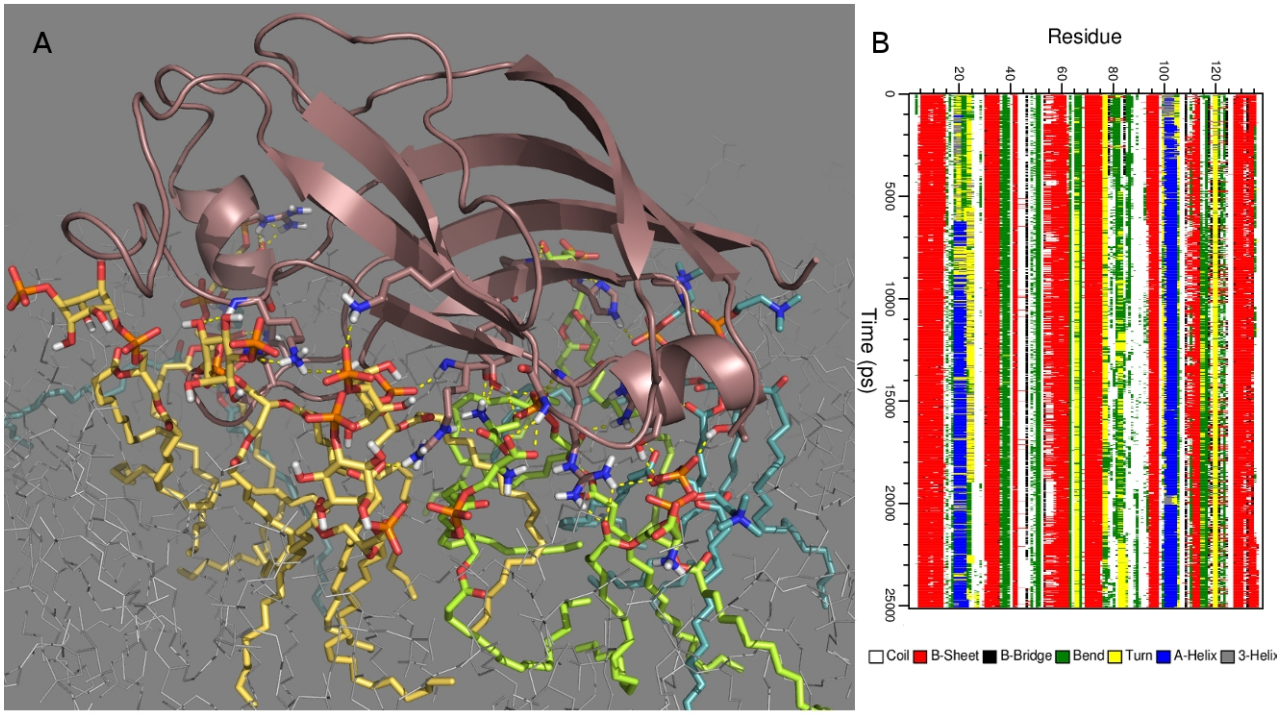

Figure 32: C2D reverse analysis with PIP4. (A) The C2D domain (*pink*) docked onto the membrane in the presence of PIP4. This is a close up of the interaction and only the interacting lipids are colored, the others are represented as *gray* lines. PIP4 are shown in *yellow*, PLPC in *light blue* and PLPS in *light green*. Only the side chains and/or main chains of the residues that are involved in polar contacts are represented as sticks. Phosphate atoms are *orange*, oxygen are *red*, nitrogen *blue* and polar hydrogen *white*. The polar contacts are displayed through the *yellow* dotted lines. **(B)** DSSP plot of the reverse simulation.

7/ *In vivo* mutant analysis

7.1/ Full length NbMCTP11 locates at PD

Confocal microscopy co-localization experiments on the full-length protein NbMCTP11 together with the ER marker HDEL and PD-PM marker PDCB1 proves the location of the protein in the ER network (weak) and at PD (strong) but not at the PM (fig. 33). PlasmoDesmata Callose Binding protein 1 (PDCB1) has been shown to locate on the PM at the neck region of the PD (C. Simpson, C. Thomas, K. Findlay et al, 2009) and thus is a good PD marker. The HDEL sequence is a retention signal at the C-term of a protein, maintaining it at the Endoplasmic Reticulum (ER) (V. Gomord, L. Denmat, A. Fitchette-Lainé et al, 1997). The ER and PD localization is in agreement with the tethering hypothesis of the MCTP family, being ER-integral membrane proteins docking to the PM inside the PD pore. Note that this experiment was already performed before the start of the bioinformatics work on NbMCTP11, in order to verify the legitimacy of this protein to be part of the project.

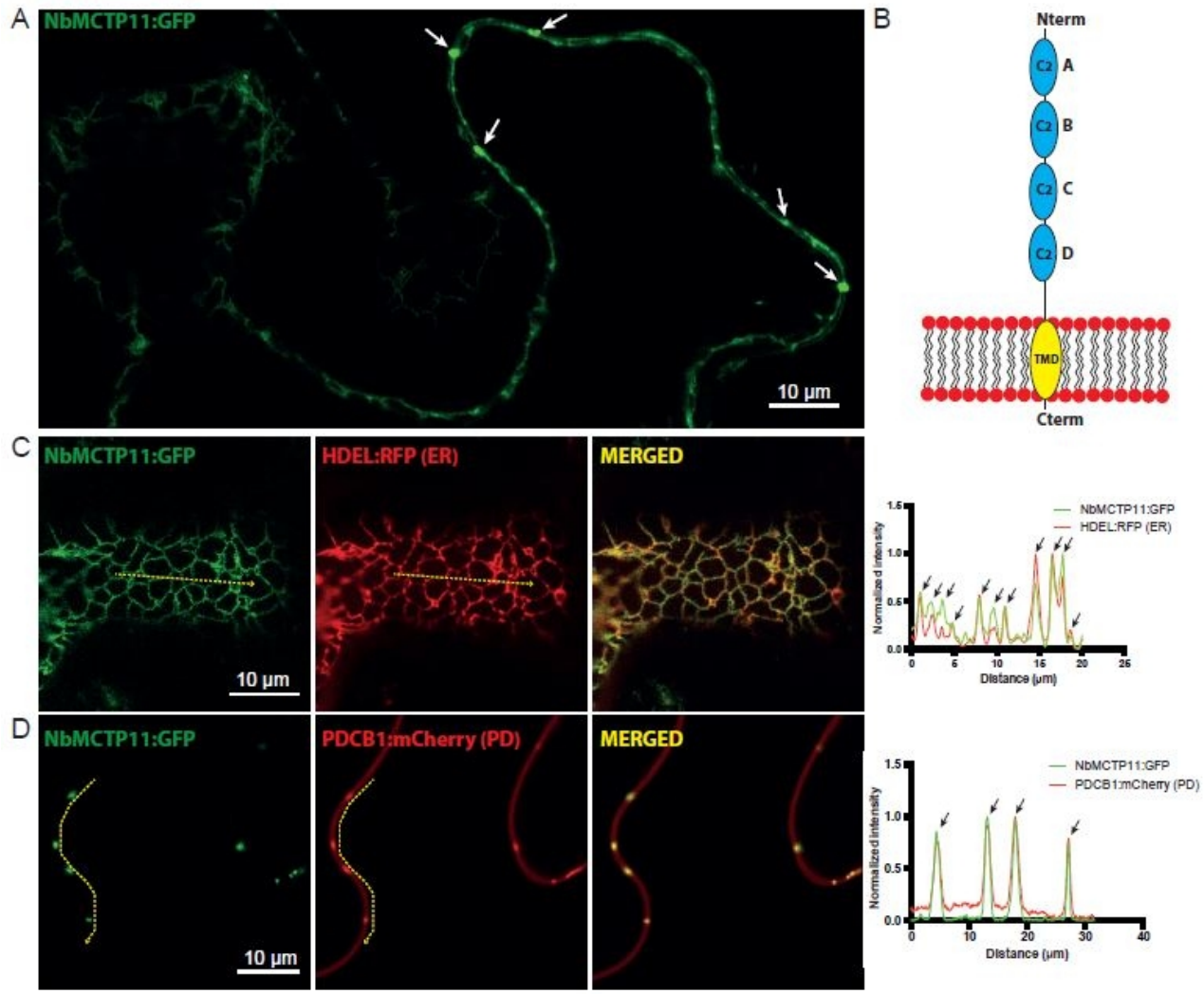

Figure 33: Localization of GFP-NbMCTP11 in *N. benthamiana* epidermal cells visualized by confocal microscopy. (A) NbMCTP11:GFP associates with immobile dots at the cell periphery (*white arrows*) and labels a reticulated network at the cell surface resembling the cortical ER. **(B)** Drawing of the protein architecture with the C2 domain in blue and the TMD region (*yellow*) inserted in a membrane (*red*). **(C)** Cell surface visualization of ER co-localization of NbMCTP11:GFP with the ER marker HDEL:RFP. **(D)** Optical section of PD co-localization of NbMCTP11:GFP with the PD-PM marker PDCB1:mCherry. The right graphs of **(C)** and **(D)** qualifies the co-localization by displaying the normalized intensity of the fluorescence along the dotted *yellow* line shown on the left images. (Figure from M. Brault, F. Immel, W. Nicolas *et al.*, unpublished).

7.2/ Analysis of the NbMCTP11 truncated mutants

Three mutant constructs were analyzed: the transmembrane region alone (TMD), domains C2A to C2C (no C2D nor TMD) and domains C2B to C2C (no C2A, C2D nor TMD). Figure 34 displays the results of their co-localization with HDEL and PDCB1.

Transient expression in *N. benthamiana* leaves showed that the C2A-C and C2B-C mutant constructs (tagged with Yellow Fluorescent Protein; YFP) do not associate with the ER nor PD. The mutants, especially the C2A-B construct, show a blurry pattern that corresponds to cytosolic

location. The blurry but yet ER-like pattern in figure 34A is caused by the greater density of the cytosol around the ER network. The cell edges are uniformly fluorescent and there are no spotty signals that could indicate PD localization. For the C2A-B, the signal at the cell periphery is not well delimited and too thick to correspond to PM but this pattern becomes thinner for C2A-C, suggesting partial membrane docking. Furthermore, the fluorescent signal is very dynamic, in agreement with a cytosolic localization of both constructs.

The TMD mutant show ER co-localization, as the pattern is more refined and perfectly matches the HDEL signal. The edges have two kinds of signal: a dynamic one, corresponding to the ER, and a fixed one, which seems to partially co-localize PD (as shown by co-localization with PDCB1) even if it less well defined (fig. 34B). These are likely to correspond the cortical ER at the proximity of PD rather than specific PD signal.

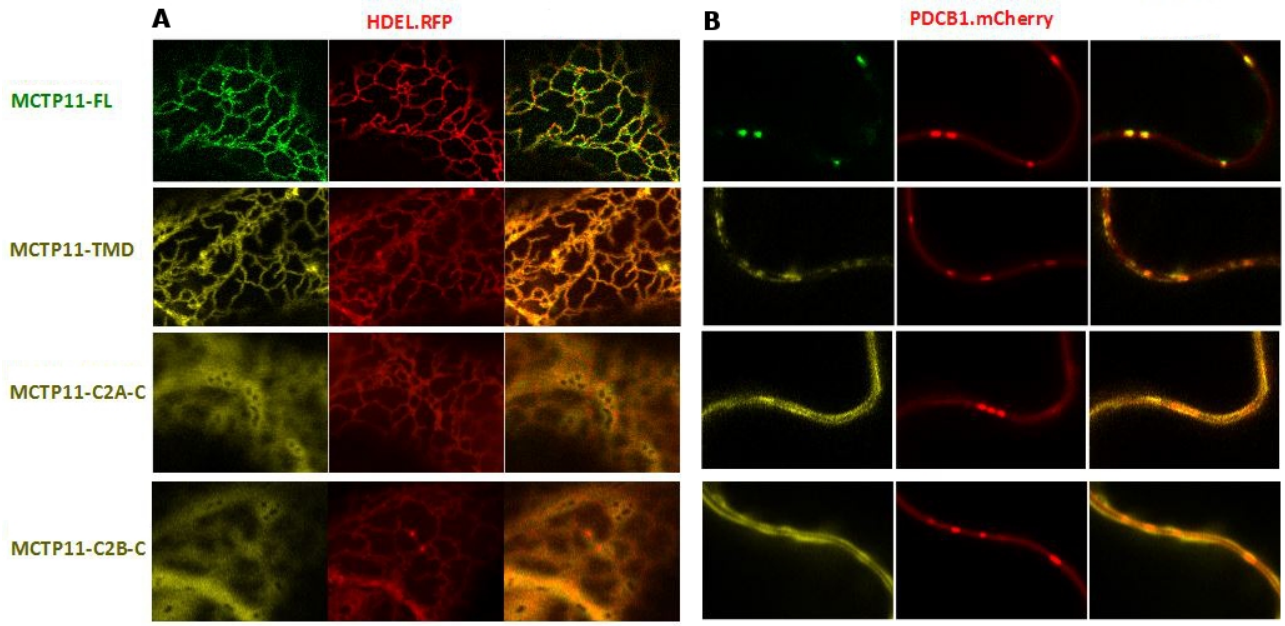

Figure 34: Localization of YFP-NbMCTP11 truncated mutants in *N. benthamiana* epidermal cells visualized by confocal microscopy. (A) Cell surface visualization of ER co-localization of GFP:NbMCTP11 full length and YFP:NbMCTP11 mutants with the ER marker HDEL:RFP. **(B)** Optical section of PD co-localization of GFP:NbMCTP11 and YFP:NbMCTP11 mutants with the PD-PM marker PDCB1:mCherry. (M. Brault, F. Immel, W. Nicolas *et al.*, unpublished)

We observed a significant difference between the C2-only mutants and the TMD mutant. The latter is more similar to the full length protein, since it follows the dynamic ER, but fails to incorporate into PD.

However, we discovered during the *in vivo* experiments that the delimitation of the domains used for the constructs was based on non refined sequence alignments and thus quite approximate. Indeed, the TMD construct was not made of the TMD only: it included the forty last amino acid residues of the C2D domain, which unfortunately correspond to the two β-strands and the loop

involved in the lipid interaction. This issue stops us to draw conclusions about the role of the TMD for now. Further construct, based on the present work, will help to clarify the different roles of each domain from MCTP protein.

Discussion

First of all, C2 domain delimitation is critical for their analysis, as proven by the necessity of complete models for bioinformatics analysis but also by the *in vivo* experiments on truncated mutants. The issue discovered in the NbMCTP11-TMD mutant is a perfect example: wrong delimitation leads to the impossibility to interpret the data properly. MD on the predicted models supports the structure autonomy of individualized C2 domains from whole MCTPs and thus supports the possibility to perform biophysical assays on purified domains.

The C2 domains possess two main characteristics: docking, or lipid interaction, and calcium binding. These typical features can be found individually or combined for each C2 domain but they were studied separately in this work. The docking mechanisms and lipid interactions in *Nicotiana benthamiana* NbMCTP11 and *Arabidopsis thaliana* AtMCTP5 will be discussed first. The calcium-binding abilities as second and the biological assays at last.

1/ Docking and lipid interaction

In a general manner, almost all C2 domains we have studied showed membrane docking during the MD CG simulations but in various manners. Before going in more details about the differences, the docking mechanisms still have common points.

The most common behavior between the C2 domains is that the interaction with the lipid leaflet is relatively superficial and mainly rely on electrostatic interactions involving the polar heads and charged/polar amino acid residues. This shallow interaction doesn't seem to be able to induce membrane curvature, as the APL and membrane thickness were not modified. Docking time seems to vary depending on the domain, but usually occurs in less than 2µs.

We noticed important differences in the way C2 domains of NbMCTP11 interacted with the membrane. The major one is the orientation of the domain, the angle between the protein and the leaflet: C2A is docking via the loops only and thus stays in an upright position whereas C2D is completely flatted since β-strands residues also interact. The C2C domain showed variability in orientation in the different repetitions, suggesting a less defined electrostatic patch. In the case of C2A, the smaller area of contact together with the relatively low penetrance of the loops could explain the lower probability of interaction. Along with that, there was no strong lipid specificity for the main electrostatic patches, since phosphate groups play a significant role in the interactions. However, the nature and arrangement of the interaction still showed slight differences in the contact

distribution between PLPC and PLPS during simulations: C2A interaction is equally distributed between PLPS and PLPC but C2D interacts more with PLPS and C2C interacts more with PLPC. In the C2C CG docking simulation, the fact that C2C interaction in oriented toward neutral lipids can be linked to the non-negligible apolar and aromatic residues (tyrosines) involved in the interaction (fig. 26A; fig. 27A), as mentioned in the literature (D. Murray & B. Honig, 2002). The light and slow docking, in comparison to C2A and C2D, could be due to partial incompatibility with the studied membrane composition and/or ionic environment.

The affinity of the C2D domain for PIP4 lipids is an important information for the tethering hypothesis, as this kind of lipids are specific to the PM (M. Simon, M. Platre, M. Marquès-Bueno *et al.*, 2016). Since the C2D domain is the closest to the TMD and we hypothesize the TMD would rather be in the ER membrane, the tethering of MCTPs could therefore be associated with the newly described type I PD (W. Nicolas, M. Grison, S. Trépout *et al.*, 2017) by maintaining very close contact between ER and PM membranes in 'immature' PD. The density and isosurface analysis show high affinity in the β-groove binding site and lower affinity in the rest of the identified areas of the domain. In either case, the interaction mechanism is dynamic, as PIP4 molecules come and go from the sites, interacting for a more or less long period. Trajectory visualization displayed peculiar behavior in the establishment of multiple PIP4 interactions: PIP4 seem to first dock in and near the β-groove pocket and then gradually toward the loop region. This conduct would need further analysis to pin out what could trigger such a spacio-temporal sequential interaction. Potential position and conformation changes in the side chains and loops respectively may be a reason. We could also verify the role of the α-helix formation in relationship with the PIP4 interaction.

Lack of time made impossible for us to perform docking simulation on all QUIRKY domains or fully analyze the docking mechanism of QKY C2D. However, this domain seems to dock in a similar way as the NbMCTP11 C2D: lying down position and rapid interaction, even if the interaction is not as 'buried' as NbMCTP11. Atomistic structure comparison between the two show global similarity in the basic residues distribution around the domain. Moreover, β-groove residues similarity indicates putative PIP-binding abilities: the important lysines 91 and 94 identified in *N. benthamiana* are found in *A. thaliana* as an arginine and a lysine respectively. PIP4 simulations could reveal the possible impact in affinity of lysine-to-arginine modification in the β-groove pocket.

2/ Calcium binding

The D. Zhang & L. Aravind (2010) statement about the fact that at least one of the two binding regions is functional in each C2 domain seem relevant in the case of NbMCTP11. Indeed,

C2B is the only domain that doesn't show any interaction with the lipids of the membrane but it's nonetheless the first candidate for calcium binding, looking at the first step of the calcium prediction protocol. If the other steps of the protocol prove calcium binding, we could say that all the C2 domains of this MCTP member are functional, even if they don't all interact with the membrane. Calcium-only dependence can be associated with protein conformational changes or trigger specific responses, such as extended synaptotagmin 1 (Y. Saheki & P. De Camilli, 2017). The cationic residues of the C2C domain could also indicate calcium-binding abilities. Calcium-binding site prediction on this domain may give more information about calcium dependence. Calcium-mediated docking is however very difficult to predict. A first glimpse on such an interaction might be given by Adaptative Poisson-Boltzmann Solver (APBS) (S. Unni, Y. Huang, R. Hanson *et al.*, 2011) electrostatic isosurface comparison with and without calcium ions bound to the predicted sites (if there are some), as discussed in literature (D. Murray & B. Honig, 2002). The calcium dependence is a paramount question to investigate regulation-associated mechanisms: MCTPs could regulate the aperture and closure of the PD in a calcium-dependent manner for example. It is also to keep in mind that some C2 domains are able to interact with other proteins, with or without calcium requirement (W. Cho & R. Stahelin, 2006).

About the Human extended synaptotagmin 2 used as prediction control during the protocol establishment, it is interesting to see how FEATURE scores, MD coordination strength and affinity constant (KD1 < 10µM; KD2 = 100-200µM; KD3 = 2-3mM; J. Xu, T. Bacaj, A. Zhou *et al.*, 2014) are coupled. From this, we could estimate the affinity constant of the QKY C2D domain to be around 100µM, based on comparison of the scores and the time of coordination during the simulation.

3/ Biological assays

In vivo experiments on the full length NbMCTP11 prove that the protein localizes at PD and truncated mutants show different phenotypes, revealing different roles of the different parts of the protein. The cytosolic localization of the C2-only mutants (C2A to C2C and C2B to C2C) is in correlation to the relatively weak or non-existent interaction, uncovered by MD, these domains have with the membrane. P. Vaddepalli, A. Herrmann, L. Fulton *et al.* (2014) states that the C-term, starting at the C2C domain, is important for the PD localization. However, our results indicate the C2C domain is not sufficient for the PD localization. The ER-faint PD localization of the partial C2D-TMD mutant is however pointing toward the importance of C2D and/or TMD for the localization. This is interesting since the C2D show the strongest overall interaction and peculiar affinity for PIP4 lipids. Due to the delimitation problem, it is unfortunately impossible to present at the moment a final conclusion about those mutants: additional constructs, especially with the C2D domain are necessary.

Conclusions and Perspectives

Among analyzed C2 domains of QUIRKY/AtMCTP5 and NbMCTP11 some are predicted to interact with calcium, by the mean of aspartate residue cluster in the loop region, some with membrane lipids and some with both. The PLPS/PLPC interaction was mainly mediated through positively charged residues, such as Lysines and Arginines, distributed in electrostatic patches at the surface of the protein. Interaction with PIP4 molecules, a PM-specific lipid essential for cellular signaling, is also observed in the C2D domain of Nb MCTP11 (fig. 35). Further analysis predicted a multiple PIP4 interaction ability, with a main binding site, similar to those of other PIP-binding C2 domains, and several secondary sites.

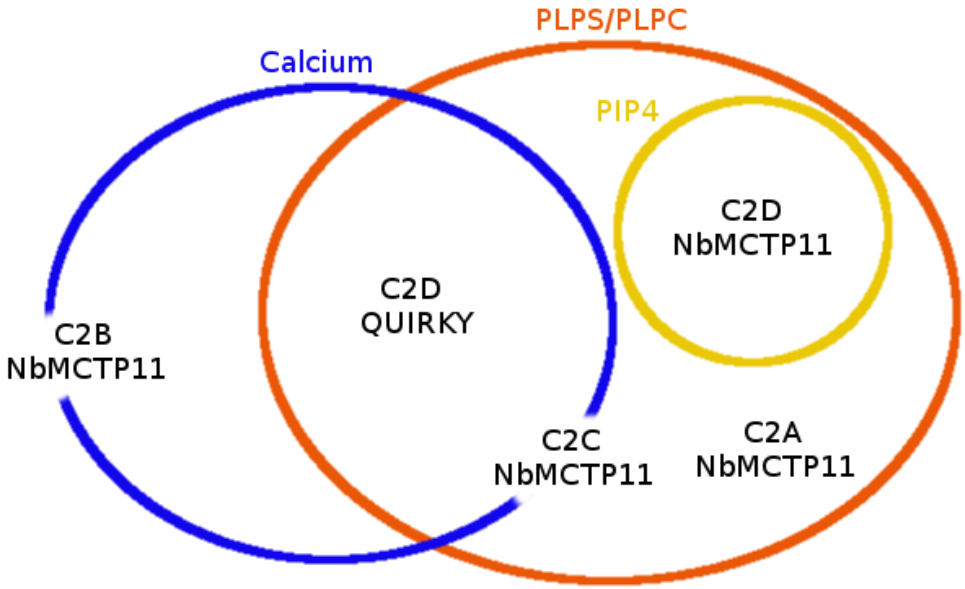

Figure 35: Interactions summary. The analyzed C2 domains seen in interaction types clusters: blue circle for calcium binding prediction, orange circle for PLPS/PLPC membrane docking and yellow circle for PIP4 interaction. Partial inclusion stands for incomplete prediction.

Detailed analysis of the interacting residues enables us to sort out possible key residues responsible for the interactions and use them to verify the predictions by making potential function-deficient MCTP mutants. As calcium-binding relies on loop aspartates, they are target for calcium-binding loss-of-function mutants in QKY/AtMCTP5 C2D domain (D30, D49, D76, D87, D90) and NbMCTP11 C2B domain (D23, D29, D76, D78, D82, D114). Membrane interaction of the C2A domain involves a small area of the protein and thus few residues (R86, R115, R120, S116, K91, K114, I117, F118). Point mutation on the phenylalanine residue 118 could inform us on its role as

apolar anchor in the membrane leaflet. Mutations on the MCTP11 C2D domain would be more difficult, as many polar and apolar residues have significant implication in the lipid interaction (K123, K94, K124, K91, T101, T104, R98, R106, R96, H110…). The PIP4 interaction is however more concentrated on some polar residues (K94, K91, K123, K20, K35, K25, K88, R22, R96, T70, T120). Point mutations in the major binding-site (K94, K91, K35, R96) could be interesting to check if it is the only one (the others could, for example, serve as PIP4 guides toward this pocket) necessary for functional PIP4 binding, i.e. MCTP protein loss of function and/or PD localization.

The many differences observed in the results support the need to do such individual C2 domain analysis, in order to fully understand the interactions properties and mechanisms. Concerning the identified specific features like the PIP-binding pocket, results of the multiple alignment and sequence comparison can bring a first idea on other C2 domains abilities. However, the low sequence identity hinders definitive conclusion without further analysis.

Beyond the NbMCTP11 specific analysis, which gave a first sight into some MCTP C2 domain specificities, the project enables us to set up a guideline analysis on newly discovered and original proteins. Indeed, the protocols and analysis methods established during this work can easily be used, adapted and/or improved for other MCTP C2 domains.

The study of MCTP C2 domains is meant to be continued in both bioinformatic and molecular biology disciplines, among others. Regarding the molecular modeling and dynamics, membrane docking of the domains could be more complete by performing it with more complex but more representative membranes (containing for example PC, PS, sitosterol, PIP, etc). MD on mutants could give an idea on the importance of dedicated amino residues on specific interactions before performing *in vivo* mutants. Refining the calcium prediction, because larger loop conformational changes could better coordinate calcium ions, and establishing a complete calcium dependent membrane docking protocol would be other very interesting perspectives. About the *in vivo* experiments, the direct perspectives from the results explained here are already being or soon to be performed: more truncated mutants are being made, including the C2D domain; PIP-pathway defective mutants experiments to see potential difference in the PD localization of the full length and C2D constructs; purification of individual C2 domains for biophysical assays and perform experiments to test the membrane and/or calcium binding.

Bibliography

Abraham, Mark James, Teemu Murtola, Roland Schulz, Pall Szilard, Jeremy C Smith, Berk Hess, and Erik Lindahl. 2015. “GROMACS : High Performance Molecular Simulations through Multi-Level Parallelism from Laptops to Supercomputers.” *SoftwareX* 1 (2): 19–25. doi:10.1016/j.softx.2015.06.001.

Ananthanarayanan, Bharath, Sudipto Das, Sue Goo Rhee, Diana Murray, and Wonhwa Cho. 2002. “Membrane Targeting of C2 Domains of Phospholipase C-Delta Isoforms.” *The Journal of Biological Chemistry* 277: 3568–75.

Arnarez, C, S J Marrink, and X Periole. 2013. “Identification of Cardiolipin Binding Sites on Cytochrome c Oxidase at the Entrance of Proton Channels.” *Scientific Reports* 3 (1263): 1–8. doi:0.1038/srep01263.

Arnold, Konstantin, Lorenza Bordoli, Jürgen Kopp, and Torsten Schwede. 2006. “Structural Bioinformatics The SWISS-MODEL Workspace : A Web-Based Environment for Protein Structure Homology Modelling.” *Bioinformatics* 22 (2): 195–201. doi:10.1093/bioinformatics/bti770.

Ausili, Alessio, Mattias Berglin, Hans Elwing, Antonio L Egea-jiménez, Senena Corbalán-garcía, and Juan C Gómez-fernández. 2013. “Membrane Docking Mode of the C2 Domain of PKC ε : An Infrared Spectroscopy and FRET Study.” *BBA - Biomembranes* 1828. Elsevier B.V.: 552–60. doi:10.1016/j.bbamem.2012.10.015.

Baker, Sharon F, Roohaida Othman, and David C Wilton. 1998. “Tryptophan-Containing Mutant of Human (Group IIa) Secreted Phospholipase A 2 Has a Dramatically Increased Ability To Hydrolyze Phosphatidylcholine Vesicles.” *Biochemistry* 37: 13203–11.

Ball, Andy, Robert Nielsen, Michael H Gelb, and Bruce H R Obinson. 1999. “Interfacial Membrane Docking of Cytosolic Phospholipase A 2 C2 Domain Using Electrostatic Potential-Modulated Spin.” *PNAS* 96: 6637–42.

Banci, Lucia, Gabriele Cavallaro, Viktoria Kheifets, and Daria Mochly-rosen. 2002. “Molecular Dynamics Characterization of the C2 Domain of Protein Kinase CB *.” *The Journal of Biological Chemistry* 277 (15): 12988–97. doi:10.1074/jbc.M106875200.

Beffa, Roland S, Rose-marie Hofer, Monique Thomas, Frederick Meins, and The Friedrich. 1996. “Decreased Susceptibility to Vira1 Disease of B-1,3-Glucanase-Deficient Plants Generated by Antisense Transformation.” *The Plant Cell* 8: 1001–11.

Benitez-alfonso, Yoselin, Michelle Cilia, Adrianna San Roman, Carole Thomas, Andy Maule, Stephen Hearn, and David Jackson. 2009. “Control of Arabidopsis Meristem Development by Thioredoxin-Dependent Regulation of Intercellular Transport.” *PNAS* 106 (9): 3615–20.

Benitez-alfonso, Yoselin, Christine Faulkner, Ali Pendle, Shunsuke Miyashima, Ykä Helariutta, and Andrew Maule. 2013. “Symplastic Intercellular Connectivity Regulates Lateral Root

Patterning.” *Developmental Cell* 26: 136–47. doi:10.1016/j.devcel.2013.06.010.

Berendsen, Herman J. C., J. P. M. Postma, W. F. van Gunsteren, and J. Hermans. 1981. “Interaction Models for Water in Relation to Protein Hydration.” In *Intermolecular Forces*, 331–42.

Berendsen, Herman J. C., J. V. Postma, W. F. van Gunsteren, A. R. H. J. DiNola, and J. R. Haak. 1984. “Molecular Dynamics with Coupling to an External Bath.” *The Journal of Chemical Physics* 81 (8): 3684–90.

Bergmans, Annette C J, A Douwe De Boer, Jan W M Derksen, and Chris Van Der Schoot. 1997. “The Symplasmic Coupling of L2 -Cells Diminishes in Early Floral Development of Iris.” *Planta* 203: 245–52.

Bilska, Anna, and Pawel Sowinski. 2010. “Closure of Plasmodesmata in Maize (Zea Mays) at Low Temperature : A New Mechanism for Inhibition of Photosynthesis.” *Annals of Botany* 106: 675–86. doi:10.1093/aob/mcq169.

Bittova, Lenka, Marius Sumandea, and Wonhwa Cho. 1999. “A Structure-Function Study of the C2 Domain Cytosolic Phospholipase A2: Identification of Essential Calcium Ligands and Hydrophobic Membrane Binding Residues.” *The Journal of Biological Chemistry* 274: 9665–72.

Brault, Marie, Françoise Immel, William J Nicolas, Amélia Gaston, Jules Petit, J M Crowet, Magali S Grison, et al. 2017. “A Role for Multiple C2 Domains and Transmembrane Region Proteins (MCTPs) in Membrane Tethering at Plasmodesmata.” *Unpublished*.

Brunkard, Jacob O, Anne M Runkel, and Patricia C Zambryski. 2013. “Plasmodesmata Dynamics Are Coordinated by Intracellular Signaling Pathways.” *Current Opinion in Plant Biology* 16 (5). Elsevier Ltd: 614–20. doi:10.1016/j.pbi.2013.07.007.

Brunkard, Jacob O, Anne M Runkel, and Patricia C Zambryski. 2015. “The Cytosol Must Flow : Intercellular Transport through Plasmodesmata.” *Current Opinion in Cell Biology* 35. Elsevier Ltd: 13–20. doi:10.1016/j.ceb.2015.03.003.

Brunkard, Jacob O, and Patricia C Zambryski. 2017. “Plasmodesmata Enable Multicellularity : New Insights into Their Evolution, Biogenesis, and Functions in Development and Immunity.” *Current Opinion in Plant Biology* 35. Elsevier Ltd: 76–83. doi:10.1016/j.pbi.2016.11.007.

Buchan, Daniel W. A., Federico Minneci, Tim C. O. Nugent, Kevin Bryson, and David T. Jones. 2013. “Scalable Web Service for the PSIPRED Protein Analysis Workbench.” *Nucleic Acids Research* 41: 349–57.

Bucher, Gregor L, Corina Tarina, Manfred Heinlein, Francesco Di Serio, Fred Meins, and Victor Alejandro Iglesias. 2001. “Local Expression of Enzymatically Active Class I B-1,3-Glucanase Enhances Symptoms of TMV Infection in Tobacco.” *The Plant Journal* 28 (3): 361–69.

Bunney, Tom D, and Matilda Katan. 2011. “PLC Regulation : Emerging Pictures for Molecular Mechanisms.” *Trends in Biochemical Sciences* 36 (2). Elsevier Ltd: 88–96. doi:10.1016/j.tibs.2010.08.003.

Burch-smith, Tessa M, Solomon Stonebloom, Min Xu, and Patricia C Zambryski. 2011. “Plasmodesmata during Development : Re-Examination of the Importance of Primary, Secondary, and Branched Plasmodesmata Structure versus Function.” *Protoplasma* 248: 61–74. doi:10.1007/s00709-010-0252-3.

Chang, Chi-lun, Ting-sung Hsieh, T Tony Yang, Karen G Rothberg, D Berfin Azizoglu, Elzibeth Volk, Jung-chi Liao, and Jen Liou. 2013. “Feedback Regulation of Receptor-Induced Ca 2 + Signaling Mediated by E-Syt1 and Nir2 at Endoplasmic Reticulum-Plasma Membrane Junctions.” *CellReports* 5. The Authors: 813–25. doi:10.1016/j.celrep.2013.09.038.

Chapman, Edwin R. 2008. “How Does Synaptotagmin Trigger Neurotransmitter Release?” *Annual Review of Biochemistry* 77: 615–41.

Chapman, Edwin R., and Reinhard Jahn. 1994. “Calcium-Dependent Interaction of the Cytoplasmic Region of Synaptotagmin with Membranes. Autonomous Function of a Single C2-Homologous Domain.” *The Journal of Biological Chemistry* 269: 5735–41.

Chavent, Matthieu, Anna L Duncan, and Mark S P Sansom. 2016. “Molecular Dynamics Simulations of Membrane Proteins and Their Interactions : From Nanoscale to Mesoscale.” *Current Opinion in Structural Biology* 40. The Author(s): 8–16. doi:10.1016/j.sbi.2016.06.007.

Chevalier, David, Martine Batoux, Lynette Fulton, Karen Pfister, Ram Kishor Yadav, Maja Schellenberg, and Kay Schneitz. 2005. “STRUBBELIG Defines a Receptor Kinase-Mediated Signaling Pathway Regulating Organ Development in Arabidopsis.” *PNAS* 102 (25): 9074–79.

Cho, Wonhwa, and Robert V Stahelin. 2006. “Membrane Binding and Subcellular Targeting of C2 Domains.” *Biochimica et Biophysica Acta (BBA)* 1761: 838–49. doi:10.1016/j.bbalip.2006.06.014.

Chon, Nara Lee, J Ryan Osterberg, Jack Henderson, Hanif M Khan, Nathalie Reuter, D Knight, and Hai Lin. 2015. “Membrane Docking of the Synaptotagmin 7 C2A Domain: Computation Reveals Interplay between Electrostatic and Hydrophobic Contributions.” *Biochemistry* 54: 5696–5711. doi:10.1021/acs.biochem.5b00421.

Cilia, Michelle Lynn, and David Jackson. 2004. “Plasmodesmata Form and Function.” *Cell Biology* 16: 500–506. doi:10.1016/j.ceb.2004.08.002.

Clark, James D., Lih-Ling Lin, Ronald W. Kriz, Chakkodabylu S. Ramesha, Lisa A. Sultzman, Alice Y. Lin, Nina Milona, and John L. Knopf. 1991. “A Novel Arachidonic Acid-Selective Cytosolic PLA2 Contains a Ca2+-Dependent Translocation Domain with Homology to PKC and GAP.” *Cell* 65 (6): 1043–51.

Corbalan-garcia, Senena, and Juan C Gómez-fernández. 2014. “Signaling through C2 Domains : More than One Lipid Target.” *BBA - Biomembranes* 1838. Elsevier B.V.: 1536–47. doi:10.1016/j.bbamem.2014.01.008.

Crawford, Katrina M, and Patricia C Zambryski. 2000. “Subcellular Localization Determines the Availability of Non-Targeted Proteins to Plasmodesmatal Transport.” *Current Biology* 10: 1032–40.

Creutz, C E, S L Snyder, and T A Schulz. 2004. “Characterization of the Yeast Tricalbins : Membrane-Bound Multi-C2-Domain Proteins That Form Complexes Involved in Membrane Trafficking.” *Cellular and Molecular Life Sciences* 61: 1208–20. doi:10.1007/s00018-004-4029-8.

Cui, Hongchang, Mitchell P Levesque, Teva Vernoux, Jee W Jung, and Alice J Paquette. 2007. “An Evolutionarily Conserved Mechanism Delimiting SHR Movement Defines a Single Layer of Endodermis in Plants.” *Science* 316: 421–25.

Darden, Tom, Darrin York, and Lee Pedersen. 1993. “Particle Mesh Ewald : An N # Log (N) Method for Ewald Sums in Large Systems Particle Mesh Ewald : An N -Log (N) Method for Ewald Sums in Large Systems.” *The Journal of Chemical Physics* 98: 1–5. doi:10.1063/1.464397.

Davletov, B. A., and Thomas C. Südhof. 1993. “A Single C2 Domain from Synaptotagmin I Is Sufficient for High Affinity Ca2+/phospholipid Binding.” *The Journal of Biological Chemistry* 268: 26386–90.

De Storme, Nico, and Danny Geelen. 2014. “Callose Homeostasis at Plasmodesmata : Molecular Regulators and Developmental Relevance.” *Frontiers in Plant Science* 5: 1–23. doi:10.3389/fpls.2014.00138.

Dobnik, David, Spela Baebler, Polona Kogovsek, Marusa Pompe-Novak, Dejan Stebih, Gabriela Panter, Nikolaja Janez, Dany Morrisset, Jana Zel, and Kristina Gruden. 2013. “B-1,3-Glucanase Class III Promotes Spread of PVY NTN and Improves in Planta Protein Production.” *Plant Biotechnology Reports* 7: 547–55. doi:10.1007/s11816-013-0300-5.

Ehlers, K., and R. Kollmann. 2001. “Primary and Secondary Plasmodesmata : Structure, Origin, and Functioning.” *Protoplasma* 216: 1–30.

Ehlers, Katrin, and Rainer Kollmann. 2000. “Synchronization of Mitotic Activity in Protoplast-Derived Solanum Nigrum L . Microcalluses Is Correlated with Plasmodesmal Connectivity.” *Planta* 210: 269–78.

Ehlers, Katrin, and Maike Grobe Westerloh. 2013. “Developmental Control of Plasmodesmata Frequency, Structure, and Function.” In *Symplasmic Transport in Vascular Plants*, 41–82.

Eisenberg-bord, Michal, Nadav Shai, Maya Schuldiner, and Maria Bohnert. 2016. “A Tether Is a Tether Is a Tether : Tethering at Membrane Contact Sites.” *Developmental Cell* 39. Elsevier Inc.: 395–409. doi:10.1016/j.devcel.2016.10.022.

Erickson, Ralph. 1986. “Symplastic Growth and Symplasmic Transport.” *Plant Physiology* 82: 1153.

Faulkner, Christine, Ozgur E Akman, Karen Bell, Chris Jeffree, and Karl Oparka. 2008. “Peeking into Pit Fields : A Multiple Twinning Model of Secondary Plasmodesmata Formation in Tobacco.” *The Plant Cell* 20: 1504–18. doi:10.1105/tpc.107.056903.

Faulkner, Christine, and Emmanuelle M F Bayer. 2017. “Isolation of Plasmodesmata.” In *Isolation of Plant Organelles and Structures*, 187–98.

Faure, Guilhem, and Isabelle Callebaut. 2013. “Sequence Analysis Identification of Hidden Relationships from the Coupling of Hydrophobic Cluster Analysis and Domain Architecture Information.” *Bioinformatics* 29 (14): 1726–33. doi:10.1093/bioinformatics/btt271.

Fernández-busnadiego, Rubén, Yasunori Saheki, and Pietro De Camilli. 2015. “Three-Dimensional Architecture of Extended Reticulum – Plasma Membrane Contact Sites.” *PNAS*. doi:10.1073/pnas.1503191112.

Fernandez-calvino, Lourdes, Christine Faulkner, John Walshaw, Gerhard Saalbach, Yoselin Benitez-alfonso, and Andrew Maule. 2011. “Arabidopsis Plasmodesmal Proteome.” *Plos One* 6 (4). doi:10.1371/journal.pone.0018880.

Foreman, Julia, Vadim Demidchik, John H. F. Bothwell, Panagiota Mylona, Henk Miedema, Miguel Angel Torres, Paul Linstead, et al. 2003. “Reactive Oxygen Species Produced by NADPH Oxidase Regulate Plant Cell Growth.” *Nature* 422: 442–46.

Frazier, April A, Mark A Wisner, Nathan J Malmberg, Kenneth G Victor, Gail E Fanucci, Eric A Nalefski, Joseph J Falke, and David S Cafiso. 2002. “Membrane Orientation and Position of the C2 Domain from cPLA2 by Site-Directed Spin Labeling.” *Biochemistry* 41: 6282–92.

Fulton, Lynette, Martine Batoux, Prasad Vaddepalli, Ram Kishor, Wolfgang Busch, Stig U. Andersen, Sangho Jeong, Jan U. Lohmann, and Kay Schneitz. 2009. “DETORQUEO, QUIRKY, and ZERZAUST Represent Novel Components Involved in Organ Development Mediated by the Receptor-Like Kinase STRUBBELIG in Arabidopsis Thaliana.” *Plos Genetics* 5 (1). doi:10.1371/journal.pgen.1000355.

Furt, Fabienne, Sabine König, Jean-jacques Bessoule, Françoise Sargueil, Rémi Zallot, Thomas Stanislas, Elodie Noirot, et al. 2010. “Polyphosphoinositides Are Enriched in Plant Membrane Rafts and Form Microdomains in the.” *Plant Physiology* 152: 2173–87. doi:10.1104/pp.109.149823.

Gaboriaud, C., V Bissery, T. Benchetrit, and J. P. Mornon. 1987. “Hydrophobic Cluster Analysis : An Efficient New Way to Compare and Analyse Amino Acid Sequences.” *FEBS Letters* 224 (1): 149–55.

Gelb, Michael H, Wonhwa Cho, and David C Wilton. 1999. “Interfacial Binding of Secreted Phospholipases Electrostatics and a Major Role for Tryptophan A 2: More than.” *Current Opinion in Structural Biology* 9: 428–32.

Giordano, Francesca, Yasunori Saheki, Olof Idevall-hagren, Sara Francesca Colombo, Michelle Pirruccello, Ira Milosevic, Elena O Gracheva, Sviatoslav N Bagriantsev, Nica Borgese, and Pietro De Camilli. 2013. “PI(4,5)P2-Dependent and Ca^{2+}-Regulated ER-PM Interactions Mediated by the Extended Synaptotagmins.” *CELL* 153. Elsevier: 1494–1509. doi:10.1016/j.cell.2013.05.026.

Gisel, Andreas, Sandra Barella, Frederick D Hempel, and Patricia C Zambryski. 1999. “Temporal and Spatial Regulation of Symplastic Trafficking during Development in Arabidopsis Thaliana Apices.” *Development* 126: 1879–89.

Gisel, Andreas, Frederick D Hempel, Sandra Barella, and Patricia Zambryski. 2002. “Leaf-to-Shoot Apex Movement of Symplastic Tracer Is Restricted Coincident with Flowering in *Arabidopsis*.” *PNAS* 99 (3): 1713–17.

Globisch, Christoph, Venkatramanan Krishnamani, Markus Deserno, and Christine Peter. 2013. “Optimization of an Elastic Network Augmented Coarse Grained Model to Study CCMV Capsid Deformation.” *Plos One* 8 (4). doi:10.1371/journal.pone.0060582.

Glover, Louise, and Robert H Brown Jr. 2007. “Dysferlin in Membrane Trafficking and Patch Repair.” *Traffic* 8: 785–94. doi:10.1111/j.1600-0854.2007.00573.x.

Gomord, Véronique, Lise-Anne Denmat, Anne-Catherine Fitchette-Lainé, Béatrice Satiat-Jeunemaitre, Chris Hawes, and Loïc Faye. 1997. “The C-Terminal HDEL Sequence Is Sufficient for Retention of Secretory Proteins in the Endoplasmic Reticulum (ER) but Promotes Vacuolar Targeting of Proteins That Escape the ER.” *The Plant Cell* 11 (2): 313–25.

Goodwin, P B. 1983. “Molecular Size Limit for Movement in the Symplast of the Elodea Leaf.” *Planta* 157: 124–30.

Gowers, Richard J., Max Linke, Jonathan Barnoud, Tyler J. E. Reddy, Manuel N. Melo, S. L. Seyler, D. L. Dotson, et al. 2016. “MDAnalysis: A Python Package for the Rapid Analysis of Molecular Dynamics Simulations.” In *Proceedings of the 15th Python in Science Conference*, edited by In S. Benthall and S. Rostrup, 102–9. Austin, TX: SciPy.

Gradilla, Ana-citlali, and Isabel Guerrero. 2013. “Cytoneme-Mediated Cell-to-Cell Signaling during Development.” *Cell and Tissue Research* 352 (1): 59–66. doi:10.1007/s00441-013-1578-x.

Grison, Magali S, Lysiane Brocard, Laetitia Fouillen, William Nicolas, Vera Wewer, and Peter Dörmann. 2015. “Specific Membrane Lipid Composition Is Important for Plasmodesmata Function in *Arabidopsis*.” *The Plant Cell* 27: 1228–50. doi:10.1105/tpc.114.135731.

Grobler, Jay A., Lars-Oliver Essen, Roger L. Williams, and James H. Hurley. 1996. “C2 Domain Conformational Changes in Phospholipase C-delta1.” *Nature Structural Biology* 3 (9): 788–95.

Guenoune-gelbart, Dana, Michael Elbaum, Guy Sagi, Amit Levy, and Bernard L Epel. 2008. “Tobacco Mosaic Virus (TMV) Replicase and Movement Protein Function Synergistically in Facilitating TMV Spread by Lateral Diffusion in the Plasmodesmal Desmotubule of *Nicotiana Benthamiana*.” *Molecular Plant-Microbe Interactions* 21 (3): 335–45.

Guerrero-valero, Marta, Cristina Ferrer-orta, Jordi Querol-audí, Consuelo Marin-vicente, Ignacio Fita, Juan C. Gomez-Fernandez, Nuria Verdaguer, and Senena Corbalán-garcía. 2009. “Structural and Mechanistic Insights into the Association of PKCa-C2 Domain to PtdIns (4,5) P2.” *PNAS* 106 (16): 6603–7.

Guerrero-valero, Marta, Consuelo Marín-vicente, Juan C Gómez-fernández, and Senena Corbalán-garcía. 2007. “The C2 Domains of Classical PKCs Are Specific PtdIns (4,5)P2 -Sensing Domains with Different Affinities for Membrane Binding.” *Journal of Molecular Biology* 371: 608–21. doi:10.1016/j.jmb.2007.05.086.

Guex, Nicolas, and Manuel C Peitsch. 1997. “SWISS-MODEL and the Swiss-PdbViewer : An Environment for Comparative Protein Modeling.” *Electrophoresis* 18: 2714–23.

Guillen, Jaime, Cristina Ferrer-orta, Monica Buxaderas, Dolores Pérez-Sanchez, Marta Guerrero-valero, Ginés Luengo-Gill, Joan Pous, et al. 2013. “Structural Insights into the Ca^{2+} and PI(4,5)P2 Binding Modes of the C2 Domains of Rabphilin 3A and Synaptotagmin 1.” *PNAS* 110 (51): 20503–8. doi:10.1073/pnas.1316179110.

Gustavsson, Natalia, and Weiping Han. 2009. “Calcium-Sensing beyond Neurotransmitters : Functions of Synaptotagmins in Neuroendocrine and Endocrine Secretion.” *Bioscience Report* 29 (4): 245–59. doi:10.1042/BSR20090031.

Hammond, Gerald R V, Michael J Fischer, Karen E Anderson, Jon Holdich, Ardita Koteci, Tamas Balla, and Robin F Irvine. 2012. “PI4P and PI(4,5)P2 Are Essential But Independent Lipid Determinants of Membrane Identity.” *Science* 337: 727–30.

Han, Dai, Shin Ok-Ho, Mischa Machius, Diana R. Tomchick, Thomas C. Südhof, and Josep Rizo. 2004. “Structural Basis for the Evolutionary Inactivation of Ca2+ Binding to Synaptotagmin 4.” *Nature Structural & Molecular Biology* 11 (9): 844–49.

Han, Sang Kyou, Kwang Pyo Kim, Rao Koduri, Lenka Bittova, Nilda M. Munoz, R. Leff, Alan, David C. Wilton, Michael H Gelb, and Wonhwa Cho. 1999. “Roles of TRP31 in High Membrane Binding and Proinflammatory Activity of Human Group V Phospholipase A2.” *The Journal of Biological Chemistry* 274: 11881–88.

Helle, Sebastian C J, Gil Kanfer, Katja Kolar, Alexander Lang, Agnès H Michel, and Benoît Kornmann. 2013. “Organization and Function of Membrane Contact Sites.” *Biochimica et Biophysica Acta (BBA)* 1833. Elsevier B.V.: 2526–41. doi:10.1016/j.bbamcr.2013.01.028.

Henne, W Mike, Jen Liou, and Scott D Emr. 2015. “Molecular Mechanisms of Inter-Organelle ER – PM Contact Sites.” *Current Opinion in Cell Biology* 35. Elsevier Ltd: 123–30. doi:10.1016/j.ceb.2015.05.001.

Hess, Berk, Henk Bekker, Herman J. C. Berendsen, and Johannes G E M Fraaije. 1997. “LINCS : A Linear Constraint Solver for Molecular Simulations.” *The Journal of Computational Chemistry* 18: 1463–72.

Holdaway-clarke, Terena L, N Alan Walker, Peter K Hepler, and Robyn L Overall. 2000. “Physiological Elevations in Cytoplasmic Free Calcium by Cold or Ion Injection Result in Transient Closure of Higher Plant Plasmodesmata.” *Planta* 210: 329–35.

Huang, Jing, and Alexander D Mackerell Jr. 2013. “CHARMM36 All-Atom Additive Protein Force Field : Validation Based on Comparison to NMR Data.” *Journal of Computational Chemistry* 34: 2135–45. doi:10.1002/jcc.23354.

Humphrey, William, Andrew Dalke, and Klaus Schulten. 1996. “VMD : Visual Molecular Dynamics.” *Journal of Molecular Graphics* 14: 33–38.

Iglesias, Victor Alejandro, and Frederick Meins. 2000. “Movement of Plant Viruses Is Delayed in a B-1,3-Glucanase- de ® Cient Mutant Showing a Reduced Plasmodesmatal Size Exclusion Limit and Enhanced Callose Deposition.” *The Plant Journal* 21 (2): 157–66.

Jorgensen, W. L., J. Chandrasekhar, J. D. Madura, R. W. Impey, and M. L. Klein. 1983. "Comparison of Simple Potential Functions for Simulating Liquid Water." *The Journal of Chemical Physics* 79 (2): 926–35.

Kabsch, Wolfgang, and Christian Sander. 1983. "Dictionary of Protein Secondary Structure: Pattern Recognition of Hydrogen-Bonded and Geometrical Features." *Biopolymers* 22 (12): 2577–2637.

Kim, David E, Dylan Chivian, and David Baker. 2004. "Protein Structure Prediction and Analysis Using the Robetta Server." *Nucleic Acids Research* 32: 526–31. doi:10.1093/nar/gkh468.

Kim, I., F.D Hempel, K. Sha, J. Pfluger, and Patricia C Zambryski. 2002. "Identification of a Developmental Transition in Plasmodesmatal Function during Embryogenesis in *Arabidopsis thaliana*." *Development* 129 (5): 1261–72.

Kim, Insoon, Euna Cho, Katrina Crawford, Frederick D Hempel, and Patricia C Zambryski. 2005. "Cell-to-Cell Movement of GFP during Embryogenesis and Early Seedling Development in *Arabidopsis*." *PNAS* 102 (6): 2227–31.

Kim, Insoon, Ken Kobayashi, Euna Cho, and Patricia C Zambryski. 2005. "Subdomains for Transport via Plasmodesmata Corresponding to the Apical – Basal Axis Are Established during *Arabidopsis* Embryogenesis." *PNAS* 102 (33): 11945–50.

Kim, Insoon, and Patricia C Zambryski. 2005. "Cell-to-Cell Communication via Plasmodesmata during *Arabidopsis* Embryogenesis." *Current Opinion in Plant Biology* 8: 593–99. doi:10.1016/j.pbi.2005.09.013.

Knox, J Paul, and Yoselin Benitez-alfonso. 2014. "Roles and Regulation of Plant Cell Walls Surrounding Plasmodesmata." *Current Opinion in Plant Biology* 22. Elsevier Ltd: 93–100. doi:10.1016/j.pbi.2014.09.009.

Knox, Kirsten, Pengwei Wang, Verena Kriechbaumer, Jens Tilsner, Lorenzo Frigerio, Imogen Sparkes, Chris Hawes, and Karl Oparka. 2015. "Putting the Squeeze on Plasmodesmata : A Role for Reticulons in Primary Plasmodesmata Formation 1." *Plant Physiology* 168: 1563–72. doi:10.1104/pp.15.00668.

Kobayashi, Ken, Marisa S Otegui, Sujatha Krishnakumar, Michael Mindrinos, and Patricia Zambryski. 2007. "INCREASED SIZE EXCLUSION LIMIT2 Encodes a Putative DEVH Box RNA Helicase Involved in Plasmodesmata Function during *Arabidopsis* Embryogenesis." *The Plant Cell* 19: 1885–97. doi:10.1105/tpc.106.045666.

Köhler, Piotr, and Denis J Carr. 2006. "A Somewhat Obscure Discoverer of Plasmodesmata : Eduard Tangl (1848 – 1905)." In *2nd ICESHS*, edited by M. Kokowski, 208–11. Cracow.

Kohout, Susy C, Senena Corbalan-garcia, Juan C. Gomez-Fernandez, and Joseph J Falke. 2003. "C2 Domain of Protein Kinase C R : Elucidation of the Membrane Docking Surface by Site-Directed Fluorescence and Spin Labeling." *Biochemistry* 42: 1254–65.

Kopec, Klaus O, Vikram Alva, and Andrei N Lupas. 2010. "Homology of SMP Domains to the TULIP Superfamily of Lipid-Binding Proteins Provides a Structural Basis for Lipid Exchange between ER and Mitochondria" 26 (16): 1927–31. doi:10.1093/bioinformatics/btq326.

Kopp, Jürgen, and Torsten Schwede. 2004. “Automated Protein Structure Homology Modeling: A Progress Report.” *Pharmacogenomics* 5 (4): 405–16.

Kwak, Su-Hwan, Ronglai Shen, and John Schiefelbein. 2005. “Positional Signaling Mediated by a Receptor-like Kinase in *Arabidopsis*.” *Science* 307 (5712): 1111–13.

Lai, Chun-liang, Kyle E Landgraf, Gregory A Voth, and Joseph J Falke. 2010. “Membrane Docking Geometry and Target Lipid Stoichiometry of Membrane-Bound PKC α C2 Domain : A Combined Molecular Dynamics and Experimental Study.” *Journal of Molecular Biology* 402. Elsevier Ltd: 301–10. doi:10.1016/j.jmb.2010.07.037.

Lee, Ji-young, Juliette Colinas, Jean Y Wang, Daniel Mace, Uwe Ohler, and Philip N Benfey. 2006. “Transcriptional and Posttranscriptional Regulation of Transcription Factor Expression in *Arabidopsis* Roots.” *PNAS* 103 (15): 6055–60.

Lee, Jung-youn, Xu Wang, Weier Cui, Ross Sager, Shannon Modla, Kirk Czymmek, Boris Zybaliov, et al. 2011. “A Plasmodesmata-Localized Protein Mediates Crosstalk between Cell-to-Cell Communication and Innate Immunity in *Arabidopsis*.” *The Plant Cell* 23: 3353–73. doi:10.1105/tpc.111.087742.

Levy, Amit, Judy Y Zheng, and Sondra G Lazarowitz. 2015. “Synaptotagmin SYTA Forms ER-Plasma Membrane Junctions That Are Recruited to Plasmodesmata for Plant Virus Movement.” *Current Biology* 25. Elsevier Ltd: 2018–25. doi:10.1016/j.cub.2015.06.015.

Lins, Laurence, Alain Couvineau, Christiane Rouyer-Fessard, Pascal Nicole, Jean-José Maoret, Moussa Benhamed, Robert Brasseur, Annick Thomas, and Marc Laburthe. 2001. “The Human VPAC1 Receptor: Three-Dimensional Model and Mutagenesis of the N-Terminal Domain.” *The Journal of Biological Chemistry* 276: 10153–60.

Liu, Lu, Chang Liu, Xingliang Hou, Wanyan Xi, Lisha Shen, Zhen Tao, Yue Wang, and Hao Yu. 2012. “FTIP1 Is an Essential Regulator Required for Florigen Transport.” *Plos Biology* 10 (4).

Lopez-Saez, J.F., G. Giménez-Martin, and M.C. Risueno. 1966. “Fine Structure of the Plasmodesm.” *Protoplasma* 61: 81–84.

Lucas, William J, and Jung-youn Lee. 2004. “Plasmodesmata as a Supracellular Control Network in Plants.” *Nature Reviews* 5: 712–27. doi:10.1038/nrm1470.

Malkova, Sarka, Fei Long, Robert V. Stahelin, Sai V. Pingali, Diana Murray, Wonhwa Cho, and Mark L. Schlossman. 2005. “X-Ray Reflectivity Studies of cPLA 2 Alpha -C2 Domains Adsorbed onto Langmuir Monolayers of SOPC.” *Biophysical Journal* 89: 1861–73. doi:10.1529/biophysj.105.061515.

Malmberg, Nathan J, David R Van Buskirk, and Joseph J Falke. 2003. “Membrane-Docking Loops of the cPLA2 C2 Domain : Detailed Structural Analysis of the Protein-Membrane Interface via Site-Directed Spin-Labeling.” *Biochemistry* 42: 13227–40.

Malmersjö, Seth, and Tobias Meyer. 2013. “Inside-Out Connections : The ER Meets the Plasma Membrane.” *Cell* 153: 1423–24. doi:10.1016/j.cell.2013.05.054.

Manna, Debasis, Nitin Bhardwaj, Mohsin S. Vora, Robert V. Stahelin, Hui Lu, and Wonhwa Cho. 2008. “Differential Roles of Phosphatidylserine, PtdIns (4,5)P2, and PtdIns (3,4,5)P3 in Plasma Membrane Targeting of C2 Domains.” *The Journal of Biological Chemistry* 283 (38): 26047–58. doi:10.1074/jbc.M802617200.

Manford, Andrew G, Christopher J Stefan, Helen L Yuan, Jason A Macgurn, and Scott D Emr. 2012. “Article ER-to-Plasma Membrane Tethering Proteins Regulate Cell Signaling and ER Morphology.” *Developmental Cell* 23 (6). Elsevier Inc.: 1129–40. doi:10.1016/j.devcel.2012.11.004.

Marrink, Siewert J, Herre J Risselada, Serge Yefimov, D. Peter Tieleman, and Alex H de Vries. 2007. “The MARTINI Force Field: Coarse Grained Model for Biomolecular Simulations.” *Journal of Physical Chemistry B* 111: 7812–24.

Maule, Andrew J, Rocio Gaudioso-pedraza, Yoselin Benitez-alfonso, Andrew J Maule, Rocio Gaudioso-pedraza, and Yoselin Benitez-alfonso. 2013. “Callose Deposition and Symplastic Connectivity Are Regulated prior to Lateral Root Emergence Callose Deposition and Symplastic Connectivity Are Regulated prior to Lateral Root Emergence.” *Communicative & Integrative Biology* 6 (6). doi:10.4161/cib.26531.

McLaughlin, Stuart, and Diana Murray. 2005. “Plasma Membrane Phosphoinositide Organization by Protein Electrostatics.” *Nature* 438: 605–11.

Medkova, Martina, and Wonhwa Cho. 1998. “Mutagenesis of the C2 Domain of Protein Kinase C-Alpha: Differential Roles of Ca^{2+} Ligands and Membrane Binding Residues.” *The Journal of Biological Chemistry* 273: 17544–52.

Michaud-Agrawal, Naveen, Elizabeth J. Denning, Thomas B. Woolf, and Oliver Beckstein. 2011. “MDAnalysis: A Toolkit for the Analysis of Molecular Dynamics Simulations.” *Journal of Computational Chemistry* 32: 2319–27.

Murray, Diana, and Barry Honig. 2002. “Electrostatic Control of the Membrane Targeting of C2 Domains.” *Molecular Cell* 9: 145–54.

Nalefski, Eric A, and Joseph J Falke. 1996. “The C2 Domain Calcium-Binding Motif : Structural and Functional Diversity.” *Protein Science* 5: 2375–90.

Nalefski, Eric A, Lisa A. Sultzman, D. M. Martin, Ronald W. Kriz, P. S. Towler, John L. Knopf, and James D. Clark. 1994. “Delineation of Two Functionally Distinct Domains of Cytosolic Phospholipase A2, a Regulatory Ca(2+)-Dependent Lipid-Binding Domain and a Ca(2+)-Independent Catalytic Domain.” *The Journal of Biological Chemistry* 269: 18239–49.

Newton, Alexandra C. 1995. “Protein Kinase C : Structure, Function, and Regulation.” *The Journal of Biological Chemistry* 270 (48): 28495–98.

Nicolas, William J, Magali S Grison, Sylvain Trépout, Amélia Gaston, Mathieu Fouché, Fabrice P Cordelières, Karl Oparka, Jens Tilsner, Lysiane Brocard, and Emmanuelle M Bayer. 2017. “Architecture and Permeability of Post-Cytokinesis Plasmodesmata Lacking Cytoplasmic Sleeves.” *Nature Plants* 3. Nature Publishing Group. doi:10.1038/nplants.2017.82.

Oparka, Karl J, Alison G Roberts, Petra Boevink, Simon Santa Cruz, Ian Roberts, Katja S Pradel, Astrid Imlau, Guy Kotlizky, Norbert Sauer, and Bernard Epel. 1999. “Simple, but Not Branched, Plasmodesmata Allow the Nonspecific Trafficking of Proteins in Developing Tobacco Leaves.” *Cell* 97: 743–54.

Ormenese, Sandra, Andrée Havelange, Georges Bernier, and Chris van der Schoot. 2002. “The Shoot Apical Meristem of *Sinapis alba* L. Expands Its Central Symplasmic Field during the Floral Transition.” *Planta* 215: 67–78. doi:10.1007/s00425-002-0746-0.

Ormenese, Sandra, Andrée Havelange, Roger Deltour, and Georges Bernier. 2000. “The Frequency of Plasmodesmata Increases Early in the Whole Shoot Apical Meristem of *Sinapis alba* L. during ¯ Oral Transition.” *Planta* 211: 370–75.

Otegui, Marisa S, Koen J Verbrugghe, and Ahna R Skop. 2005. “Midbodies and Phragmoplasts : Analogous Structures Involved in Cytokinesis.” *Trends in Cell Biology* 15 (8): 404–13. doi:10.1016/j.tcb.2005.06.003.

Overall, Robyn L, Danny Y T Liu, and Deborah A Barton. 2006. “Plasmodesmata : New Perspectives on Old Questions.” In *Symplasmic Transport in Vascular Plants*, edited by K. Sokolowska and P. Sowinski, 217–44. New York: Springer Science. doi:10.1007/978-1-4614-7765-5.

Palevitz, B A, and P K Hepler. 1985. “Changes in Dye Coupling of Stomatal Cells of Allium and Commelina Demonstrated by Microinjection of Lucifer Yellow.” *Planta* 164: 473–79.

Parrinello, M., and A. Rahman. 1981. “Polymorphic Transitions in Single Crystals: A New Molecular Dynamics Method.” *Journal of Applied Physics* 52 (12): 7182–90.

Paultre, Danae Simone Genevieve, Marie-paule Gustin, Attila Molnar, and J Karl. 2016. “Lost in Transit : Long-Distance Trafficking and Phloem Unloading of Protein Signals in *Arabidopsis* Homografts.” *Plant Cell*. doi:10.1105/tpc.16.00249.

Pérez-lara, Ángel, and Reinhard Jahn. 2015. “Extended Synaptotagmins (E-Syts): Architecture and Dynamics of Membrane Contact Sites Revealed.” *PNAS* 112 (16): 4837–38. doi:10.1073/pnas.1504487112.

Pérez-sancho, Jessica, Jens Tilsner, A Lacey Samuels, Miguel A Botella, Emmanuelle M Bayer, and Abel Rosado. 2016. “Stitching Organelles : Organization and Function of Specialized Membrane Contact Sites in Plants.” *Trends in Cell Biology* 26 (9). Elsevier Ltd: 705–17. doi:10.1016/j.tcb.2016.05.007.

Pérez-sancho, Jessica, Steffen Vanneste, Eunkyoung Lee, Heather E Mcfarlane, Alicia Esteban del Valle, Victoriano Valpuesta, Jiri Friml, Miguel A Botella, and Abel Rosado. 2015. “The *Arabidopsis* Synaptotagmin1 Is Enriched in Endoplasmic Reticulum-Plasma Membrane Contact Sites and Confers Cellular Resistance to Mechanical Stresses.” *Plant Physiology* 168: 132–43. doi:10.1104/pp.15.00260.

Periole, X, and Siewert J Marrink. 2013. “The Martini Coarse-Grained Force Field.” In *Biomolecular Simulations*, 533–65.

Periole, Xavier, Marco Cavalli, Siewert-jan Marrink, and Marco A Ceruso. 2009. “Combining an Elastic Network With a Coarse-Grained Molecular Force Field : Structure, Dynamics, and Intermolecular Recognition.” *Journal of Chemical Theory and Computation* 5: 2531–43.

Pickard, W. F. 2003. “The Role of Cytoplasmic Streaming in Symplastic Transport.” *Plant, Cell and Environment* 26: 1–15.

Prinz, William A. 2012. “Bridging the Gap : Membrane Contact Sites in Signaling, Metabolism, and Organelle Dynamics.” *The Journal of Cell Biology* 205 (6): 759–69. doi:10.1083/jcb.201401126.

Radford, Janine E, and Rosemary G White. 2011. “Inhibitors of Myosin, but Not Actin, Alter Transport through Tradescantia Plasmodesmata.” *Protoplasma* 248: 205–16. doi:10.1007/s00709-010-0244-3.

Ramachandran, G.N., C. Ramakrishnan, and V. Sasisekharan. 1963. “Stereochemistry of Polypeptide Chain Configurations.” *Journal of Molecular Biology* 7 (1): 95–99.

Raven, John A. 2005. “Evolution of Plasmodesmata.” In *Annual Plant Reviews, Plasmodesmata*, 33–52.

Roberts, A G, and K J Oparka. 2003. “Plasmodesmata and the Control of Symplastic Transport.” *Plant, Cell and Environment* 26: 103–24.

Rouse, Sarah, Timothy Carpenter, and Mark S. Sansom. 2010. “Coarse-Grained Molecular Dynamics Simulations of Membrane Proteins.” In *Molecular Simulations and Biomembranes: From Biophysics to Function*, 56–75.

Sager, Ross, and Jung-youn Lee. 2014. “Plasmodesmata in Integrated Cell Signalling : Insights from Development and Environmental Signals and Stresses.” *Journal of Experimental Botany* 65 (22): 6337–58. doi:10.1093/jxb/eru365.

Saheki, Yasunori, and Pietro De Camilli. 2017. “The Extended-Synaptotagmins.” *BBA-Molecular Cell Research* 1864 (9). Elsevier: 1490–93. doi:10.1016/j.bbamcr.2017.03.013.

Salmon, Magali S, and Emmanuelle M F Bayer. 2013. “Dissecting Plasmodesmata Molecular Composition by Mass Spectrometry-Based Proteomics.” *Frontiers in Plant Science* 3: 1–8. doi:10.3389/fpls.2012.00307.

Schapire, Arnaldo L., Boris Voigt, Jan Jasik, Abel Rosado, Rosa Lopez-Cobollo, Diedrik Menzel, Julio Salinas, et al. 2008. “*Arabidopsis* Synaptotagmin 1 Is Required for the Maintenance of Plasma Membrane Integrity and Cell Viability.” *The Plant Cell* 20: 3374–88. doi:10.1105/tpc.108.063859.

Schapire, Arnaldo L, Victoriano Valpuesta, and Miguel A Botella. 2009. “Plasma Membrane Repair in Plants.” *Trends in Plant Science* 14 (12): 645–52. doi:10.1016/j.tplants.2009.09.004.

Schauder, Curtis M, Xudong Wu, Yasunori Saheki, Pradeep Narayanaswamy, Federico Torta, Markus R. Wenk, Pietro De Camilli, and Karin M Reinisch. 2014. “Structure of a Lipid-Bound Extended-Synaptotagmin Indicates a Role in Lipid Transfer.” *Nature* 510 (7506): 552–55. doi:10.1038/nature13269.Structure.

Schauder, Curtis M, Xudong Wu, Yasunori Saheki, Pradeep Narayanaswamy, Federico Torta, Markus R Wenk, Pietro De Camilli, and Karin M Reinisch. 2014. “Structure of a Lipid-Bound Extended Synaptotagmin Indicates a Role in Lipid Transfer.” *Nature* 510. Nature Publishing Group: 552–55. doi:10.1038/nature13269.

Schiefelbein, John, Ling Huang, and Xiaohua Zheng. 2014. “Regulation of Epidermal Cell Fate in *Arabidopsis* Roots : The Importance of Multiple Feedback Loops LATERAL INHIBITION.” *Frontiers in Plant Science* 5: 1–4. doi:10.3389/fpls.2014.00047.

Schulz, Timothy A, and Carl E Creutz. 2004. “The Tricalbin C2 Domains : Lipid-Binding Properties of a Novel, Synaptotagmin-Like Yeast Protein Family.” *Biochemistry* 43: 3987–95.

Shao, Xuguang, Cai Li, Imma Fernandez, Xiangyang Zhang, Thomas C Sudhof, and Josep Rizo. 1997. “Synaptotagmin – Syntaxin Interaction : The C2 Domain as a Ca^{2+} -Dependent Electrostatic Switch.” *Neuron* 18: 133–42.

Simon, Mathilde Laetitia Audrey, Matthieu Pierre Platre, Maria Mar Marquès-bueno, Laia Armengot, Thomas Stanislas, Vincent Bayle, Marie-cécile Caillaud, and Yvon Jaillais. 2016. “A PtdIns(4)P-Driven Electrostatic Field Controls Cell Membrane Identity and Signalling in Plants.” *Nature Plants*. Nature Publishing Group, 1–10. doi:10.1038/nplants.2016.89.

Simpson, Clare, Carole Thomas, Kim Findlay, Emmanuelle Bayer, and Andrew J Maule. 2009. “An *Arabidopsis* GPI-Anchor Plasmodesmal Neck Protein with Callose Binding Activity and Potential to Regulate Cell-to-Cell Trafficking.” *The Plant Cell* 21: 581–94. doi:10.1105/tpc.108.060145.

Sosinsky, Gina E, and Bruce J Nicholson. 2005. “Structural Organization of Gap Junction Channels.” *Biochimica et Biophysica Acta (BBA) - Biomembranes* 1711 (2): 99–125. doi:10.1016/j.bbamem.2005.04.001.

Sparkes, Imogen, Nicholas Tolley, Isabel Aller, Julia Svozil, Anne Osterrieder, Stanley Botchway, Christopher Mueller, Lorenzo Frigerio, and Chris Hawes. 2010. “Five *Arabidopsis* Reticulon Isoforms Share Endoplasmic Reticulum Location, Topology, and Membrane-Shaping Properties.” *The Plant Cell* 22: 1333–43. doi:10.1105/tpc.110.074385.

Stahelin, Robert V., John D. Rafter, Sudipto Das, and Wonhwa Cho. 2003. “The Molecular Basis of Differential Subcellular Localization of C2 Domains of Protein Kinase C-Alpha and Group IVa Cytosolic Phospholipase A2.” *The Journal of Biological Chemistry* 278: 12452–60.

Stonebloom, Solomon, Tessa Burch-smith, Insoon Kim, David Meinke, Michael Mindrinos, and Patricia Zambryski. 2009. “Loss of the Plant DEAD-Box Protein ISE1 Leads to Defective Mitochondria and Increased Cell-to-Cell Transport via Plasmodesmata.” *PNAS* 106 (40): 17229–34.

Su, Shengzhong, Zhaohui Liu, Cheng Chen, Yan Zhang, Xu Wang, Lei Zhu, Long Miao, Xue-chen Wang, and Ming Yuan. 2010. “Cucumber Mosaic Virus Movement Protein Severs Actin Filaments to Increase the Plasmodesmal Size Exclusion Limit in Tobacco.” *The Plant Cell* 22: 1373–87. doi:10.1105/tpc.108.064212.

Südhof, Thomas C. 2004. “The Synaptic Vesicle Cycle.” *Annual Review Neurosciences* 27: 509–47.

Thomas, Carole L, Emmanuelle M Bayer, Christophe Ritzenthaler, Lourdes Fernandez-calvino, and Andrew J Maule. 2008. “Specific Targeting of a Plasmodesmal Protein Affecting Cell-to-Cell Communication.” *Plos Biology* 6 (1). doi:10.1371/journal.pbio.0060007.

Tilsner, Jens, William Nicolas, Abel Rosado, and Emmanuelle M Bayer. 2016. “Staying Tight : Plasmodesmal Membrane Contact Sites and the Control of Cell-to-Cell Connectivity in Plants.” *Annual Review Plant Biology* 67: 337–64. doi:10.1146/annurev-arplant-043015-111840.

Tilsner, Jens, Michael E Taliansky, and Lesley Torrance. 2014. “Plant Virus Movement.” *eLS*.

Tironi, I. G., R. Sperb, P. E. Smith, and W. F. van Gunsteren. 1995. “A Generalized Reaction Field Method for Molecular Dynamics Simulations.” *The Journal of Chemical Physics* 102 (13): 5451–59.

Toulmay, Alexandre, and William A Prinz. 2011. “A Conserved Membrane-Binding Domain Targets Proteins to Organelle Contact Sites.” *Journal of Cell Science* 125: 49–58. doi:10.1242/jcs.085118.

Trehin, Christophe, Sandra Schrempp, Aurélie Chauvet, Annick Berne-dedieu, Anne-marie Thierry, Jean-emmanuel Faure, Ioan Negrutiu, and Patrice Morel. 2013. “QUIRKY Interacts with STRUBBELIG and PAL OF QUIRKY to Regulate Cell Growth Anisotropy during Arabidopsis Gynoecium Development.” *The Company of Biologists Ltd - Development* 140: 4807–17. doi:10.1242/dev.091868.

Tucker, E B. 1982. “Translocation in the Staminal Hairs of *Setcreasea purpurea* . I . A Study of Cell Ultrastructure and Cell-to-Cell Passage of Molecular Probes.” *Protoplasma* 113: 193–201.

Tucker, Edward B. 1990. “Planta in Staminal Hairs of *Setcreasea Purpurea*.” *Planta* 182: 34–38.

Ubach, Josep, Xiangyang Zhang, Xuguang Shao, Thomas C. Südhof, and Josep Rizo. 1998. “Ca2+ Binding to Synaptotagmin: How Many Ca^{2+} Ions Bind to the Tip of a C2-Domain?” *The EMBO Journal* 17: 3921–30.

Ueki, Shoko, Roman Spektor, Danielle M Natale, and Vitaly Citovsky. 2010. “ANK, a Host Cytoplasmic Receptor for the Tobacco Mosaic Virus Cell-to-Cell Movement Protein, Facilitates Intercellular Transport through Plasmodesmata.” *Plos Pathogens* 6 (11). doi:10.1371/journal.ppat.1001201.

Unni, Samir, Yong Huang, Robert M Hanson, Malcolm Tobias, Sriram Krishnan, Wilfred W Li, Jens E Nielsen, and Nathan A Baker. 2011. “Web Servers and Services for Electrostatics Calculations with APBS and PDB2PQR.” *Journal of Computational Chemistry* 32 (7): 1488–91. doi:10.1002/jcc.

Vaddepalli, Prasad, Lynette Fulton, Martine Batoux, Ram Kishor, and Kay Schneitz. 2011. “Structure-Function Analysis of STRUBBELIG, an Arabidopsis Atypical Receptor-Like Kinase Involved in Tissue Morphogenesis.” *Plos One* 6 (5). doi:10.1371/journal.pone.0019730.

Vaddepalli, Prasad, Anja Herrmann, Lynette Fulton, Maxi Oelschner, Stefan Hillmer, Thomas F Stratil, Astrid Fastner, et al. 2014. “The C2-Domain Protein QUIRKY and the Receptor-like Kinase STRUBBELIG Localize to Plasmodesmata and Mediate Tissue Morphogenesis in Arabidopsis Thaliana.” *The Company of Biologists Ltd - Development* 141: 4139–48. doi:10.1242/dev.113878.

Verdaguer, Nuria, Senena Corbalán-garcía, Wendy F. Ochoa, Ignacio Fita, and Juan C. Gomez-Fernandez. 1999. “Ca^{2+} Bridges the C2 Membrane-Binding Domain of Protein Kinase C Alpha Directly to Phosphatidylserine.” *The EMBO Journal* 18 (22): 6329–38.

Vogler, Hannes, Myoung-ok Kwon, Vy Dang, Adrian Sambade, and Monika Fasler. 2008. “Tobacco Mosaic Virus Movement Protein Enhances the Spread of RNA Silencing.” *Plos Pathogens* 4 (4). doi:10.1371/journal.ppat.1000038.

Wang, Pengwei, Timothy J Hawkins, Christine Richardson, Ian Cummins, Michael J Deeks, Imogen Sparkes, Chris Hawes, and Patrick J Hussey. 2014. “Report The Plant Cytoskeleton, NET3C, and VAP27 Mediate the Link between the Plasma Membrane and Endoplasmic Reticulum.” *Current Biology* 24. Elsevier Ltd: 1397–1405. doi:10.1016/j.cub.2014.05.003.

Wang, Pengwei, Christine Richardson, Timothy J Hawkins, Imogen Sparkes, Chris Hawes, and Patrick J Hussey. 2016. “Plant VAP27 Proteins : Domain Characterization, Intracellular Localization and Role in Plant Development.” *New Phytologist* 210: 1311–26.

Wang, Xu, Ross Sager, Weier Cui, Chong Zhang, Hua Lu, and Jung-youn Lee. 2013. “Salicylic Acid Regulates Plasmodesmata Closure during Innate Immune Responses in *Arabidopsis*.” *The Plant Cell* 25: 2315–29. doi:10.1105/tpc.113.110676.

Ward, Katherine E, James P Ropa, Emmanuel Adu-gyamfi, and Robert V Stahelin. 2012. “C2 Domain Membrane Penetration by Group IVA Cytosolic Phospholipase A 2 Induces Membrane Curvature Changes.” *Journal of Lipid Research* 53: 2656–66. doi:10.1194/jlr.M030718.

Wassenaar, Tsjerk A, Helgi I. Ingolfsson, Rainer Böckmann, D. Peter Tieleman, and Siewert J Marrink. 2015. “Computational Lipidomics with Insane : A Versatile Tool for Generating Custom Membranes for Molecular Simulations.” *Journal of Chemical Theory and Computation* 11: 2144–55. doi:10.1021/acs.jctc.5b00209.

Wassenaar, Tsjerk A, Kristyna Pluhackova, Rainer A Böckmann, Siewert J Marrink, and D Peter Tieleman. 2014. “Going Backward : A Flexible Geometric Approach to Reverse Transformation from Coarse Grained to Atomistic Models.” *Journal of Chemical Theory and Computation* 10: 676–90.

Wayne, Randy. 2009. *Plant Cell Biology.*

Webb, Benjamin, and Andrej Sali. 2014. “Protein Structure Modeling with MODELLER.” In *Protein Structure Prediction*, 1–15.

Weiner, Hendrik, James N Burnell, I A N E Woodrow, Hans W Heldt, and Marshall D Hatch. 1988. “Metabolite Diffusion into Bundle Sheath Cells from C4 Plants.” *Plant Physiology* 88: 815–22.

White, Rosemary G, and Deborah A Barton. 2011. “The Cytoskeleton in Plasmodesmata : A Role in Intercellular Transport ?” *Journal of Experimental Botany* 62 (15): 5249–66. doi:10.1093/jxb/err227.

Wiederstein, Markus, and Manfred Sippl. 2007. “ProSA-Web: Interactive Web Service for the Recognition of Errors in Three-Dimensional Structures of Proteins.” *Nucleic Acids Research* 35: 407–10.

Willmer, C.M., and R Sexton. 1979. “Stomata and Protoplasma.” *Protoplasma* 100: 113–24.

Wolburg, Hartwig, and Arstrid Rolhmann. 1995. “Structure-Function Relationships in Gap Junctions.” *International Review of Cytology* 157: 315–73.

Xie, Bo, Xiaomin Wang, Maosheng Zhu, Zhongming Zhang, and Zonglie Hong. 2011. “CalS7 Encodes a Callose Synthase Responsible for Callose Deposition in the Phloem.” *The Plant Journal* 65: 1–14. doi:10.1111/j.1365-313X.2010.04399.x.

Xu, Junjie, Taulant Bacaj, Amy Zhou, Diana R Tomchick, Thomas C Sudhof, and Josep Rizo. 2014. “Article Structure and Ca^{2+} -Binding Properties of the Tandem C 2 Domains of E-Syt2.” *Structure* 22: 269–80. doi:10.1016/j.str.2013.11.011.

Xu, Min, Euna Cho, Tessa M Burch-smith, and Patricia C Zambryski. 2012. “Plasmodesmata Formation and Cell-to-Cell Transport Are Reduced in Decreased Size Exclusion Limit 1 during Embryogenesis in *Arabidopsis*.” *PNAS* 109 (13). doi:10.1073/pnas.1202919109/-/DCSupplemental.www.pnas.org/cgi/doi/10.1073/pnas.1202919109.

Xu, Xianfeng Morgan, Jing Wang, Zhenyu Xuan, Alexander Goldshmidt, Philippa G M Borrill, Nisha Hariharan, Jae Yean Kim, and David Jackson. 2011. “Chaperonins Facilitate KNOTTED1 Cell-to-Cell Trafficking and Stem Cell Function.” *Science* 333: 1141–45.

Yamaguchi, T., H. Shirataki, S. Kishida, M. Miyazaki, J. Nishikawa, K. Wada, S. Numata, K. Kaibuchi, and Y Takai. 1993. “Two Functionally Different Domains of Rabphilin-3A, Rab3A p25/smg p25A-Binding and Phospholipid- and Ca(2+)-Binding Domains.” *The Journal of Biological Chemistry* 268: 27164–70.

Yamazaki, Tomokazu, Yukio Kawamura, Anzu Minami, and Matsuo Uemura. 2008. “Calcium-Dependent Freezing Tolerance in *Arabidopsis* Involves Membrane Resealing via Synaptotagmin SYT1.” *The Plant Cell* 20: 3389–3404. doi:10.1105/tpc.108.062679.

Yau, Wai-ming, William C Wimley, Klaus Gawrisch, and Stephen H White. 1998. “The Preference of Tryptophan for Membrane Interfaces.” *Biochemistry* 37: 14713–18.

Zanetti, Maria N, Oscar D Bello, Jing Wang, Jeff Coleman, Yiying Cai, Charles V Sindelar, James E Rothman, and Shyam S Krishnakumar. 2016. “Ring-like Oligomers of Synaptotagmins and Related C2 Domain Proteins.” *eLife* 5: 1–15. doi:10.7554/eLife.17262.

Zhang, Dapeng, and L Aravind. 2010. “Identification of Novel Families and Classification of the C2 Domain Superfamily Elucidate the Origin and Evolution of Membrane Targeting Activities in Eukaryotes.” *Gene* 469. Elsevier B.V.: 18–30. doi:10.1016/j.gene.2010.08.006.

Zhang, Xiangyang, Josep Rizo, and Thomas C Sudhof. 1998. “Mechanism of Phospholipid Binding by the C 2 A-Domain of Synaptotagmin I.” *Biochemistry* 37: 12395–403.

Zhou, Weizhuang, Grace W Tang, and Russ B Altman. 2015. “High Resolution Prediction of Calcium-Binding Sites in 3D Protein Structures Using FEATURE.” *Journal of Chemical Information and Modeling* 55: 1663–72. doi:10.1021/acs.jcim.5b00367.

Zhu, T, and T L Rost. 2000. “Directional Cell-to-Cell Communication in the Arabidopsis Root Apical Meristem III . Plasmodesmata Turnover and Apoptosis in Meristem and Root Cap Cells.” *Protoplasma* 213: 99–107.

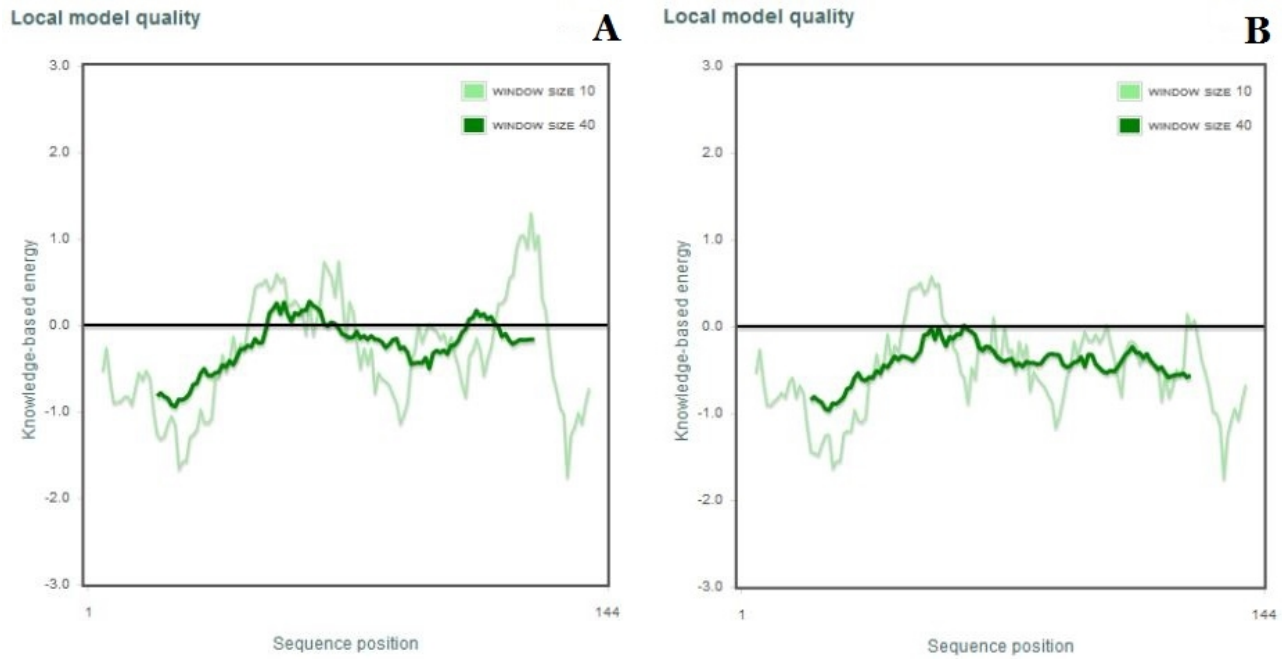

Supp. Figure 1: PROSA-WEB energy plots of the AtMCTP5 C2A domain model. (**A**) Modeller model before loop refining. (**B**) Final 3D structure after refining.

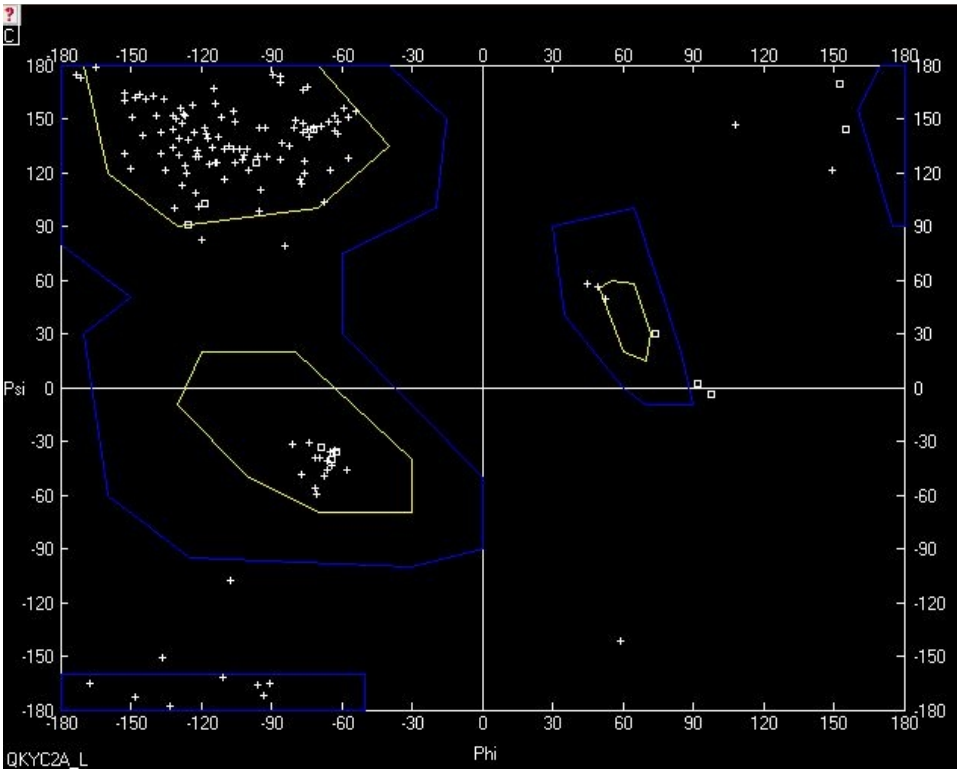

Supp. Figure 2: Ramachandran plot of AtMCTP5 C2A domain final model. Squares represent Glycines residues and crosses all the other residues.

Annexe 2

Name	Uniprot	C2_A		C2_B		C2_C		C2_D		TMD	Total Length
		Position	*Length*	*Position*	*Length*	*Position*	*Length*	*Position*	*Length*		
MCTP1	Q9C8H3	/	/	{L34-A166}	133	{P198-G335}	138	{P360-C498}	139	* – {574-591} – {604-636} – {717-748}	776
MCTP2	O64492	{G9-A140}	132	{L274-G397}	124	{P431-G574}	144	{P599-G735}	137	* – {850-872} – {956-978}	1012
MCTP3	Q9FIZ1	/	/	{L33-G154}	122	{P188-G299}	112	/	/	(*)	478
MCTP4	Q9FL59	/	/	{L50-G180}	131	{P214-G354}	141	{P379-L517}	139	*{510-532}* – {590-612} – {627-649} – {737-759}	794
MCTP5	**B8XCH5**	**{P12-T155}**	**144**	**{P333-P473}**	**141**	**{P494-A650}**	**157**	**{P666-P803}**	**138**	*** – {919-941} – {1024-1046}**	**1081**
MCTP6	Q9LXU2	/	/	{L35-G164}	130	{P198-G334}	137	{P359-L492}	134	* – {602-624} – {712-734}	769
MCTP7	Q9SS68	{M1-P137}	137	{L276-G406}	131	{P436-A584}	149	{P601-P739}	139	{851-873} – {960-982}	1017
MCTP8	Q9SKA3	{M1-G133}	133	{L288-A423}	132	{P454-A594}	141	{P619-T752}	134	{862-884} – {972-994}	1029
MCTP9	Q8RXU9	{M1-P133}	133	{L263-G392}	130	{P429-G568}	140	{A594-T729}	136	{844-866} – {949-971}	1006
MCTP10	Q9M2R0	/	/	{L34-A166}	133	{P198-G334}	137	{P359-C495}	137	{571-588} – {601-633} – {714-745}	773
MCTP11	Q84TJ7	{M1-A135}	135	{L273-A405}	133	{P439-G584}	146	{P602-C733}	132	{809-826} – {839-861} – {952-981}	1011
MCTP12	Q9FJG3	{M1-P139}	139	{L318-G445}	128	{M472-G606}	135	{P631-P772}	142	{881-903} – {992-1014}	1049
MCTP13	O49435	/	/	{L41-A169}	129	{P200-L338}	139	{P358-A495}	138	{608-630} – {722-744}	774
MCTP14	Q9M366	/	/	{L36-G162}	127	{P196-A327}	132	{P354-G491}	138	(*) – {610-632} – {730-752} – (*)	795
MCTP15	Q9LZE5	/	/	{L35-G157}	123	{P190-A318}	129	{P345-G481}	137	{569-591} – {687-709}	745
MCTP16	Q9FI32	{M1-S133}	133	{L289-A425}	137	{P456-G596}	141	{P622-L759}	138	* – {874-896} – {979-1001}	1036
MCTP17	Q9M2D4	{M1-P137}	137	{L243-A372}	130	{P401-G532}	132	{P560-C693}	134	{814-824}* – {921-943}	972

Supp. Table 1: C2 domain and transmembrane region delimitation of the *Arabidopsis thaliana* MCTPs.

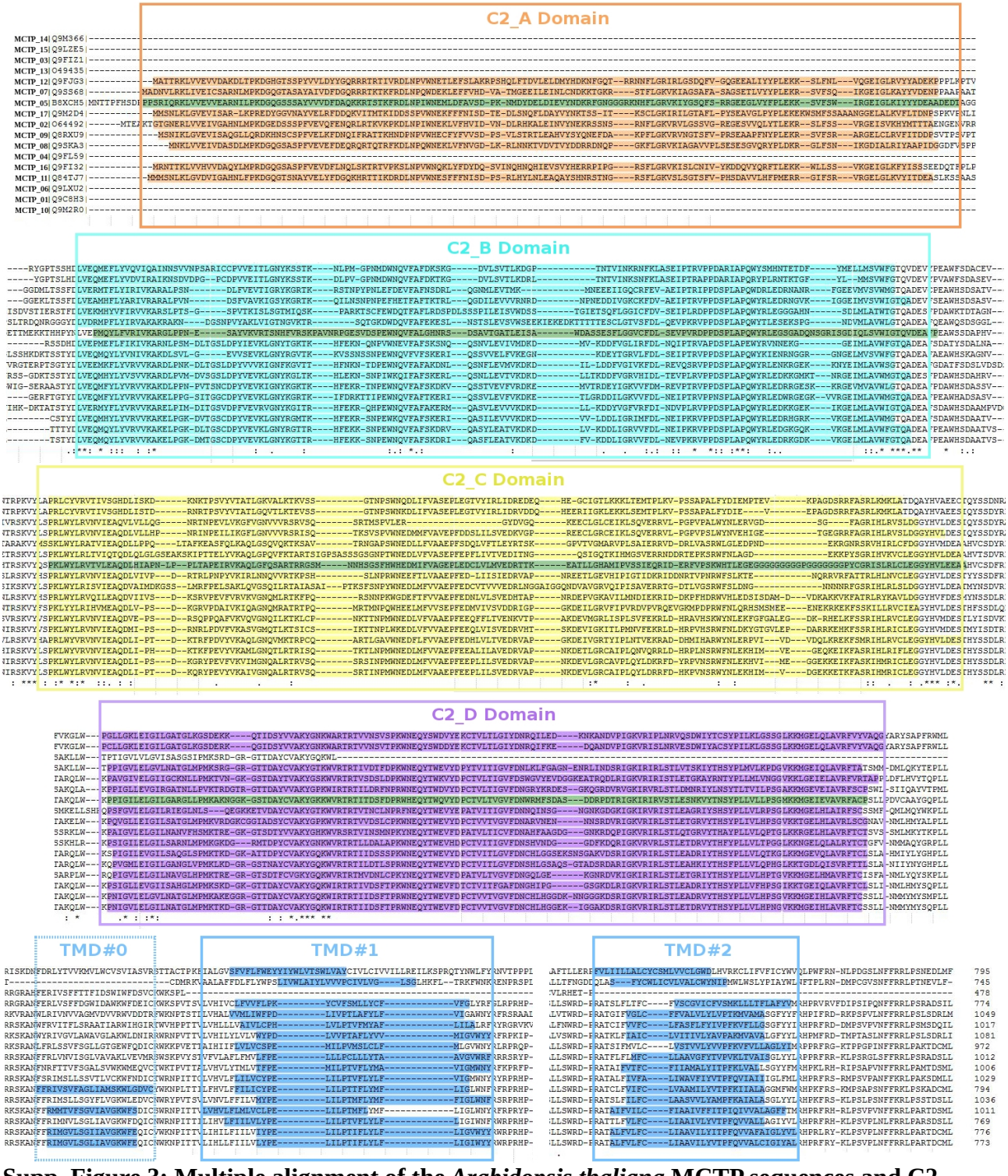

Supp. Figure 3: Multiple alignment of the *Arabidopsis thaliana* MCTP sequences and C2 domain and Transmembrane region delimitation. The green highlightening represent the modeled C2 domains of QKY.

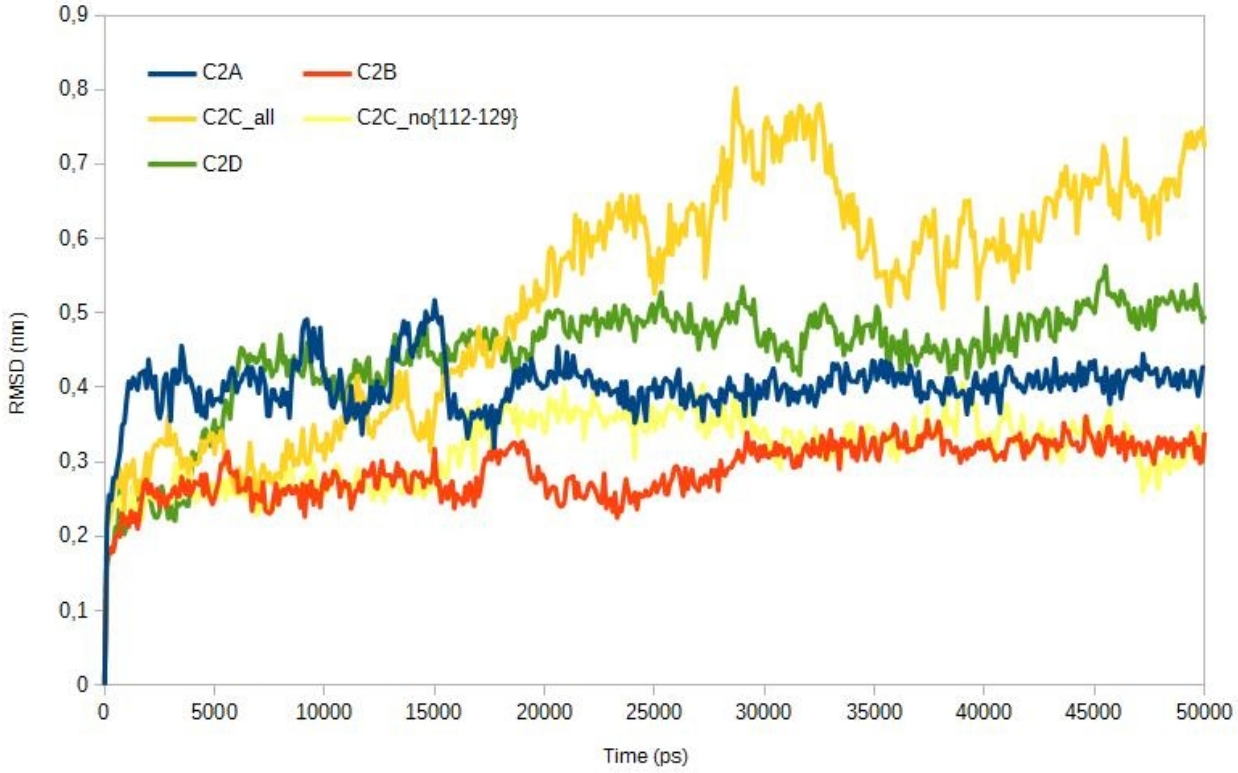

Supp. Figure 4: RMSD of the atomistic structures of the NbMCTP11 C2 domains. The RMSD was calculated on the α-carbons positions during the 50ns simulations. A loop (112-129) of the C2C domain is responsible for high RMSD, as the RMSD calculated on the domain without the loop residues is lower.

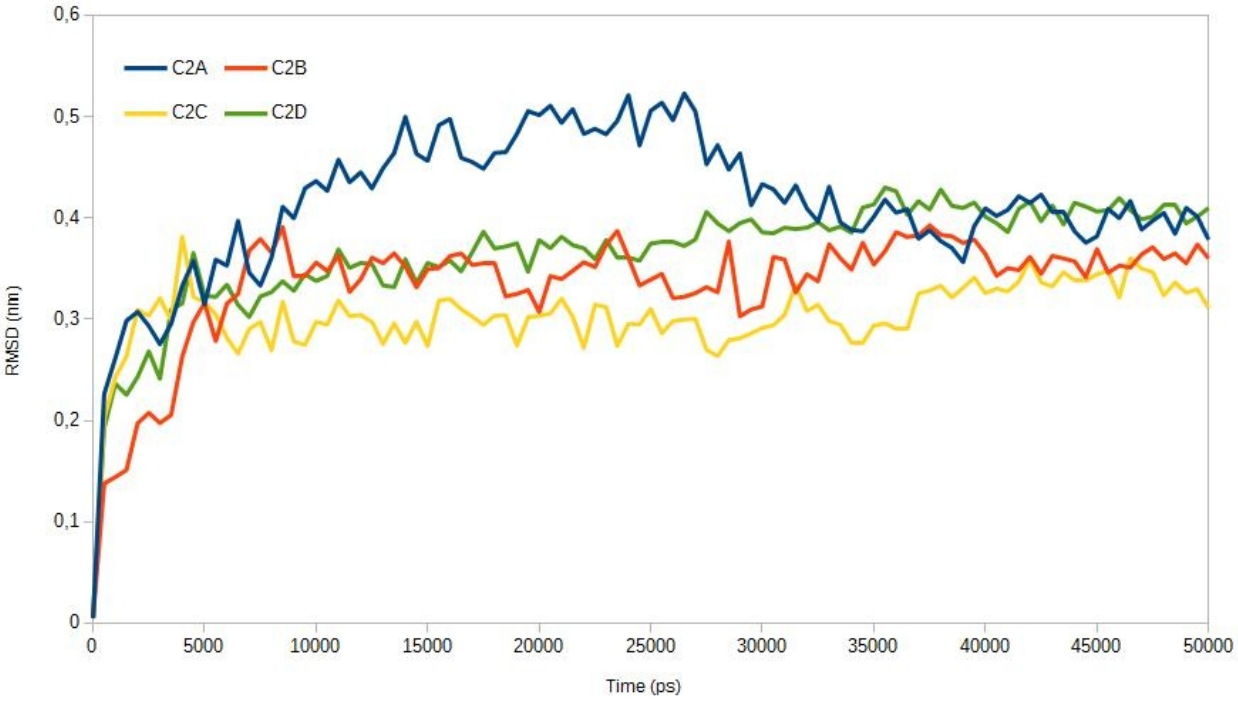

Supp. Figure 5: RMSD of the CG structures of the NbMCTP11 C2 domains. The RMSD was calculated on the BB beads positions during the 50ns simulations.

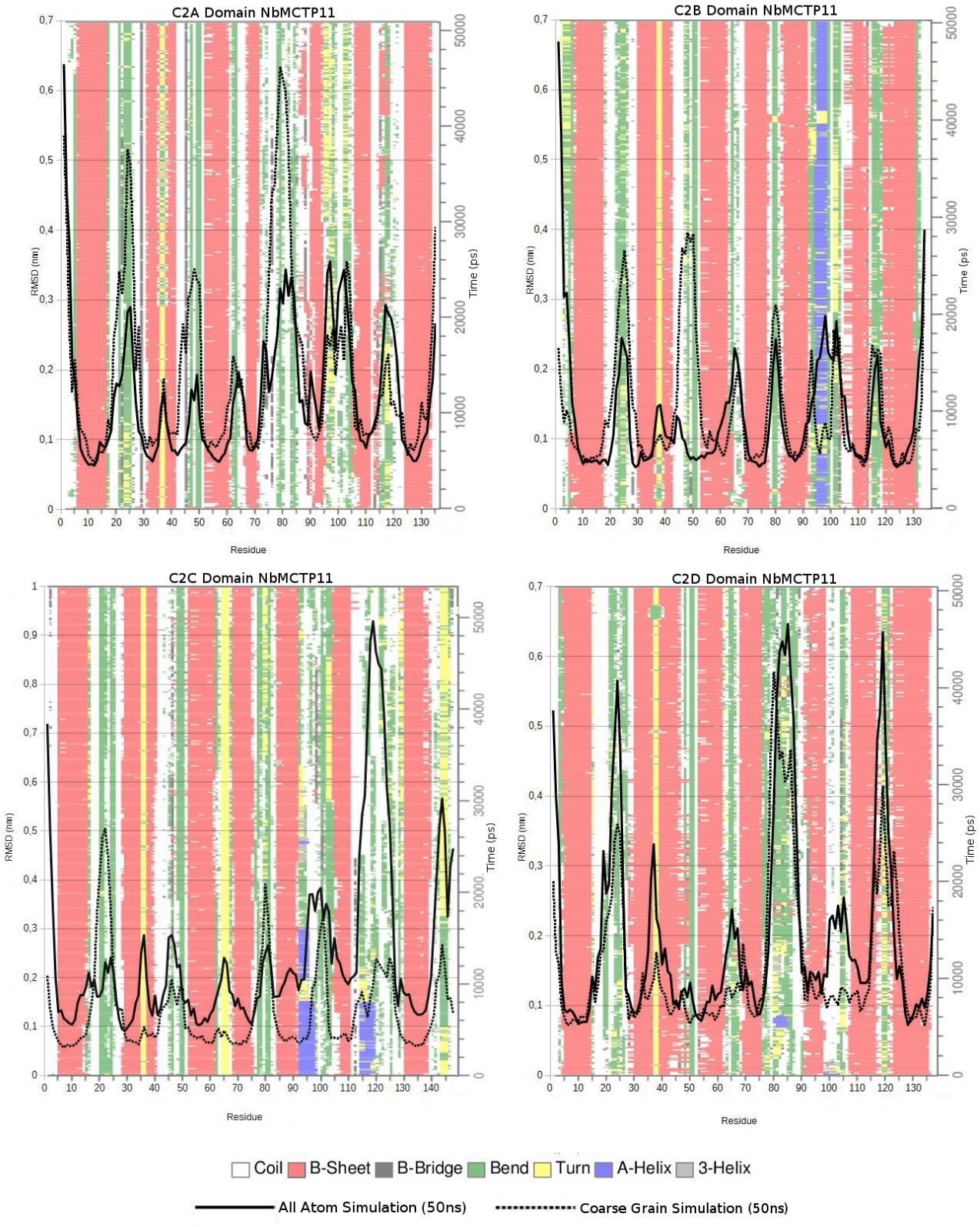

Supp. Figure 6: Atomistic and CG stand-alone simulations of the four C2 domains of NbMCTP11. The background color represents the DSSP (secondary structure over time) of the 50ns atomistic simulation. The continuous black lines are the RMSF associated with the DSSP. The dotted lines are the RMSF of the CG structure after optimization.